

Volume 5, Issue 4 (IX)
October - December 2018

ISSN 2394 - 7780



ज्ञान-विज्ञान विमुक्तये

UGC
University Grants Commission
Journal No.: 63571

International Journal of
Advance and Innovative Research
(Special Issue)

Indian Academicians and Researchers Association
www.iaaedu.com



SPECIAL ISSUE

of

E. G. S. Pillay Engineering College
Nagapattinam, Tamil Nadu



Publication Partner

Indian Academicians and Researcher's Association

Guest Editors of Special Issue

Prof. G. Ganesan

Assistant Professor

E. G. S. Pillay Engineering College, Nagapattinam, Tamilnadu

International Journal of Advance and Innovative Research

Volume 5, Issue 4 (IX): October - December 2018

Editor- In-Chief

Dr. Tazyn Rahman

Members of Editorial Advisory Board

Mr. Nakibur Rahman

Ex. General Manager (Project)
Bongaigoan Refinery, IOC Ltd, Assam

Dr. Alka Agarwal

Director,
Mewar Institute of Management, Ghaziabad

Prof. (Dr.) Sudhansu Ranjan Mohapatra

Dean, Faculty of Law,
Sambalpur University, Sambalpur

Dr. P. Malyadri

Principal,
Government Degree College, Hyderabad

Prof.(Dr.) Shareef Hoque

Professor,
North South University, Bangladesh

Prof.(Dr.) Michael J. Riordan

Professor,
Sanda University, Jiashan, China

Prof.(Dr.) James Steve

Professor,
Fresno Pacific University, California, USA

Prof.(Dr.) Chris Wilson

Professor,
Curtin University, Singapore

Prof. (Dr.) Amer A. Taqa

Professor, DBS Department,
University of Mosul, Iraq

Dr. Nurul Fadly Habidin

Faculty of Management and Economics,
Universiti Pendidikan Sultan Idris, Malaysia

Dr. Neetu Singh

HOD, Department of Biotechnology,
Mewar Institute, Vasundhara, Ghaziabad

Dr. Mukesh Saxena

Pro Vice Chancellor,
University of Technology and Management, Shillong

Dr. Archana A. Ghatule

Director,
SKN Sinhgad Business School, Pandharpur

Prof. (Dr.) Monoj Kumar Chowdhury

Professor, Department of Business Administration,
Guahati University, Guwahati

Prof. (Dr.) Baljeet Singh Hothi

Professor,
Gitarattan International Business School, Delhi

Prof. (Dr.) Badiuddin Ahmed

Professor & Head, Department of Commerce,
Maulana Azad Nationl Urdu University, Hyderabad

Dr. Anindita Sharma

Dean & Associate Professor,
Jaipuria School of Business, Indirapuram, Ghaziabad

Prof. (Dr.) Jose Vargas Hernandez

Research Professor,
University of Guadalajara, Jalisco, México

Prof. (Dr.) P. Madhu Sudana Rao

Professor,
Mekelle University, Mekelle, Ethiopia

Prof. (Dr.) Himanshu Pandey

Professor, Department of Mathematics and Statistics
Gorakhpur University, Gorakhpur

Prof. (Dr.) Agbo Johnson Madaki

Faculty, Faculty of Law,
Catholic University of Eastern Africa, Nairobi, Kenya

Prof. (Dr.) D. Durga Bhavani

Professor,
CVR College of Engineering, Hyderabad, Telangana

Prof. (Dr.) Shashi Singhal

Professor,
Amity University, Jaipur

Prof. (Dr.) Alireza Heidari

Professor, Faculty of Chemistry,
California South University, California, USA

Prof. (Dr.) A. Mahadevan

Professor
S. G. School of Business Management, Salem

Prof. (Dr.) Hemant Sharma

Professor,
Amity University, Haryana

Dr. C. Shalini Kumar

Principal,
Vidhya Sagar Women's College, Chengalpet

Prof. (Dr.) Badar Alam Iqbal

Adjunct Professor,
Monarch University, Switzerland

Prof.(Dr.) D. Madan Mohan

Professor,
Indur PG College of MBA, Bodhan, Nizamabad

Dr. Sandeep Kumar Sahratia

Professor
Sreyas Institute of Engineering & Technology

Dr. S. Balamurugan

Director - Research & Development,
Mindnotix Technologies, Coimbatore

Dr. Dhananjay Prabhakar Awasarikar

Associate Professor,
Suryadutta Institute, Pune

Dr. Mohammad Younis

Associate Professor,
King Abdullah University, Saudi Arabia

Dr. Kavita Gidwani

Associate Professor,
Chanakya Technical Campus, Jaipur

Dr. Vijit Chaturvedi

Associate Professor,
Amity University, Noida

Dr. Marwan Mustafa Shamot

Associate Professor,
King Saud University, Saudi Arabia

Prof. (Dr.) Aradhna Yadav

Professor,
Krupanidhi School of Management, Bengaluru

Prof.(Dr.) Robert Allen

Professor
Carnegie Mellon University, Australia

Prof. (Dr.) S. Nallusamy

Professor & Dean,
Dr. M.G.R. Educational & Research Institute, Chennai

Prof. (Dr.) Ravi Kumar Bommiseti

Professor,
Amrita Sai Institute of Science & Technology, Paritala

Dr. Syed Mehartaj Begum

Professor,
Hamdard University, New Delhi

Dr. Darshana Narayanan

Head of Research,
Pymetrics, New York, USA

Dr. Rosemary Ekechukwu

Associate Dean,
University of Port Harcourt, Nigeria

Dr. P.V. Praveen Sundar

Director,
Shanmuga Industries Arts and Science College

Dr. Manoj P. K.

Associate Professor,
Cochin University of Science and Technology

Dr. Indu Santosh

Associate Professor,
Dr. C. V.Raman University, Chhattisgarh

Dr. Pranjal Sharma

Associate Professor, Department of Management
Mile Stone Institute of Higher Management, Ghaziabad

Dr. Lalata K Pani

Reader,
Bhadrak Autonomous College, Bhadrak, Odisha

Dr. Pradeepta Kishore Sahoo

Associate Professor,
B.S.A, Institute of Law, Faridabad

Dr. R. Navaneeth Krishnan

Associate Professor,
Bharathiyan College of Engg & Tech, Puducherry

Dr. Mahendra Daiya
Associate Professor,
JIET Group of Institutions, Jodhpur

Dr. Parbin Sultana
Associate Professor,
University of Science & Technology Meghalaya

Dr. Kalpesh T. Patel
Principal (In-charge)
Shree G. N. Patel Commerce College, Nanikadi

Dr. Juhab Hussain
Assistant Professor,
King Abdulaziz University, Saudi Arabia

Dr. V. Tulasi Das
Assistant Professor,
Acharya Nagarjuna University, Guntur, A.P.

Dr. Urmila Yadav
Assistant Professor,
Sharda University, Greater Noida

Dr. M. Kanagarathinam
Head, Department of Commerce
Nehru Arts and Science College, Coimbatore

Dr. V. Ananthaswamy
Assistant Professor
The Madura College (Autonomous), Madurai

Dr. S. R. Boselin Prabhu
Assistant Professor,
SVS College of Engineering, Coimbatore

Dr. A. Anbu
Assistant Professor,
Acharya College of Education, Puducherry

Dr. C. Sankar
Assistant Professor,
VLB Janakiammal College of Arts and Science

Dr. G. Valarmathi
Associate Professor,
Vidhya Sagar Women's College, Chengalpet

Dr. M. I. Qadir
Assistant Professor,
Bahauddin Zakariya University, Pakistan

Dr. Brijesh H. Joshi
Principal (In-charge)
B. L. Parikh College of BBA, Palanpur

Dr. Namita Dixit
Assistant Professor,
ITS Institute of Management, Ghaziabad

Dr. Nidhi Agrawal
Assistant Professor,
Institute of Technology & Science, Ghaziabad

Dr. Ashutosh Pandey
Assistant Professor,
Lovely Professional University, Punjab

Dr. Subha Ganguly
Scientist (Food Microbiology)
West Bengal University of A. & F Sciences, Kolkata

Dr. R. Suresh
Assistant Professor, Department of Management
Mahatma Gandhi University

Dr. V. Subba Reddy
Assistant Professor,
RGM Group of Institutions, Kadapa

Dr. R. Jayanthi
Assistant Professor,
Vidhya Sagar Women's College, Chengalpattu

Dr. Manisha Gupta
Assistant Professor,
Jagannath International Management School

Copyright @ 2018 Indian Academicians and Researchers Association, Guwahati
All rights reserved.

No part of this publication may be reproduced or transmitted in any form or by any means, or stored in any retrieval system of any nature without prior written permission. Application for permission for other use of copyright material including permission to reproduce extracts in other published works shall be made to the publishers. Full acknowledgment of author, publishers and source must be given.

The views expressed in the articles are those of the contributors and not necessarily of the Editorial Board or the IARA. Although every care has been taken to avoid errors or omissions, this publication is being published on the condition and understanding that information given in this journal is merely for reference and must not be taken as having authority of or binding in any way on the authors, editors and publishers, who do not owe any responsibility for any damage or loss to any person, for the result of any action taken on the basis of this work. All disputes are subject to Guwahati jurisdiction only.



Journal - 63571

UGC Journal Details

Name of the Journal : International Journal of Advance & Innovative Research

ISSN Number :

e-ISSN Number : 23947780

Source: UNIV

Subject: Multidisciplinary

Publisher: Indian Academicians and Researchers Association

Country of Publication: India

Broad Subject Category: Multidisciplinary

CONTENTS

Research Papers

DIGITAL SIMULATION OF CLOSED LOOP FUZZY LOGIC CONTROLLED TRANSFORMER LESS UPFC WITH IMPROVED DYNAMIC RESPONSE	1 – 6
N. keerthana, M. Ramya and Anandaraj	
BATTERY BALANCING SYSTEM FOR AN ELECTRIC VEHICLE USING SOLAR PANEL	7 – 13
R. Janbaga Lakshmi, S. Sivamani and R. Anandaraj	
CONCURRENTLY POWER/DATA TRANSFER BY WIRELESS FOR ELECTRIC VEHICLE CHARGING USING IOT	14 – 20
V. Anitha, P. J. Suresh Babu and R. Anandaraj	
DESIGN OF MULTIPHASE INTERLEAVED BOOST CONVERTER	21 – 26
M. Pavithra and R. Anandaraj	
ELECTRIC VEHICLE CHARGING STATION USING VIENNA RECTIFIER AND 3L DC - DC CONVERTER WITH AN ENERGY STORAGE STAGE	27 – 34
Shree Aasha Lekshman, Dr. T. Suresh Padmanabhan and R. Anandaraj	
ENHANCEMENT OF PV MODULE BY PARTIAL SHADING DETECTION USING MAXIMUM POWER POINT TRACKING TECHNIQUE	35 – 40
B. S. Umabharathi, B. Amalorenaveenantony and R. Anandaraj	
INTELLIGENT MPPT CONTROLLER FOR FAST AND EFFICIENT TRACKING UNDER DIFFERENT ENVIRONMENT CONDITIONS	41 – 46
M. Sangeetha and S. Latha	
WIRELESS POWER TRANSFER BASED ON INTEGRATED HYBRID ENERGY HARVESTING SYSTEM	47 – 52
N. Midula and R. Anandaraj	
A DESIGN OF SELECTIVE HARMONIC MITIGATION BASED SELF-ELIMINATION OF TRIPLIN HARMONICS FOR SINGLE-PHASE SEVEN-LEVEL INVERTERS	53 – 58
N. Saraswathi	
SINGLE-STAGE SWITCHED-BOOST INVERTER WITH FOUR SWITCHES FOR AC/DC APPLICATION	59 - 64
J. Jayasri	
A COMPARATIVE ANALYSIS OF CLASSICAL THREE PHASE MULTILEVEL (FIVE LEVEL) INVERTER TOPOLOGIES	65 – 69
K. Kalaivanan and K. Nandakumar	
CONTROL AND OPERATION OF A DC GRID-BASED WIND POWER GENERATION SYSTEM IN A MICROGRID	70 – 76
D. Senthilkumar and R. Anandaraj	

EXPERIMENTAL STUDY ON STRENGTH AND DURABILITY PRPERTIES OF GGBS BASED CONCRETE IN SEA WATER 77 – 83

P. Malliga and Dr. B. Vidivelli

SINGLE PHASE BIDIRECTIONAL AC TO DC CONVERTER USING THREE PORT CONVERTER WITH MINIMISED POWER PROCESSING STAGE AND OVERALL IMPROVED EFFICIENCY 84 – 89

Chakkaravarthi C. and J. Menaka

DIGITAL SIMULATION OF CLOSED LOOP FUZZY LOGIC CONTROLLED TRANSFORMER LESS UPFC WITH IMPROVED DYNAMIC RESPONSE

N. Keerthana¹, M. Ramya² and Anandraj³

PG Scholar¹, Assistant Professor² and Associate Professor³

Department of Electrical and Electronics Engineering, E. G. S. Pillay Engineering College (Autonomous), Nagapattinam, Tamilnadu

ABSTRACT

This paper deals with simulation of closed loop MLI based UPFC (CLMLIUPFC) to improve the power - quality. The UPFC is also capable of enhancing transient – stability - limit in a power system. UPFC is a combination of series -converter and shunt- converter. The circuit model of CLMLIUPFC is developed using rectifier and multi level inverter circuits. The control angle is varied to vary the true and imaginary powers at the receiving end. The Mat-lab simulation results of PI and FL controlled CLMLIUPFC systems are presented. The results indicate that FL controlled CLMLIUPFC system gives faster response than PI controlled CLMLIUPFC system.

Keywords: UPFC, Power Quality, Multilevel Inverter (MLI), Static Series Synchronous Compensator (SSSC), Fuzzy logic control (FLC), STATCOM, Compensation and Matlab Simulink.

I. INTRODUCTION

The Static Series Synchronous Compensator (SSSC) can control lively and hasty in a transmission line of a little range by the use of storied energy in capacitor DC-link where Static Synchronous Compensator with injecting hasty power can regulate the bus voltage in a transmission line. Unified Power Flow Controller is the most important adaptable and complex supply AC Transmission Systems (FACTS) equipment that has emerge for the control and optimization of power flow in power transmission systems. This devices offer a substitute mean to mitigate power system oscillations. Thus a critical inquiry is the determination of the information signals and the embraced control strategy for these devices in order to damp power oscillations in an effective and robust manner. Much research in this domain has been true zed. Finally, a new identification method based on “state variables” was proposed.

After this presentation, the rule and operation of an UPFC associated with a system are displayed. In section II, the control strategy for UPFC is introduced. Simulation consequence are presented in sections III. Section IV describes the conclusion.

II. UPFC SYSTEM

A simplified scheme of an UPFC connected to an infinite bus via a transmission line is shown in Figure.1. The basic function of inverter -1 is to supply the true power demanded by inverter -2 through the common DC -link. Inverter -1 can also generate or absorb controllable power.

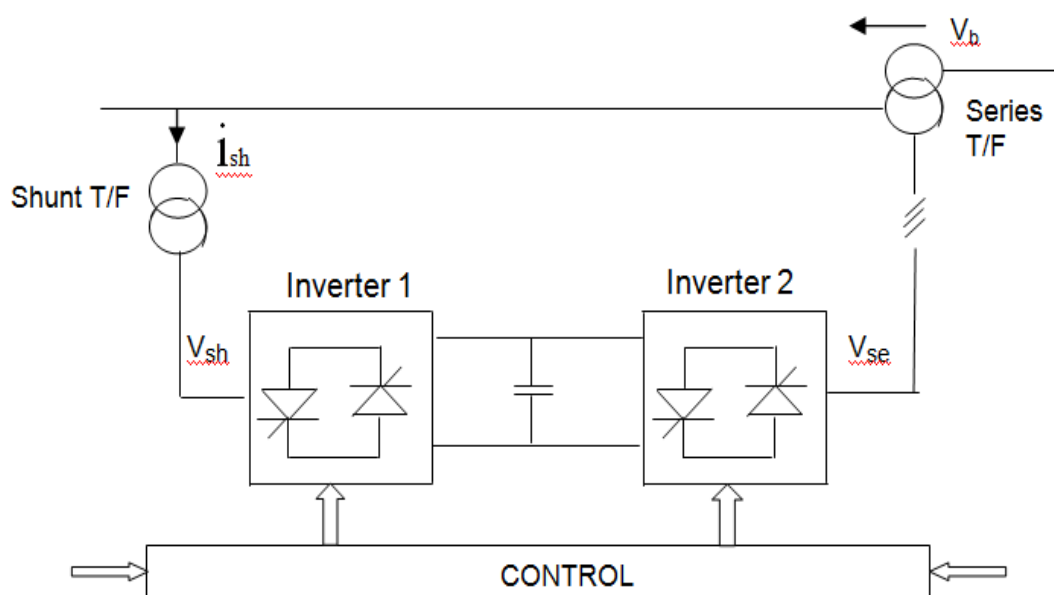


Fig-1: UPFC installed in the transmission line

The overhead information does not convenient with power-quality enhancement in Wind generation based two-bus system utilizing 'UPFC'. This work recommends 'UPFC' for the power-quality enhancement in the multi-bus system. The above papers do not compare the response of PI and FL controlled 'UPFC' systems. This work recommends FL for the control of 'UPFC' system.

III. SYSTEM DESCRIPTION

The conventional UPFC that consists of two back-to-back inverters and it requires bulky and often a complicated zigzag transformers for isolation and reaching high power rating with desired voltage waveforms. To overcome this problem, a completely transformer less UPFC based on an innovative configuration of two cascade multilevel inverters has been proposed. The new UPFC offers several advantages over the traditional technology, such as transformer less, light weight, high efficiency, low cost and fast dynamic response.

In large power plants more than one PI controller are used. Traditionally these PI controllers are tuned with constant parameters which are not robust enough when there is change in design parameters. In order to overcome this problem different methods are proposed. Fuzzy Controller is one of them.

A. Design of Fuzzy-PI controller

In order to improve the transient stability of power system two fuzzy-PI controllers have been designed to separately regulate the voltage and current. For voltage regulator the difference between V_{meas} and V_{ref} i.e. error and its derivative are taken as input for fuzzy adjuster similar for current regulator difference between I_q and I_{qref} and its derivative are taken as input for fuzzy adjuster.

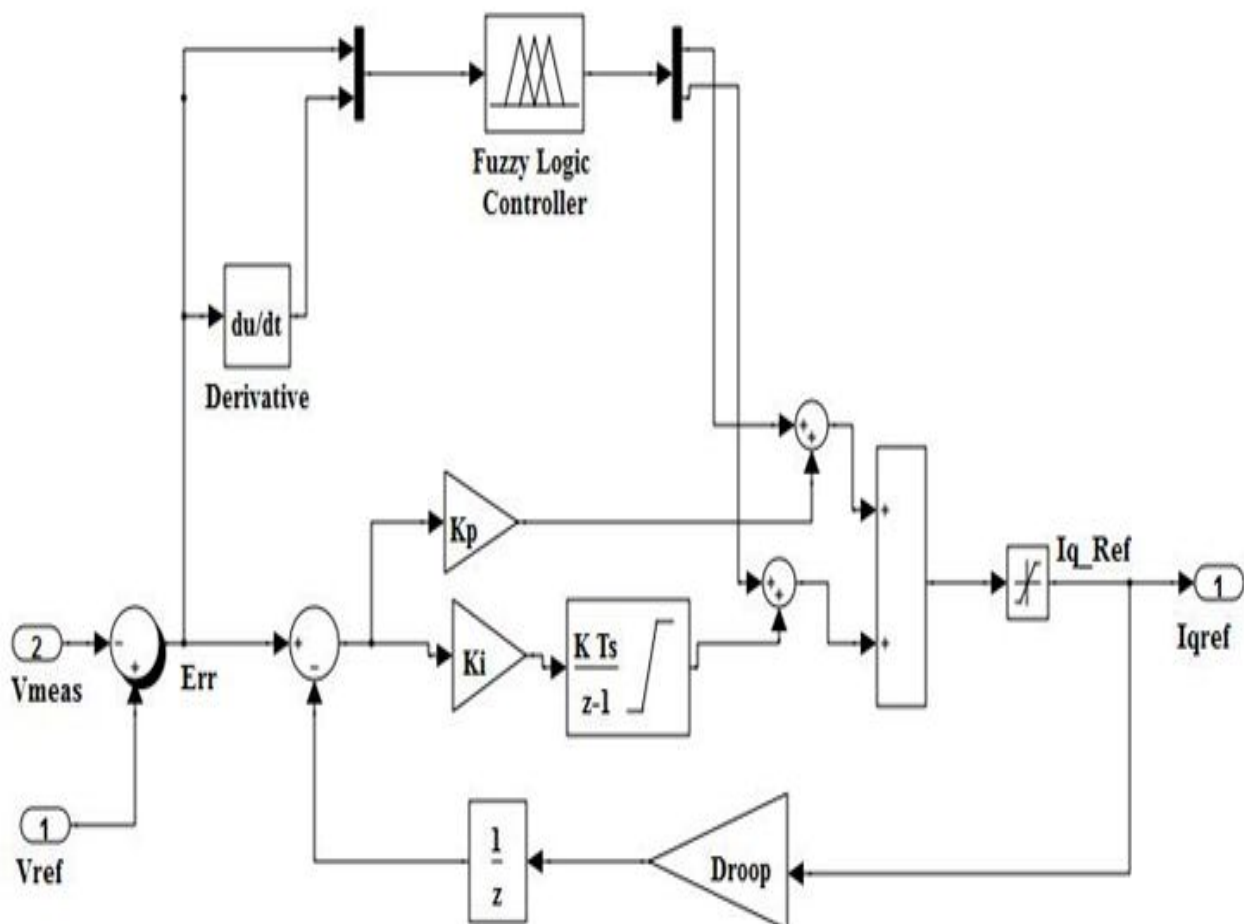


Fig-2: Fuzzy-PI arrangement for Voltage Regulator

These fuzzy adjusters are used to adjust the parameters of proportional gain and integral gain. Where and are the reference values of fuzzy-PI based controllers. The general arrangement of fuzzy-PI controller in Voltage Regulator and Current Regulator are given in Figure 2.

IV. SIMULATION RESULTS

Closed loop PI controller of transformer less UPFC is appeared in Fig 4. The receiving end voltage is related with a reference--voltage. The flaw is pragmatic to the comparator across a PI-controller. The output of comparator updates the pulse width applied to 'UPFC'.

Discrete,
 $T_s = 5e-06$ s,
powergui

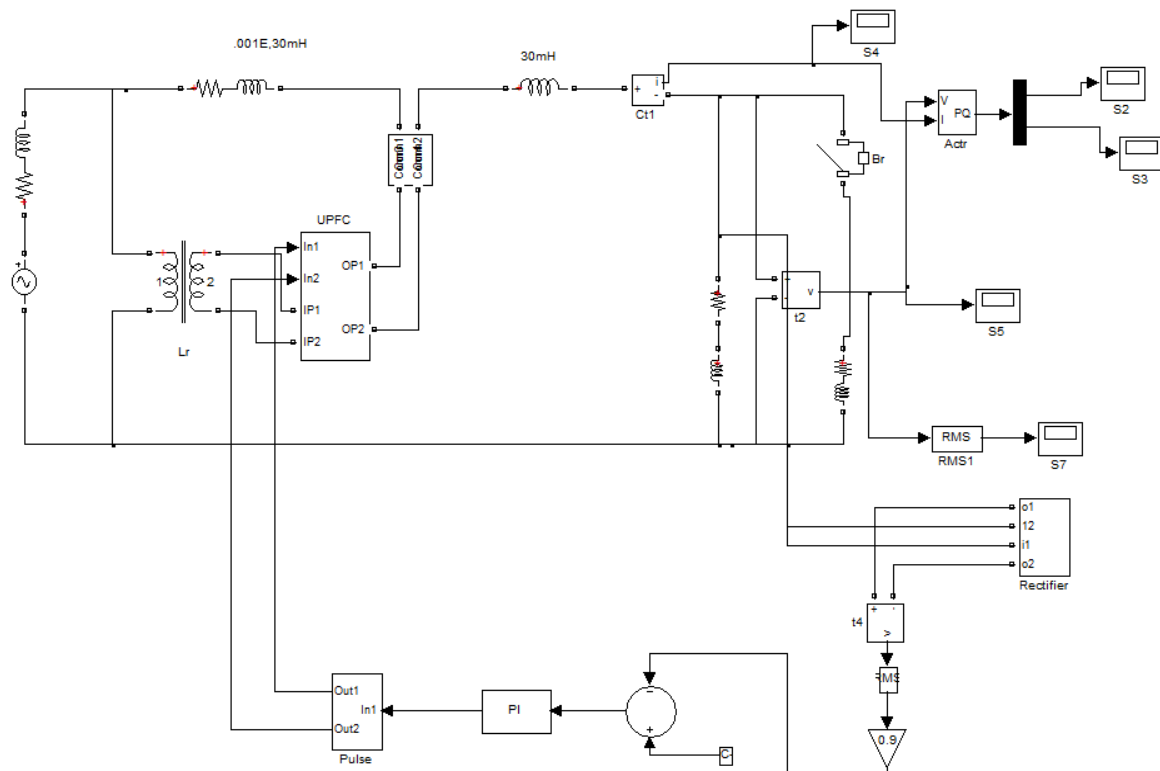


Fig-3: Closed loop PI controller of transformer less UPFC

The output voltage across load is shown in Fig 4 and its value is $0.5 \times 10^4 \text{V}$.

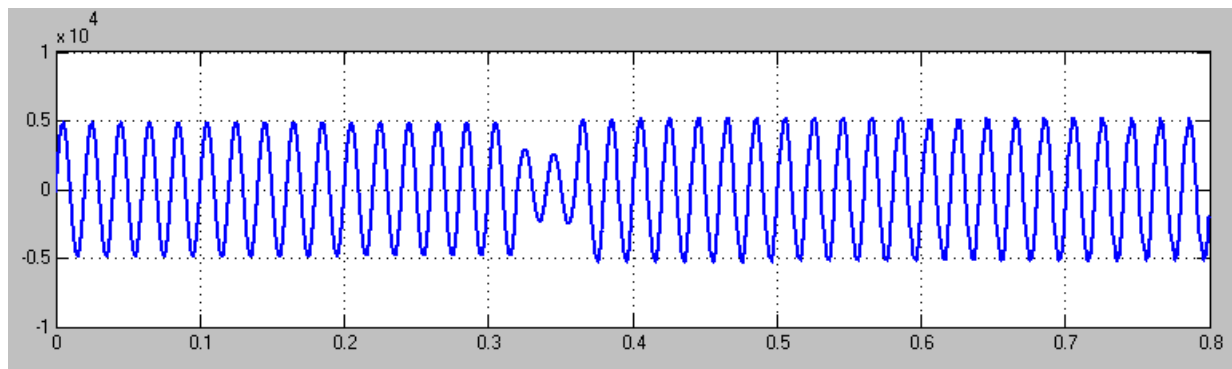


Fig-4: Output voltage across load

The Closed loop RMS output voltage of transformer less UPFC is shown in Fig 5 and it is approximately 3900V. The RMS output voltage decreases from t = 1 sec and then reaches normal value.

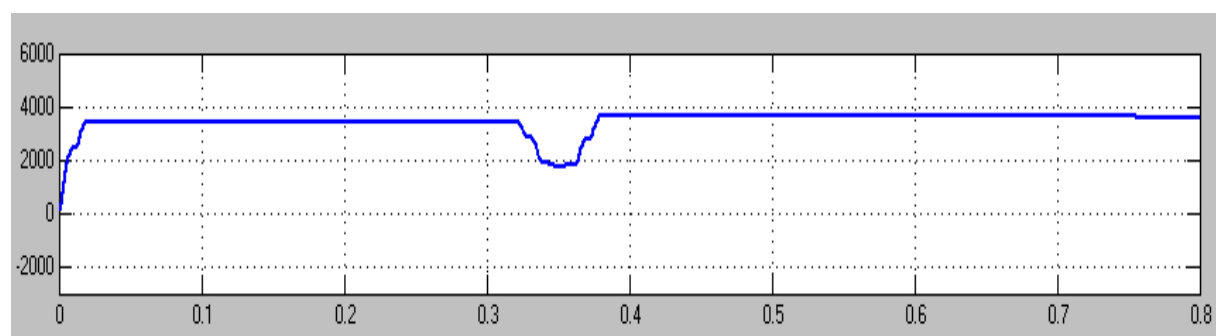


Fig-5: RMS output voltage

The Real power through load of transformer less UPFC is appeared in Fig 6 and the value of real power 2.3×10^5 Watts.

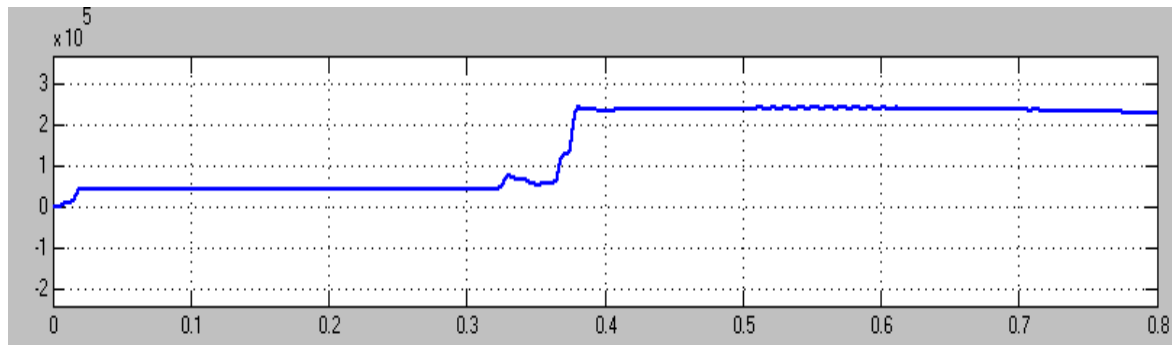


Fig-6: Real power through load

The Reactive power through load of transformer less UPFC is appeared in Fig 7 and the value of reactive power 14.5×10^4 Watts.

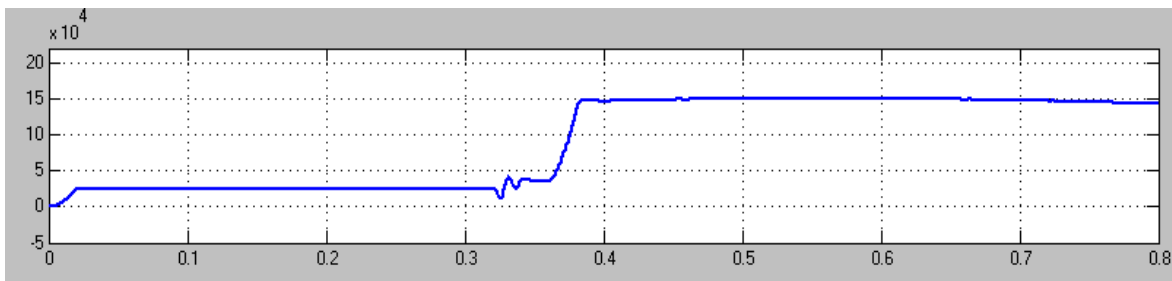


Fig-7: Reactive power through load

Closed loop Fuzzy Logic controller of transformer less UPFC is appeared in Fig 9. The receiving end --voltage is related with a reference--voltage. The flaw is pragmatic to the comparator across a FL-controller. The output of comparator updates the pulse width applied to 'UPFC'.

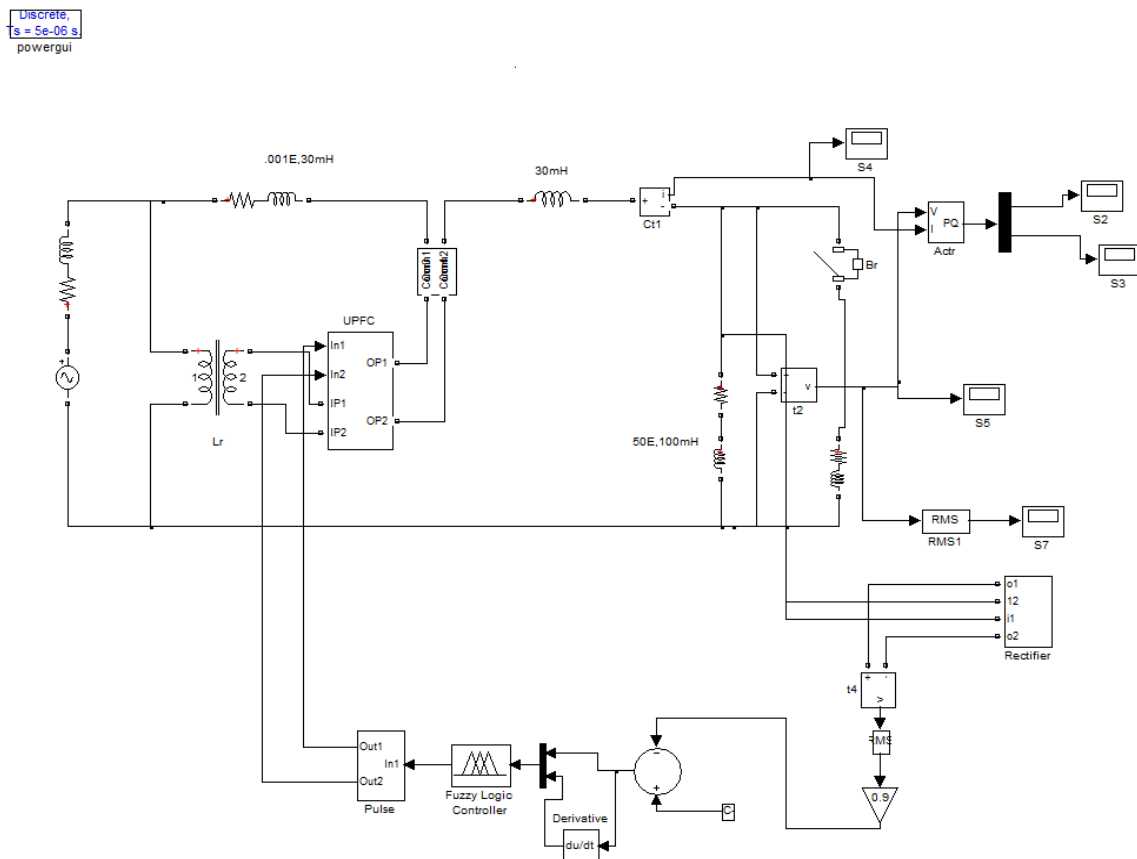


Fig-8: Closed loop FLC controller of transformer less UPFC

The output voltage across load of the transformer less UPFC is shown in Fig 9 and its value is 5000V.

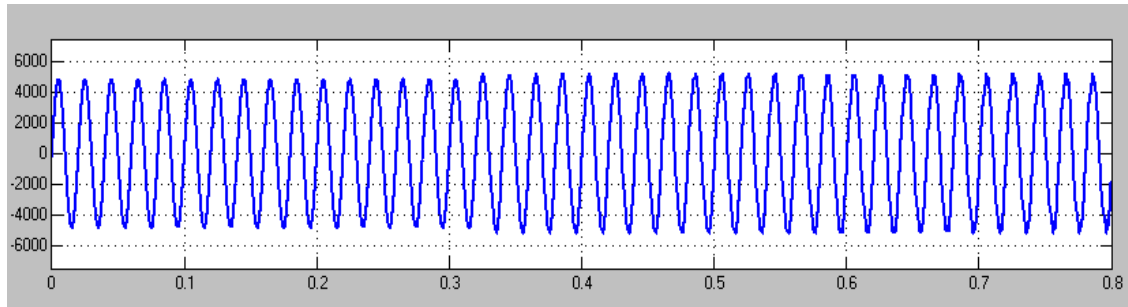


Fig-9: Output voltage across load

The Closed loop RMS output voltage of transformer less UPFC is shown in Fig 11 and it is approximately 3800V. The RMS output voltage decreases from $t = 1$ sec and then reaches normal value.

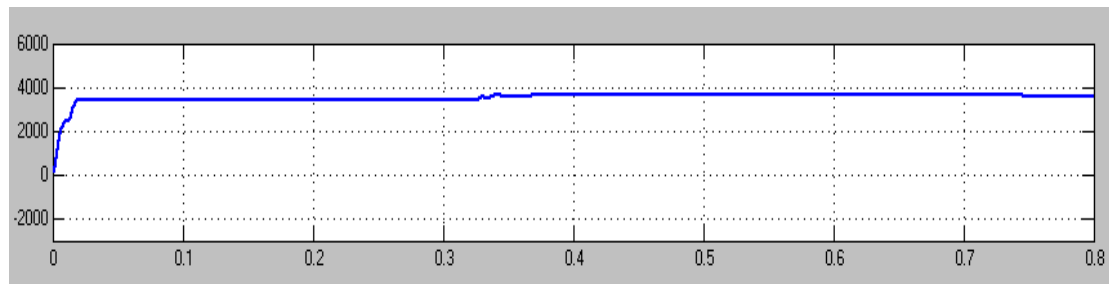


Fig-10: RMS output voltage

The Real power through load of transformer less UPFC is appeared in Fig 12 and the value of real power 2.356×10^5 Watts.

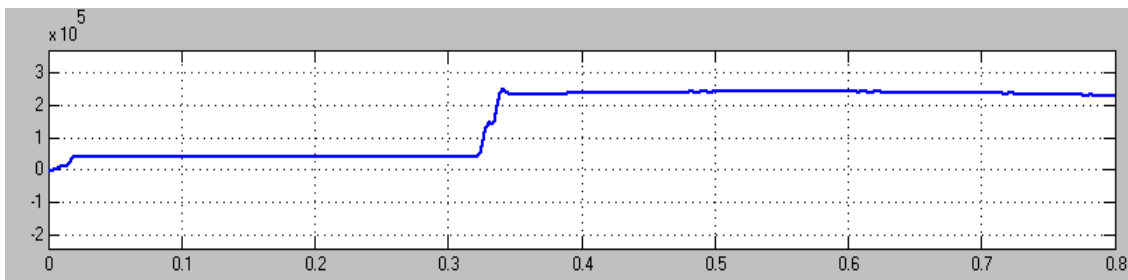


Fig-11: Real power through load

The Reactive power through load of transformer less UPFC is appeared in Fig 13 and the value of reactive power 14.59×10^4 Watts.

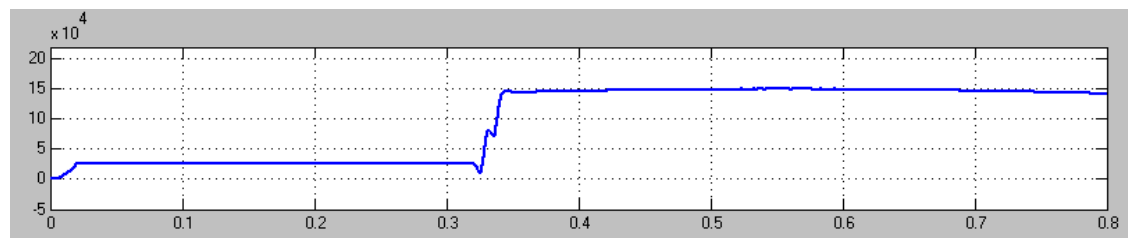


Fig-12: Reactive power through load

Here, the output power settling time is 0.06s and the steady state error is 1.6V

The comparison of time-domain-parameters is given in Table 1. The rise-time is reduced from 0.33 Secs to 0.03 Secs; the peak-time is reduced from 0.34 to 0 Secs; the Settling-time is reduced from 0.38 to 0.06 Secs and steady-state-error is reduced from 7.3 to 1.6 Volts by replacing P-I controller with FLC-controller. Dynamic-response is also improved by using FLC-controller.

Table-1: Comparison of Time domain parameters

Controllers	T_r	T_s	T_p	E_{ss}
PI	0.33	0.38	0.34	7.3
FLC	0.03	0.06	0	1.6

V. CONCLUSION

Closed loop PI controller of transformer less UPFC and Closed loop FLC controller of transformer less UPFC are modelled and simulated using Simulink. The results represent that steady state error is reduced from 7.3 V to 1.6 V by using FLC controller. Hence, closed loop FLC controller of transformer less UPFC is superior to closed loop PI controller of transformer less UPFC.

The present work deals with simulation of PI and FL controlled CLMLIUPFC systems. The simulation of Hysteretic controlled CLMLIUPFC system will be done in future.

REFERENCES

1. C.D. Schaulder et al., "Operation of unified power flow controller (UPFC) under practical constraints", IEEE Trans.Power Del., vol.13, no.2. pp. 630-639, Apr1998.
2. R.Mihalic et al., "Improvement of transient stability using unified power flow controller' IEEE Trans.Power Del., vol. 11, no. 1, pp. 485-492, Jan 1996.
3. J.Machowski et al., Power System Dynamics and Stability. New York: Wiley, 1998.
4. M. Noroozian et al., "Improving power system dynamics by series-connected FACTS devices," IEEE trans. Power Del., vol. 139, no.4, pp. 689-694, Oct. 1997.
5. Gyugyi, "Unified power-flow control concept for flexible AC transmission system," Proc. Inst. elect. Eng.C, vol. 139, no.4, pp. 323-331, Jul, 1992.
6. N.G. Hingorani and L. Gyugyi, Understanding FACTS. New York: IEEE Press, 2000.
7. E. Gholipour and S.Saadate, " A new method for improving transient stability of power systems by using UPFC," in Proc. European Power Electronics, Toulouse, France, Sep. 2003.
8. Z. Huang et al., "Application of UPFC in interconnected power systems- Modeling, interface, control strategy, and case study, " IEEE Trans. Power Syst., vol. 15, no. 2, pp. 817-824, May 2000.
9. K. Schoder, A. hasanovic, and A. feliachi, " Enhancing transient stability using fuzzy control scheme for the unified power flow controller (UPFC) within the power system toolbox (PST)," in proc. Midwest Symp. Circuits Systems, vol. 3, lansing, MI, Aug, 2000, pp. 1382-1385.
10. K.K. Sen and A.J.F. Keri, "Comparison of field results and digital simulation results of Avoltage-sourced converter-based FACTS controller," IEEE Trans. Power Del., vol. 18, no. 1, pp. 300-306, Jan. 2003.

BATTERY BALANCING SYSTEM FOR AN ELECTRIC VEHICLE USING SOLAR PANEL

R. Janbaga Lakshmi¹, S. Sivamani² and R. Anandaraj³PG Scholar¹, Assistant Professor² and Associate Professor³Department of Electrical and Electronics Engineering, E. G. S. Pillay Engineering College (Autonomous),
Nagapattinam, Tamilnadu

ABSTRACT

This paper proposes a battery balancing system of electric vehicle using solar panel. There are three operation modes of the system: Solar-Balancing, Storage-Balancing, and Charge-Balancing. The Solar Balancing mode charges the battery module, which has the lowest SOC using the solar power. This mode is operated during the vehicle is driving; the Charge-Balancing mode is operated when the vehicle is parked and it can be charged by the conventional charger. This system eliminates the energy loss that would or occur in conventional active and passive balancing schemes by equalizing the battery using solar/stored energy in the storage cell. In this paper, SEPIC converter is used instead of using DC-DC converter, it will acts as both buck converter and boost converter. Energy management system has the operation strategy Q Supplying the load with sufficient energy and power Q Optimized usage of photovoltaic energy Q Long battery life Q Minimized usage of auxiliary power generator.

Keywords: Electric vehicle, Battery Balancing, Energy Management System, Solar Panel.

I INTRODUCTION

Electric vehicle using solar charging stations are widely unrolled and it is relying on clean solar electricity. Single phase grid connection of 50 kW rapid charger station is actually made and announced in company which is located in Japan. Battery storage of bank is necessary for electric vehicle charger using solar. It is connected to low-voltage grid line to store the limited. Also it is slowly drawn the electricity (from PV and grid). After that In electric vehicle battery pack, this electricity will be ready to discharge fastly. And the charger is also needed. The battery management system (BMS) is a critical one. It is used as component in EV and EHV. The purpose of the BMS is used for safety purpose and reliable for battery operation. To maintain the both safety and reliability of the battery, state monitoring and evaluation, charge control, and cell balancing are functionalities are implemented in Battery management system. In an electrochemical product, a battery is differently acts as in both operational and environmental conditions. To implement these function a battery performance possess a challenge due to uncertainty. A battery's state evaluation, includes SOC, state of health, and state of life, is a critical task for a Battery management system. In recent methods, the state evaluation of battery has the possible solution for future challenges which are occurred in battery management system.

II RELATED AND EXISTING SYSTEM

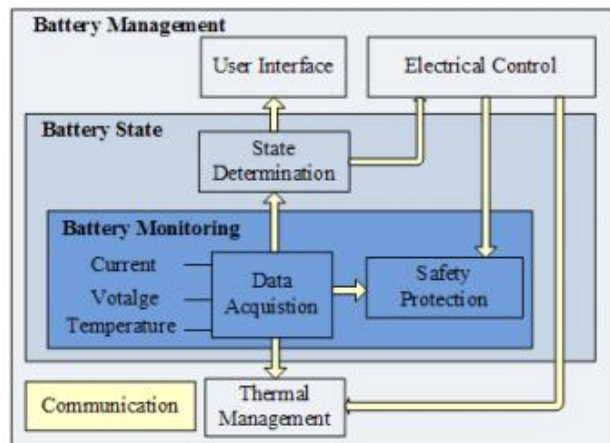
Battery management systems are found in mature range in a portable electronic devices. For example: laptop, computer, cellular phones, etc. It cannot be completely developed in electric vehicles and hybrid electric vehicles. In vehicle's battery number of cells are presented, which are hundred times greater than that of battery in portable electronics. To design a vehicle's battery, an important advantage is the main reason i.e., **long lasting of an energy system**. In both electric vehicle and hybrid electric vehicle are provided high voltage and current. When compared to portable electronics, BMS of electric vehicle are more complicated.

In BMS, there are three types of topologies are implemented in hardware structure which includes centralized, distributed and modular structures. Battery monitoring, battery state and battery management of layer structure are proposed by Meissner and Richter. In each case, the functions of BMS are similar. But Gold found out the different functions in battery management system. A generic BMS structure with basic functions are combined with these concepts, which are shown in below figure.1. At the monitoring layer, the data acquisition has various sensors. It can be installed in battery pack. In real time, data collection is used for the maintaining the system's safety. And also to determine the state of battery.

The mentioned BMUs has the following drawbacks

- 1) Limited data logging function.
- 2) Lack of state of health (SOH) and state of life (SOL) estimations.
- 3) Non-interchangeable among current BMSs

Figure 1. Illustration of a battery management system.



OPERATION

Mode 1: Solar-Balancing Mode

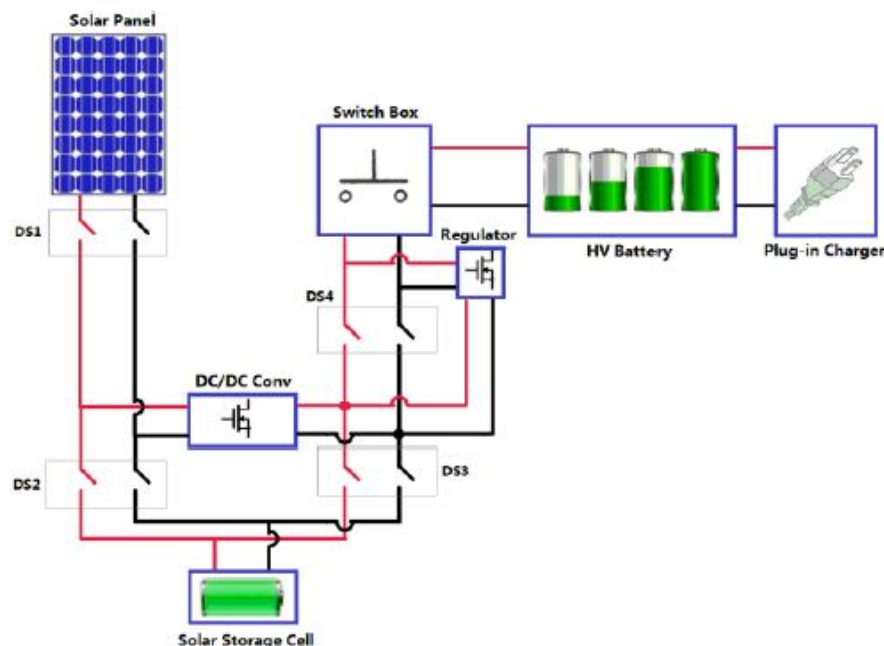
When the weather is sunny and the vehicle is under driving, DS1 and DS4 will be closed. Under this condition, the battery pack is discharged for energizing the vehicle power train. The battery module with the lowest SOC/voltage will be linked to the output of the DC/DC converter and charged by the solar panel. Once all the battery modules are balanced to the same SOC/voltage, the whole battery pack will be connected to the DC bus and charged.

Mode 2: Storage-Balancing Mode

When there is little or no solar power to harvest (such as during cloudy days or at night), DS1 and DS3 are opened and DS2 and DS4 are closed to run the Storage-Balancing mode. Under this mode, the energy saved in the storage cell will be transferred to the battery module at the lowest SOC/voltage through the DC/DC converter. Since the energy saved in the storage cell is limited, once the battery modules are balanced, the energy flow from the storage cell will be cut.

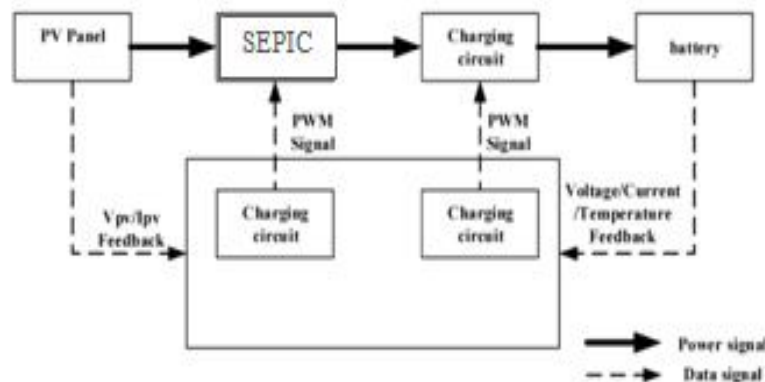
Mode 3: Charge-Balancing Mode

The two modes demonstrated above are used when the vehicle is driving and the battery pack is being discharged. When the vehicle is parked and charged, the Charge-Balancing mode will be selected by closing DS1 and DS3. Under this mode, the battery pack is being charged by a plug-in charger. The system monitors the battery module voltages and links the module with the highest voltage to the DC bus. The battery module will be discharged by the regulator.



III PROPOSED SYSTEM

This paper proposes a battery balancing system of electric vehicle using solar panel. There are three operation modes of the system: Solar-Balancing, Storage-Balancing, and Charge-Balancing. The Solar Balancing mode charges the battery module, which has the lowest SOC using the solar power. This mode is operated during the vehicle is driving; the Charge-Balancing mode is operated when the vehicle is parked and it can be charged by the conventional charger. This system eliminates the energy loss that would or occur in conventional active and passive balancing schemes by equalizing the battery using solar/stored energy in the storage cell. In this paper, SEPIC converter is used instead of using DC-DC converter, it will acts as both buck converter and boost converter.

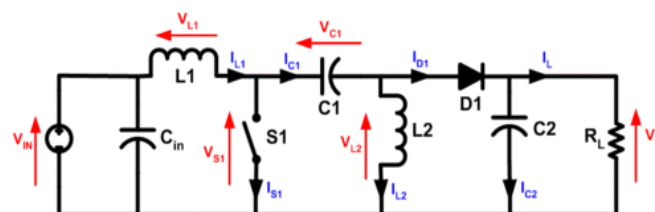


SEPIC CONVERTER

The single-ended primary-inductor converter (SEPIC) is a type of converter allowing the electrical potential (voltage) at its output to be greater than, less than, or equal to that at its input. The output of the SEPIC is controlled by the duty cycle of the control transistor.

A SEPIC is essentially a boost converter followed by a buck-boost converter, therefore it is similar to a traditional buck-boost converter, but has advantages of having non-inverted output (the output has the same voltage polarity as the input), using a series capacitor to couple energy from the input to the output (and thus can respond more gracefully to a short-circuit output), and being capable of true shutdown: when the switch is turned off, its output drops to 0 V, following a fairly hefty transient dump of charge.

SEPICs are useful in applications in which a battery voltage can be above and below that of the regulator's intended output. For example, a single lithium ion battery typically discharges from 4.2 volts to 3 volts; if other components require 3.3 volts, then the SEPIC would be effective.



OPERATION

The schematic diagram for a basic SEPIC is shown in Figure. As with other switched mode power supplies (specifically DC-to-DC converters), the SEPIC exchanges energy between the capacitors and inductors in order to convert from one voltage to another. The amount of energy exchanged is controlled by switch S1, which is typically a transistor such as a MOSFET. MOSFETs offer much higher input impedance and lower voltage drop than bipolar junction transistors (BJTs), and do not require biasing resistors as MOSFET switching is controlled by differences in voltage rather than a current, as with BJTs).

Continuous mode

A SEPIC is said to be in continuous-conduction mode ("continuous mode") if the current through the inductor L1 never falls to zero. During a SEPIC's steady-state operation, the average voltage across capacitor C1 (V_{C1}) is equal to the input voltage (V_{in}). Because capacitor C1 blocks direct current (DC), the average current through it (I_{C1}) is zero, making inductor L2 the only source of DC load current. Therefore, the average current through inductor L2 (I_{L2}) is the same as the average load current and hence independent of the input voltage.

Looking at average voltages, the following can be written

$$V_{IN} = V_{L1} + V_{C1} + V_{L2}$$

Because the average voltage of V_{C1} is equal to V_{IN} , $V_{L1} = -V_{L2}$. For this reason, the two inductors can be wound on the same core. Since the voltages are the same in magnitude, their effects of the mutual inductance will be zero, assuming the polarity of the windings is correct. Also, since the voltages are the same in magnitude, the ripple currents from the two inductors will be equal in magnitude.

The average currents can be summed as follows (average capacitor currents must be zero)

$$I_{D1} = I_{L1} - I_{L2}$$

When switch S1 is turned on, current I_{L1} increases and the current I_{L2} goes more negative. (Mathematically, it decreases due to arrow direction.) The energy to increase the current I_{L1} comes from the input source. Since S1 is a short while closed, and the instantaneous voltage V_{C1} is approximately V_{IN} , the voltage V_{L2} is approximately $-V_{IN}$. Therefore, the capacitor C1 supplies the energy to increase the magnitude of the current in I_{L2} and thus increase the energy stored in L2. The easiest way to visualize this is to consider the bias voltages of the circuit in a d.c. state, then close S1.

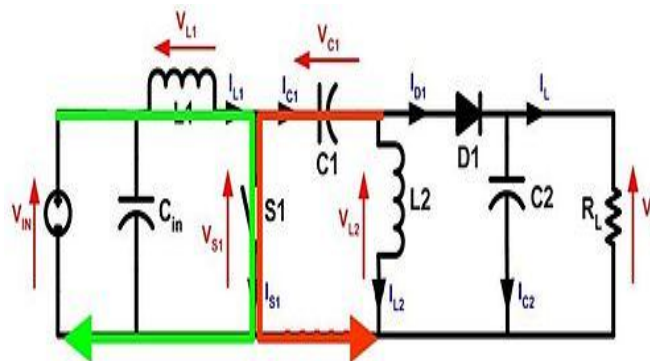


Figure-2: With S1 closed current increases through L1 (green) and C1 discharges increasing current in L2 (red).

When switch S1 is turned off, the current I_{C1} becomes the same as the current I_{L1} , since inductors do not allow instantaneous changes in current. The current I_{L2} will continue in the negative direction, in fact it never reverses direction. It can be seen from the diagram that a negative I_{L2} will add to the current I_{L1} to increase the current delivered to the load. Using Kirchhoff's Current Law, it can be shown that

$$I_{D1} = I_{C1} - I_{L2}.$$

It can then be concluded, that while S1 is off, power is delivered to the load from both L2 and L1. C1, however is being charged by L1 during this off cycle, and will in turn recharge L2 during the on cycle.

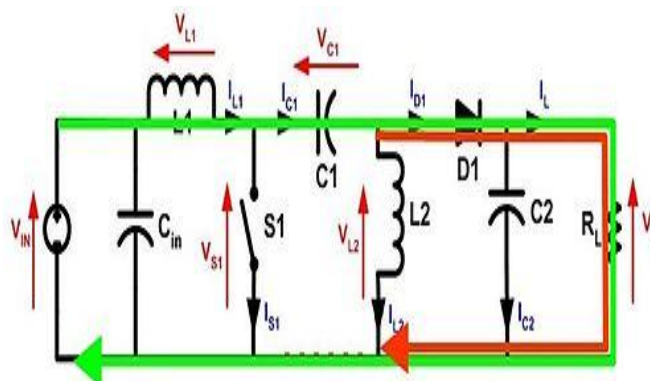


Figure-3: With S1 open current through L1 (green) and current through L2 (red) produce current through the load.

Because the potential (voltage) across capacitor C1 may reverse direction every cycle, a non-polarized capacitor should be used. However, a polarized tantalum or electrolytic capacitor may be used in some cases,^[1] because the potential (voltage) across capacitor C1 will not change unless the switch is closed long enough for a half cycle of resonance with inductor L2, and by this time the current in inductor L1 could be quite large.

The capacitor C_{IN} is required to reduce the effects of the parasitic inductance and internal resistance of the power supply. The boost/buck capabilities of the SEPIC are possible because of capacitor C1 and inductor L2.

Inductor L1 and switch S1 create a standard boost converter, which generates a voltage (V_{S1}) that is higher than V_{IN} , whose magnitude is determined by the duty cycle of the switch S1. Since the average voltage across C1 is V_{IN} , the output voltage (V_O) is $V_{S1} - V_{IN}$. If V_{S1} is less than double V_{IN} , then the output voltage will be less than the input voltage. If V_{S1} is greater than double V_{IN} , then the output voltage will be greater than the input voltage.

The evolution of switched-power supplies can be seen by coupling the two inductors in a SEPIC converter together, which begins to resemble a Fly back converter, the most basic of the transformer-isolated SMPS topologies.

Discontinuous mode

A SEPIC is said to be in discontinuous-conduction mode or discontinuous mode if the current through the inductor L1 is allowed to fall to zero.

IV SIMULATION RESULT

1. System Diagram

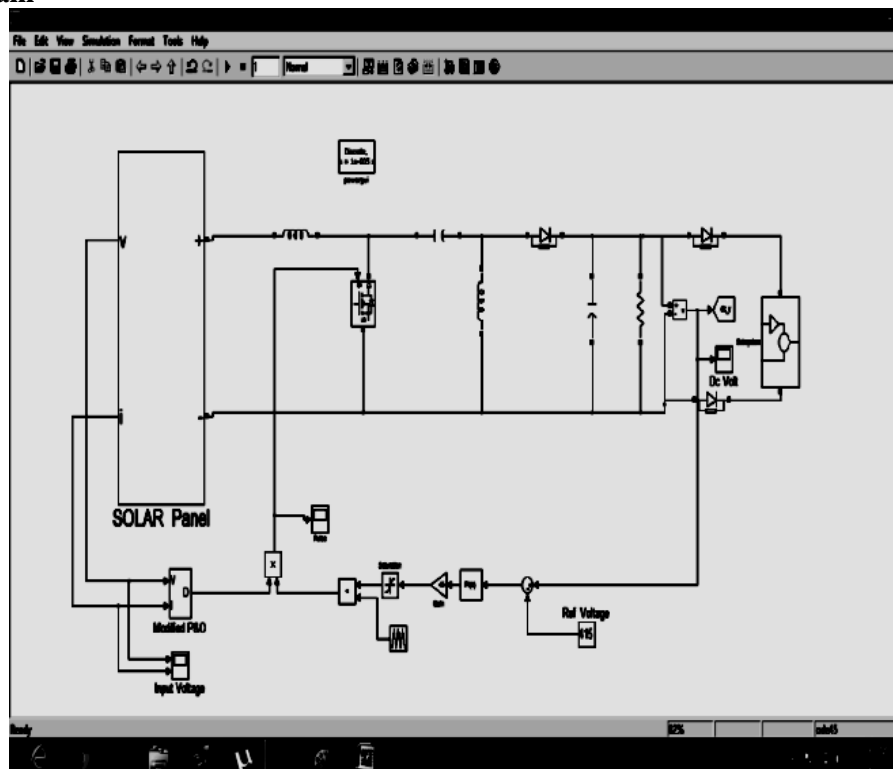


Fig-13: Simulation Diagram of Proposed System

2. Input and Output

i) Input Voltage and Current

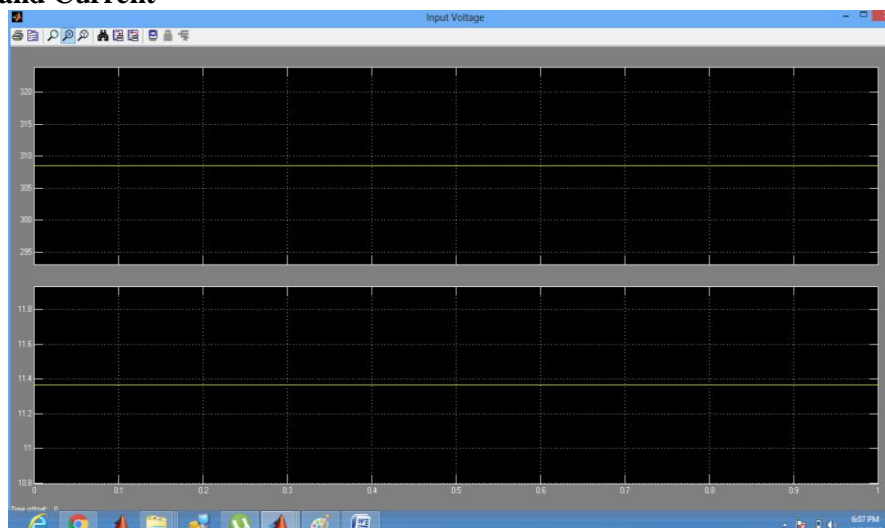


Fig-14: Input voltage and current

ii) Output Voltage

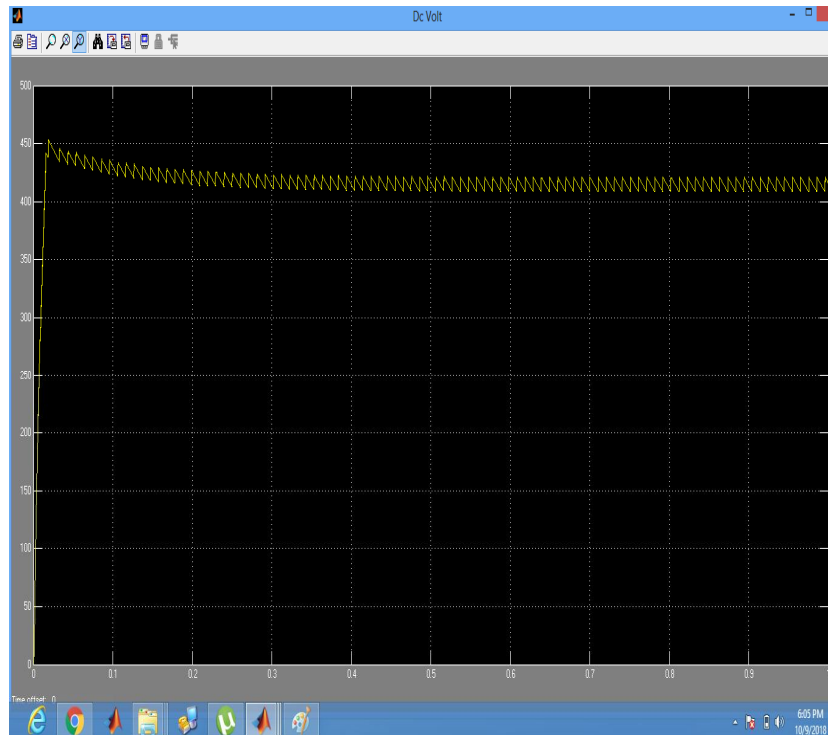


Fig-15: Output Voltage

Modes of operation

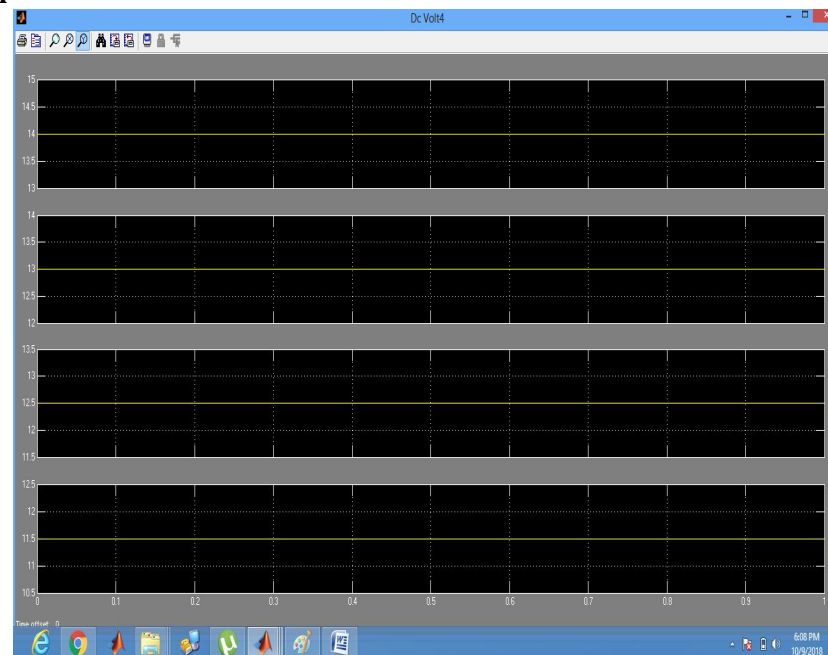


Fig-16: Modes of operation

V CONCLUSION

An intelligent power management system with innovative power-stage components is most likely to optimize the performance and lifespan of the vehicle's battery while performing the tasks to help validate the safety of the battery. Through and frequent monitoring of vital operating parameters, robust communications among all of the nodes on all of the control loops within the system, and fast decision making followed by effective control and protection mechanisms are essential in EV or HEV power systems. **It is used in the applications of automatic Control System, BMS used in many applications, such as**

- Solar vehicles,
- Street lighting, and
- Other PV systems.

VI REFERENCE

1. B.-Y. Choi, S.-R. Lee, J.-W. Kang and C.-Y. Won, "Battery balancing algorithm for parallel operation of single phase UPS Inverters", in IEEE Conference and Expo Transportation Electrification Asia-Pacific (ITEC Asia-Pacific), Aug 2014, pp. 1–6.
2. Du Shuang, Zuo Chuncheng, and Wang Lichen. "Algorithm research on maximum power point tracking of solar Electric Vehicle." In Mechatronic Sciences, Electric Engineering and Computer (MEC), Proceedings 2013 International Conference on, pp. 74-78. IEEE, 2013.
3. L. Liu, LY Wang, Z. Chen, C. Wang, F. Lin and H. Wang, "Integrated System Identification and State-of-Charge Estimation of Battery Systems," IEEE Transactions on Energy Conversion, vol. 28, no. 1, 2013.
4. M. Sitterly, L.Y. Wang, G. Yin and C. Wang, "Identification of Battery Models for Real-Time Enhanced Battery Management," IEEE Transactions on Sustainable Energy, vol. 2, no.3, pp. 300-308, July 2011.
5. Maurice Caspar, Torsten Eiler, and Soren Hohmann. "Comparison of active battery balancing systems." In Vehicle Power and Propulsion Conference (VPPC), 2014 IEEE, pp. 1-8. IEEE, 2014.
6. Michael B. Burnett, and Lawrence J. Borle. "A power system combining batteries and supercapacitors in a solar/hydrogen hybrid electric vehicle." In Vehicle Power and Propulsion, 2005 IEEE Conference, pp. 7-pp. IEEE, 2005.
7. Xiaosong Hu, Changfu Zou, Caiping Zhang, and Yang Li. "Technological developments in batteries: a survey of principal roles, types, and management needs." IEEE Power and Energy Magazine 15, no. 5 (2017): 20-31.
8. Wai Chung Lee, David Drury, and Phil Mellor. "Comparison of passive cell balancing and active cell balancing for automotive batteries." In Vehicle Power and Propulsion Conference (VPPC), 2011 IEEE, pp. 1-7. IEEE, 2011.

CONCURRENTLY POWER/DATA TRANSFER BY WIRELESS FOR ELECTRIC VEHICLE CHARGING USING IOT

V. Anitha¹, P. J. Suresh Babu² and R. Anandaraj³

PG Scholar¹, Assistant Professor² and Associate Professor³

Department of Electrical and Electronics Engineering, E. G. S. Pillay Engineering College (Autonomous), Nagapattinam, Tamilnadu

ABSTRACT

Wireless power transmission (WPT) is the scale of next implementation in power electronics. In traditional electric vehicles is the use of plug-in charging devices is the major drawbacks of battery charging. By avoiding the power loss and plug in charging method, another phenomenon is proposed. In this method transferring the electrical power from one place to another (primary to secondary) without the usage of wiring medium based on the grid. The aim of this paper is to propose battery (electric vehicle) charging by using WPT method in addition to transfer the power. This paper also transfers a data. The data includes the battery status, vehicle ID code, or emergency messages can be concurrently transferred between the grid and vehicle. In addition to using a new technology IoT is used to control the system and also proposed for sensing, actuating and transmitting the information to the control centre. This paper derives a state-space model of wireless power transfer (WPT) systems to be used for the purpose of state estimation and controller design considering the internet of things (IoT) communication networks. In this paper to complete the charging system an inductive power transfer (IPT) will be applied. IOT technology is used to monitor a data of the vehicle. The operating status of the secondary side (vehicle) can be monitor by the proposed control system (IoT). In electric vehicle, if any problem occurs in the battery side the vehicle can immediate stop. The IOT technology also used to monitor the contingency of the system.

Keywords: Electric Vehicle, Simultaneous power and data, Wireless Power Transfer, Internet of Things.

I INTRODUCTION

A wireless battery(Electric vehicle) charging method the inductive power transfer (IPT) method is used for transferring the power is transfer by the method of inductive power transfer (IPT), the data is additionally transfer. The power and data is transfer at same time. The data is feedback to the load to source. In electric vehicle data (battery status, vehicle ID code, or emergency messages) can be transferred between the grid and vehicle simultaneously. In this paper, power and data is transferred concurrently. So two way communication is possible by this method. In this paper to complete the charging system an inductive power transfer (IPT) will be applied. The data can be monitor by using the new technology is IOT. It also detects the fault of the vehicle. If any contingency occur in the system the vehicle will stop immediately.

Inductive WPT systems have two main components; a Ground Assembly (GA) unit and a Vehicle Assembly (VA) unit. The GA contains a grid-connected Power Factor Correction (PFC) converter, followed by a DC-AC inverter, a filter and impedance matching network (IMN) connected to the GA coil. The VA consists of the VA coil connected to an IMN and filter, a rectifier and an optional impedance converter that produces suitable voltages and currents to the connected battery. During charging, the magnetic energy created by the GA Coil is coupled to the VA Coil.

In this work, a wireless vehicle charger with the capacity of simultaneous data/power transmission is studied. The grid (primary) side is operated on the utility power source of single-phase 110V. The vehicle (secondary) side is to accept the power transferred from the primary side. In addition to receiving power, the secondary side will simultaneously transfer digitalized date back to the primary side via the same conduction coils.

In the recent past, city planners have been busy resolving the best trade-off among mobility, green zones and residential and commercial expansion. To address these conflict-of-interest problems, technological breakthroughs will be fundamental for future smart city planning. At a careful but steady pace, modern cities are embracing the information and communication developments. Products and services, from technological innovations, will become ubiquitous in future smart cities. From rural to urban, industrial to residential and the overlap, Wireless Power Transmission (WPT), the Internet of things (IoT) and Information and Communication Technologies (ICT) will become a cornerstone in the design of new and growth of human settlement.

II EXSITING METHOD

The proposed simultaneous wireless power and data transfer system using parallel-parallel (P-P) reactive power compensation. The parallel-compensated primary unit is used to generate a large primary current. The parallel-

compensated secondary unit looks like a current source that characteristics of the parallel secondary unit is suitable for battery charging.

To depict the idea, consider the simplified schematic diagram of the proposed system illustrated in Fig.

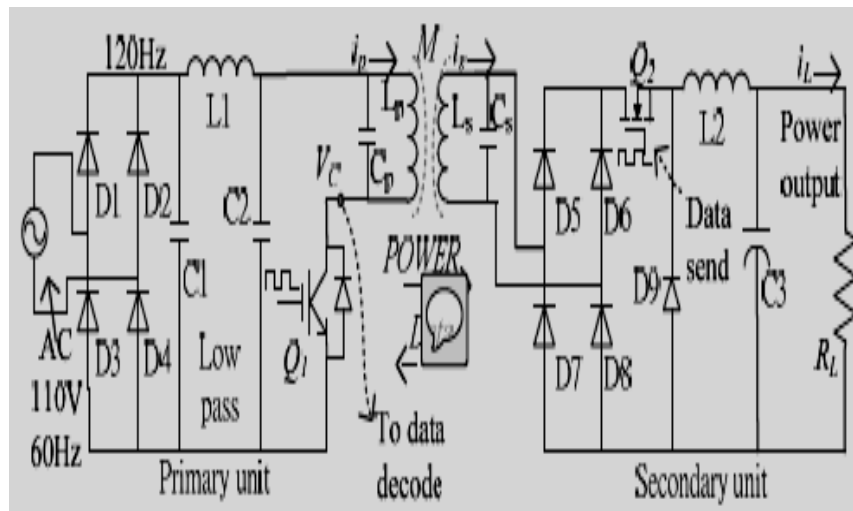


Fig-1: Circuit Diagram of Existing System

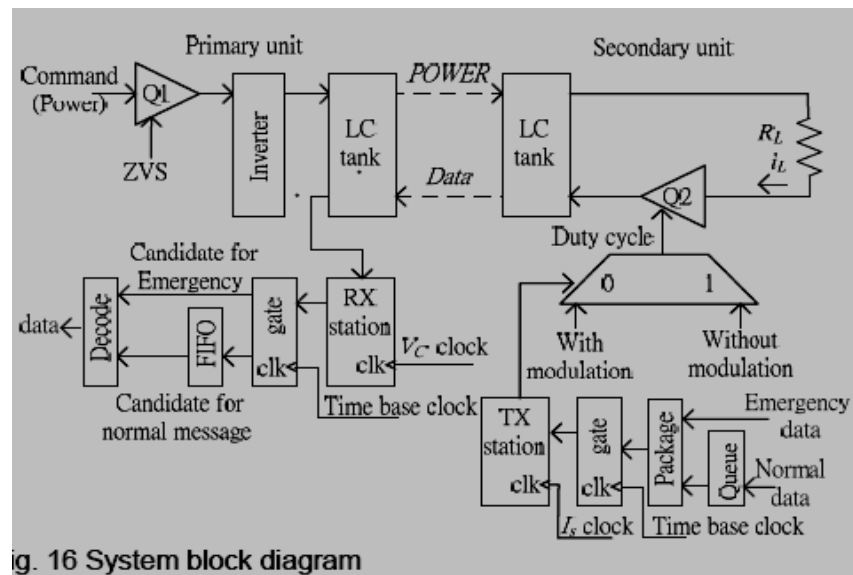


Fig-2: Block Diagram of Existing System

Referring to the system structure illustrated in Fig, the secondary unit sends data along the following steps

1. Arrange the normal messages into a queue to prevent data congestion. The emergency message possesses the highest priority. I will not be placed in the queue.
2. Pack data according to the protocol listed.
3. If data exists, it is then sent to the TX station according to the clock (related to $s I$), one bit per clock.
4. If data is normal message or emergency message, then send a data bit (for the normal message) or whole data set (for the emergency message including data, checksum and stop segments). The data bit synchronizes to the clock related to I_s .

III PROPOSED SYSTEM

This project elucidates the transfer of electrical energy from one place to another, wirelessly avoiding quotidian methods of power transfer. The phenomenon is used to transfer the power, without the use of wired medium. In this proposed system also transfer a data. The data which is related to battery status, vehicle ID code, or emergency messages can be simultaneously transferred between the grid and vehicle.

Wired technology was initially a success, but transfer of power was achieved only by cables, which ended up as a costly affair. Lately, Wireless Power Technology is emerging as a practical solution for providing energy for devices at remote distances.

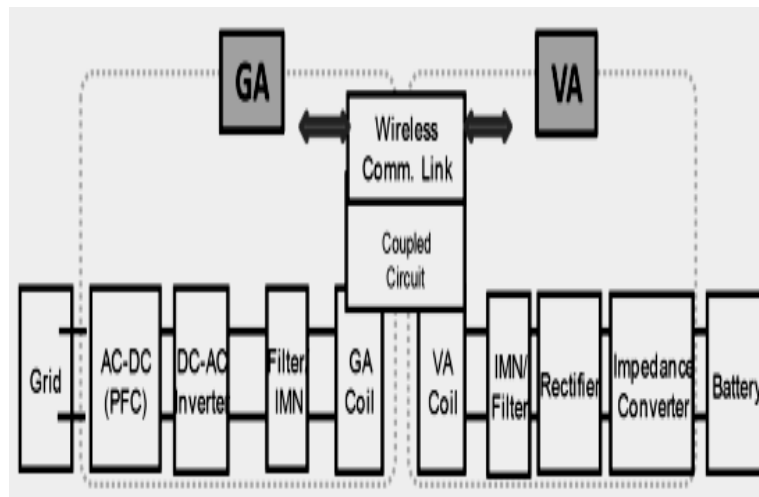


Fig-3: Functional Block Diagram of Existing System

1. Block Diagram Description

Inductive WPT systems have two main components; a Ground Assembly (GA) unit and a Vehicle Assembly (VA) unit. The GA contains a grid-connected Power Factor Correction (PFC) converter, followed by a DC-AC inverter, a filter and impedance matching network (IMN) connected to the GA coil.

The VA consists of the VA coil connected to an IMN and filter, a rectifier and an optional impedance converter that produces suitable voltages and currents to the connected battery. During charging, the magnetic energy created by the GA Coil is coupled to the VA Coil, This project is used to transmit the power using wireless and to turn ON LED's or to charge the battery after receiving power wirelessly.

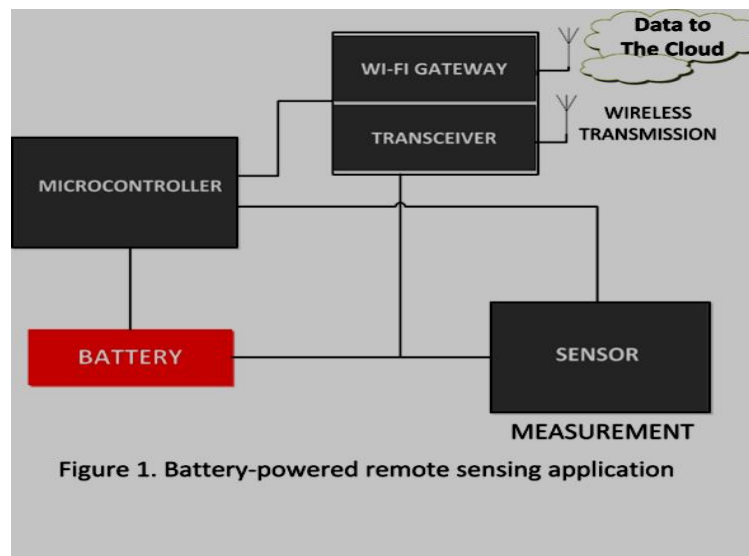


Figure 1. Battery- powered Remote Sensing Application

Fig-4: Battery- powered Remote Sensing Application

In Transmitter Side

A transformer is a device that transfers electrical energy from one circuit to another through inductively coupled conductors—the transformer's coils.

A varying current in the first or primary winding creates a varying magnetic flux in the transformer's core, and thus a varying magnetic field through the secondary winding. This varying magnetic field induces a varying electromotive force (EMF) or "voltage" in the secondary winding. This effect is called mutual induction.

The voltage we getting is AC in form and it is given to rectifier circuit to convert AC voltage to DC voltage and it is given to the MOSFET Switching Circuit (It is a device used for amplifying or switching electronic signals). Initially clock pulse is given by Crystal oscillator and given to the MOSFET driver circuit and it is driven. The DC voltage is transmitted wirelessly through Transmitter Coil.

In Receiver Side

In the Receiver Side, the DC voltage is received through Receiver Coil and it is used to turn On LED's or to charge the battery.

2. BLOCK DIAGRAM

The WPT system consists mainly of two parts; the transmitter and the receiver part. At the transmitter part there is

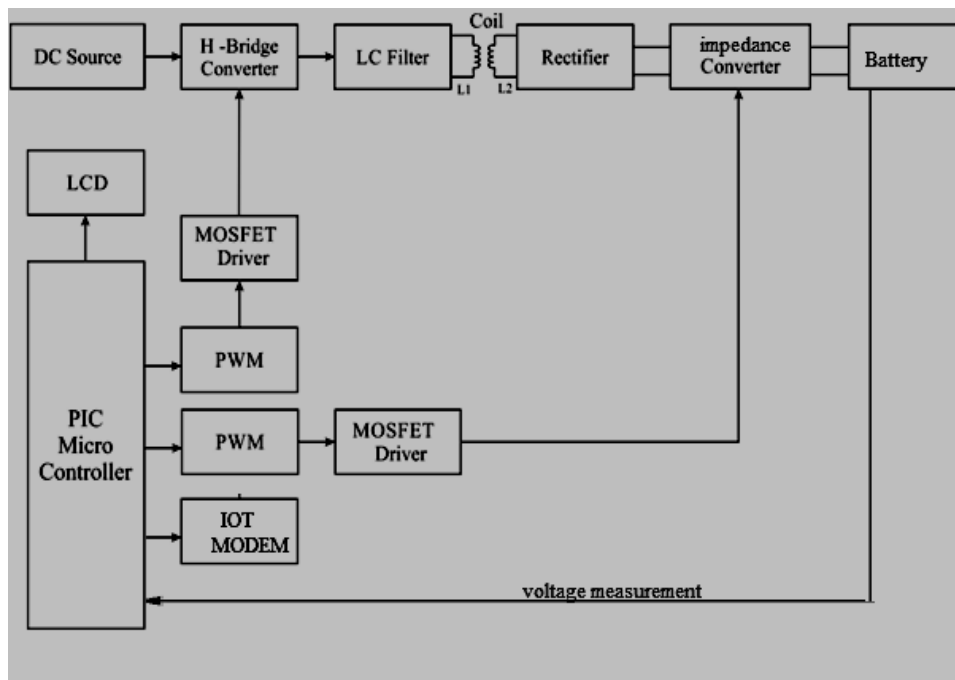


Fig-5: Block Diagram of Proposed System

a DC supply to supply power to the system. Then this DC will be converted to AC of high frequency through an inverter. Single-phase full bridge inverter is employed for this application. The AC voltage resulting from the inverter will be transferred through a coil from the transmitter side to the receiver side. This is achieved through a series resonant circuit in the transmitter and the receiver ends. After transferring the power to the secondary side of the system, it is used to charge the battery of the electric vehicle. Therefore a rectifier is needed to convert the AC to DC voltage. Data also is transferred wirelessly with the power in order to control the charging process for the electric vehicles with different proposed scenarios.

3. CIRCUIT DIAGRAM

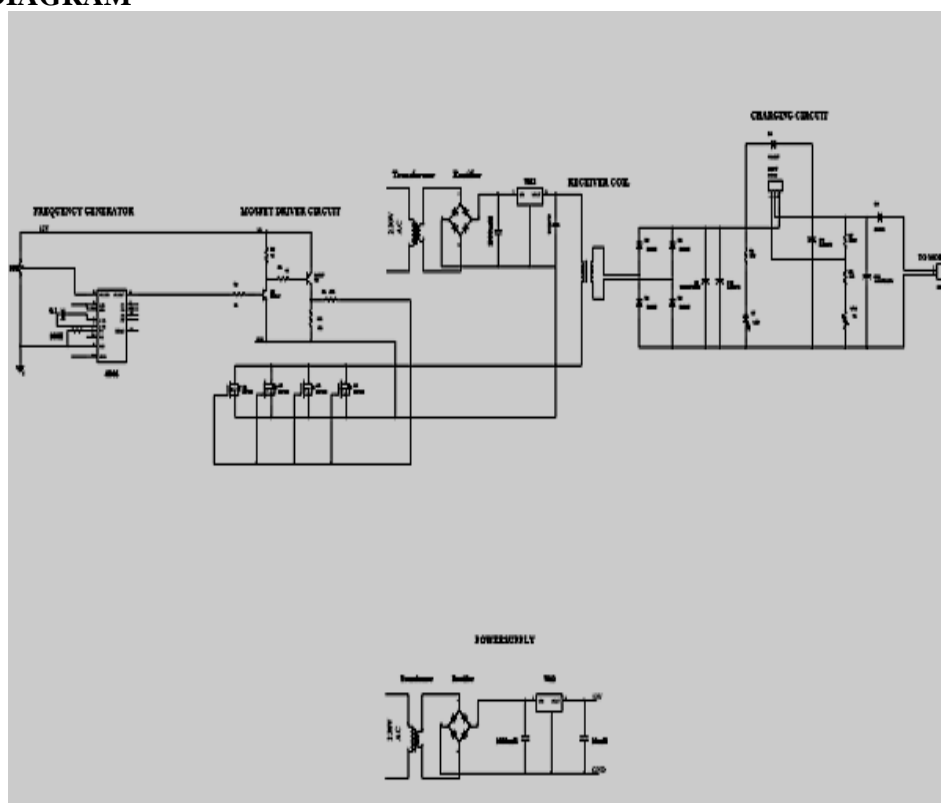


Fig-6: Circuit Diagram of Proposed System

Schematic Diagram

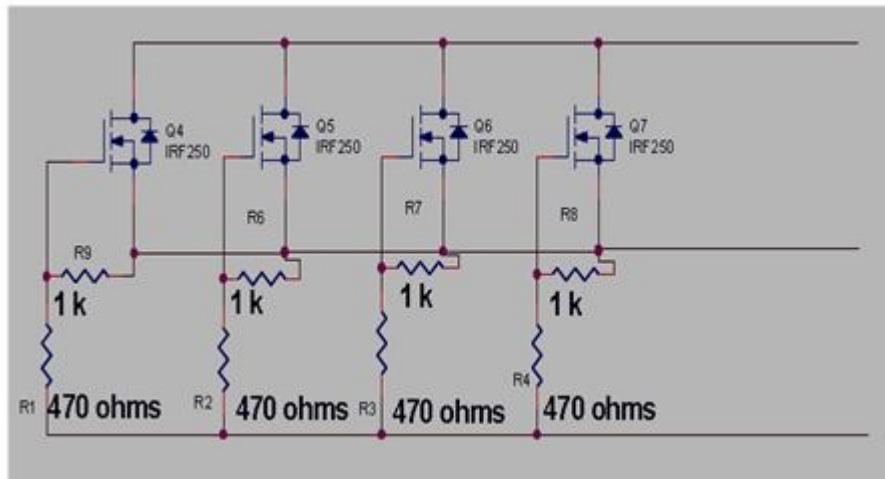


Fig-7: Schematic Diagram of MOSFETs

4) CIRCUIT DESCRIPTION

This circuit is designed to control the MOSFET depending upon the signals from PIC. In our circuit there is two transistor connected back to back. We use npn transistor as a Q1 and pnp transistor as a Q2 transistor. When high pulse signal is given to base of the Q1 transistors, the transistor is conducting and shorts the collector and emitter terminal and zero signals is given to base of the Q2 transistor. So Q2 is turned ON so MOSFET'S gate get high pulse and it will be turned ON. When low pulse is given to base of transistor Q1 transistor, the transistor is turned OFF. Now 12v is given to base of Q2 transistor so the Q2 is turned OFF. Now MOSFET'S gate get low pulse now it goes to off state.

Voltage Signal from	Transistor Q1	Transistor Q2	MOSFET	PIC Microcontroller
1	ON	ON	ON	
0	OFF	OFF	OFF	

Table-1

IV MATLAB RESULT

1. Simulink Diagram

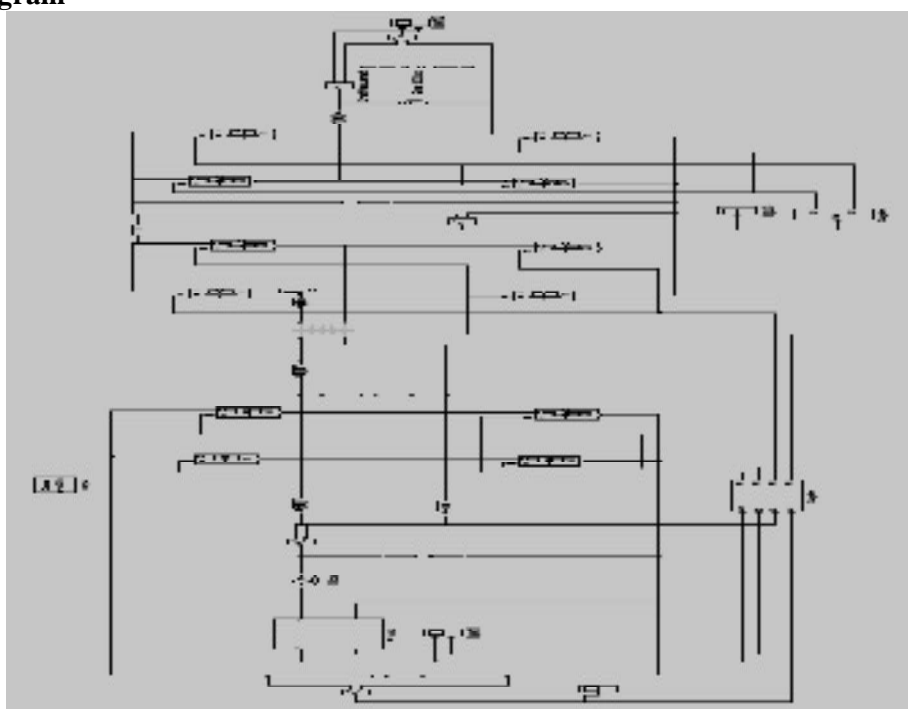


Fig-11: Simulation Diagram of Proposed system

2. INPUT

i) Input Voltage

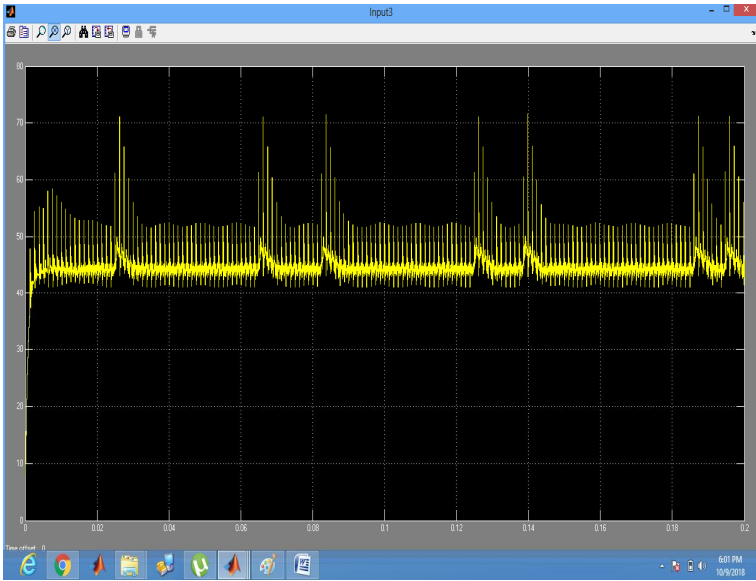


Fig-12: Input Voltage

ii) Input voltage and current from source

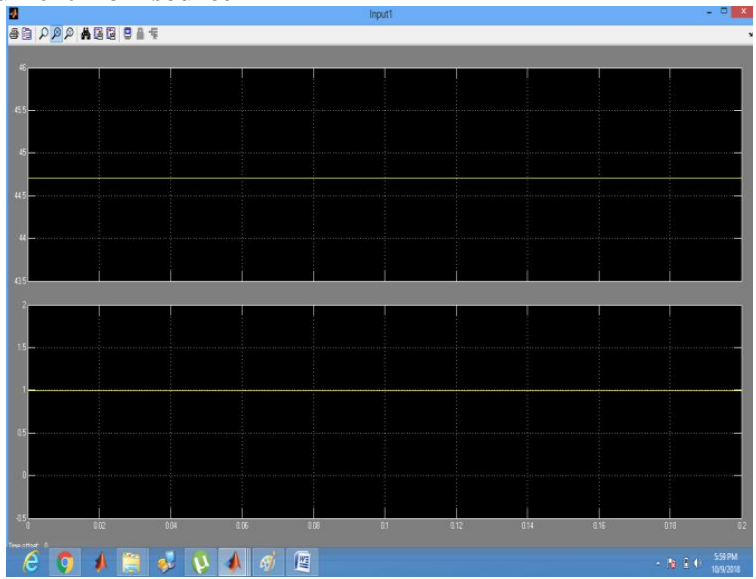


Fig-13: Input Voltage and current from source

3. OUTPUT

Wireless transferred voltage

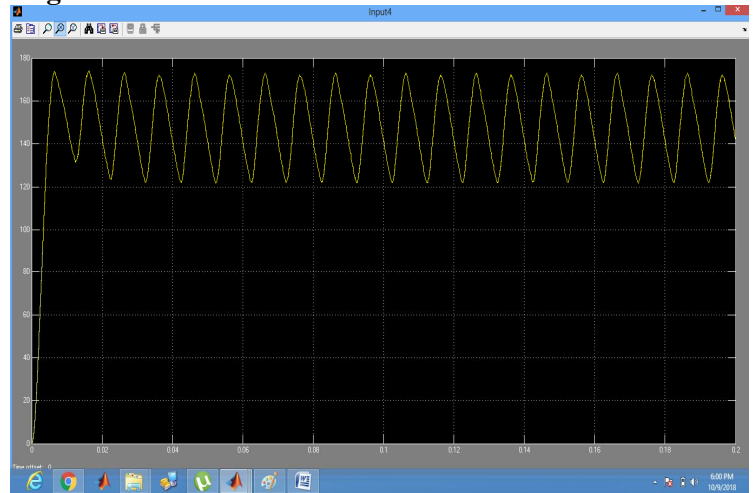


Fig-14: Wireless transferred voltage

V CONCLUSION

Overview of this project, implementing a new technologies and schemes to enable WET for IoT systems. With an emphasis on improving the efficiency of the WETT unit and reducing the energy consumption of the devices, the lifetime of WET-assisted battery-operated systems in an IoT architecture are analyzed for two different scenarios. A wireless battery charging method in addition to transfer power. This paper also transfers a data. The data which is related to battery status, vehicle ID code, or emergency messages can be simultaneously transferred between the grid and vehicle. In addition to using IOT technology is used to control the system and also proposed for sensing, actuating and transmitting the information to the control centre. A study of the specific energy requirements of IoT devices reveals that achieving self-sustainability requires improved design techniques both at circuit and system level.

VI REFERENCE

1. C. S. Wang, O. H. Stielau, and G. A. Covic, "Design considerations for a contactless electric vehicle battery charger," *IEEE Trans. Ind. Electron.*, vol. 52, no. 5, pp. 1308–1314, Oct. 2005.
2. H. H. Wu, A. Gilchrist, K. Sealy, P. Israelsen, and J. Muhs, "A review on inductive charging for electric vehicles," in *Proc. IEEE Int. Electric Machines & Drives Conf.*, 2011, pp. 143–147.
3. H. Wang, W. Sun, and P. X. Liu, "Adaptive intelligent control of non affine nonlinear time-delay systems with dynamic uncertainties," *IEEE Transactions on Systems, Man, and Cybernetics: Systems*, vol. 47, pp. 1474–1485, 2017.
4. K. Song, C. Zhu, K.-E. Koh, D. Kobayashi, T. Imura, and Y. Hori, "Modeling and design of dynamic wireless power transfer system for EV applications," in *Proc. of the Annual Conference of the Industrial Electronics Society*, 2015, pp. 005 229–005 234.
5. U. K. Madawala, and D. J. Thrimawithana, "A bidirectional inductive power interface for electric vehicles in V2G systems," *IEEE Trans. Ind. Electron.*, vol. 58, no. 10, pp. 4789–4796, Oct. 2011.
6. X. Qu, H. Han, S. C. Wong, C. K. Tse, and W. Chen, "Hybrid IPT topologies with constant current or constant voltage output for battery charging applications," *IEEE Trans. Power Electron.*, vol. 30, no. 11, pp. 6329–6337, Nov. 2015.
7. Y. Sun, P. X. Yan, Z. H. Wang, and Y. Y. Luan, "The parallel transmission of power and data with the shared channel for an inductive power transfer system", *IEEE Trans. Power Electron.*, vol. 31, no. 8, pp. 5495–5502, Aug. 2016.
8. Z. Feng, W. X. Zheng, and L. Wu, "Reachable set estimation of fuzzy systems with time-varying delay," *IEEE Transactions on Fuzzy Systems*, to appear in 2017.

DESIGN OF MULTIPHASE INTERLEAVED BOOST CONVERTER

M. Pavithra¹ and R. Anandaraj²

PG Scholar¹ and Associate Professor²

Department of Electrical and Electronics Engineering, E. G. S. Pillay Engineering College (Autonomous),
Nagapattinam, Tamilnadu

ABSTRACT

This work involves the design of Multiphase Interleaved Boost Converter (ILBC) for renewable energy based applications. The proposed converter will produce a voltage with higher gain and reduced ripples in the current which is necessary for battery charging. Using this technique, EMI can also be reduced along with lower switching Stress due to the presence of interleaving technique. The circuit will be realized through simulation using MATLAB.

Keywords: Multiphase Interleaved Boost Converter, MPPT, PV system.

I INTRODUCTION

Solar energy is converted to electricity using an electronic device called solar panel using photovoltaic effect. PV applications can be grouped into utility interactive and stand-alone application. For stand-alone systems without the utility connection uses the electricity where it is produced. The battery storage allows a stand-alone PV system to be run when the solar panels are not producing enough energy on their own with the battery storage size tied to the electrical usage. Efficiency of a PV cell is very small. So to make it efficient, some methods are to be adopted. These methods mainly equalize the load & source impedance. One such mechanism is the Maximum Power Point Tracking (MPPT). It is a technique using which we can get the maximum possible power point from the changing nonlinear source. A basic boost converter converts a DC voltage to a higher DC voltage. In the field of power electronics, application of interleaving technique can be traced back to very early days, especially in high power applications. Interleaving which adds additional benefits such as reduced ripple currents in both the input and output circuits. Higher efficiency is realized by splitting the output current into two paths, substantially reducing I^2R losses and inductor AC losses. Interleaving, also called multi-phasing, is a technique that is useful for reducing the size of filter components. When these boost converters are operated for high ratios leading to some difficulties like higher voltage and current stress on the MOSFET & higher voltage. Hence as a solution for this, an interleaving technique for boost converter have been adopted. This approach can be used for higher power applications to produce high voltage gain compared to the simple boost converter. Output of the PV module is acting as input to these converters.

In this paper has some advantage features by using interleaved technique is analysed by Multiple phases of Boost converter. The main motivation of this paper is to reduce the current ripples to create the battery charging as good performance and increase the lifetime of battery mainly for standalone PV system. The MPPT indicated the maximum power from PV module and supply to load via ILBC which boost up the voltage in high ratio. The main purpose of the paper is to examine the various operating modes of converter with lower current ripple to the inductor currents. Simulation results are obtained by using the MATAB/SIMULINK to shows the output voltage is well tracked and it improves the efficiency and reduces the current ripple.

II EXISTING SYSTEM

Existing System Boost Converter has a several problem. The high step-up voltage gain dc-dc converters are widely used as an interface between the available low voltage sources and the output loads which are operated at much higher voltage. Generally, the classical boost is a popular choice for non-isolated applications because of a simple structure and a continuous input current. However, it will be operated at extreme duty cycle, and the rectifier diode must sustain a short pulse current with high amplitude when an extreme high-voltage gain is required.

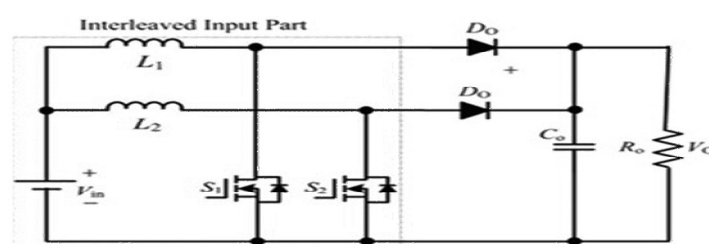


Fig-2.1: Conventional interleaved boost converter

The conventional interleaved boost converter shown in the above fig 1.1. This leads to severe reverse recovery and the electromagnetic interference (EMI) problems. Moreover, the boost switch has to block a high-output voltage and hence the ON-state resistance, $R_{DS(ON)}$, which varies almost proportionally with the square of blocking voltage, will be very high so that low-voltage-rated MOSFETs may not be adopted. For those reasons, it is hard for a basic boost converter to achieve both high voltage conversion ratio and high efficiency at the same time.

A conventional interleaved boost converter has severe voltage stress on switches are high. The active switches will suffer from high current stress during the switches in ON period for high step up applications. Large duty cycle is required for the large voltages, in practical step up the voltage leads to large volume of capacitance required. To maintain the small output ripple voltage large capacitance is required. Finally, it is concluded that the conventional boost converter requires large output capacitor to reduce current ripple and it is not suitable for high power applications.

III PROPOSED SYSTEM

In this paper proposes the multiphase interleaved boost converter for renewable energy system to increase the voltages in higher magnitude. The block diagram of proposed system is as shown in fig.3.1. A photovoltaic energy system is mainly powered by PV cells. In this figure a PV panel is used as the input to the multiphase interleaved boost converter and the output of MILBC has fed in to the input to battery. In order to increase the efficiency of the solar panel the MPPT is used. The MPPT is connected between the PV panels and to get boost up the maximum power. These powers are given to the MILBC to boost up the voltage at higher ratio. The output of battery voltages are fed in to DC load. Otherwise, by using inverter to convert DC to AC voltages for AC load.

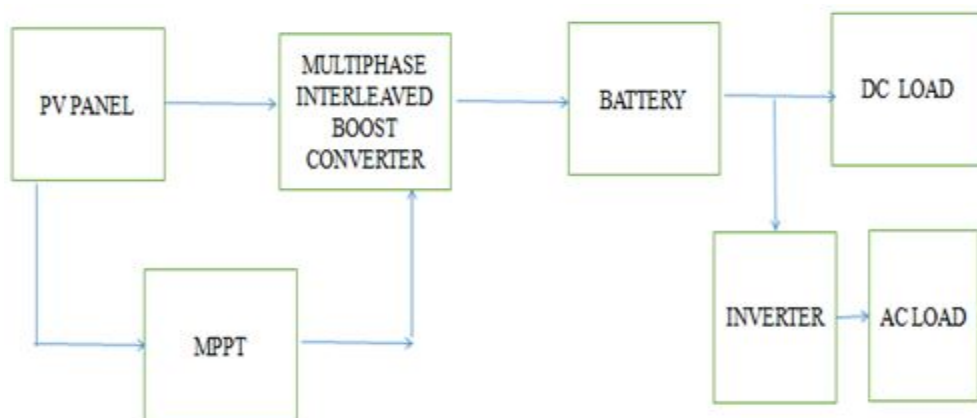


Fig-3.1: Block Diagram of Proposed System

The interleaved boost converters consists of several identical boost converters connected in parallel and controlled by the interleaved method which has the same switching frequency and phase shift. The circuit diagram for multi phase interleaved boost converter is shown in fig.3.2.

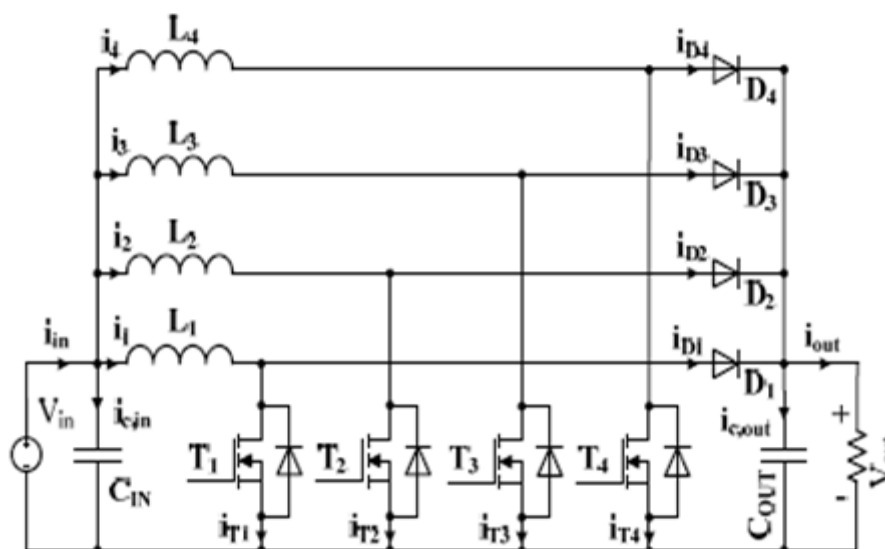


Fig-3.2: Multi-phase interleaved boost converter

It is simply four boost converters connected in parallel with each phase operating 90° out of phase. It consists of four inductors $L1, L2, L3, L4$, switches $T1, T2, T3, T4$ and diodes $D1, D2, D3, D4$ which are operating in parallel. The load used here is a resistive load. At any time, at least one of the phases is supplying to the load in addition to the output capacitor. The input current is the sum of four inductor currents $IL1, IL2, IL3$ and $IL4$ and $I_{1pp}, I_{2pp}, I_{3pp}$, and I_{4pp} are the peak to peak amplitudes. Since the inductor ripple currents are out of phase, they tend to cancel and thus reduce the input ripple caused by the interleaved boost inductors.

The drawbacks of conventional interleaved boost converter are listed below

- Interleaved boost converter leads to severe reverse recovery and the electromagnetic interference (EMI) problems.
- The converters are operated in hard switching results in large switching losses.
- High ripples in current.
- The active switches are suffering high current stress during the switch-on period for high step up applications.
- To maintain the small output ripple voltage large capacitance is required.

In proposed converter by using multiple phasing interleaving techniques has to overcome the above problem that means reduced the current ripple and increased output voltage.

IV SIMULATION RESULTS

Conventional Simulink Model

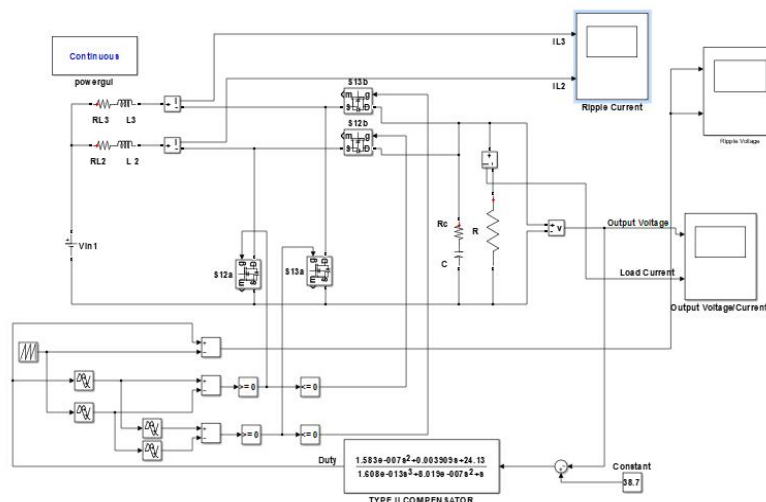


Fig-4.1: Two Phase SIMULINK Model

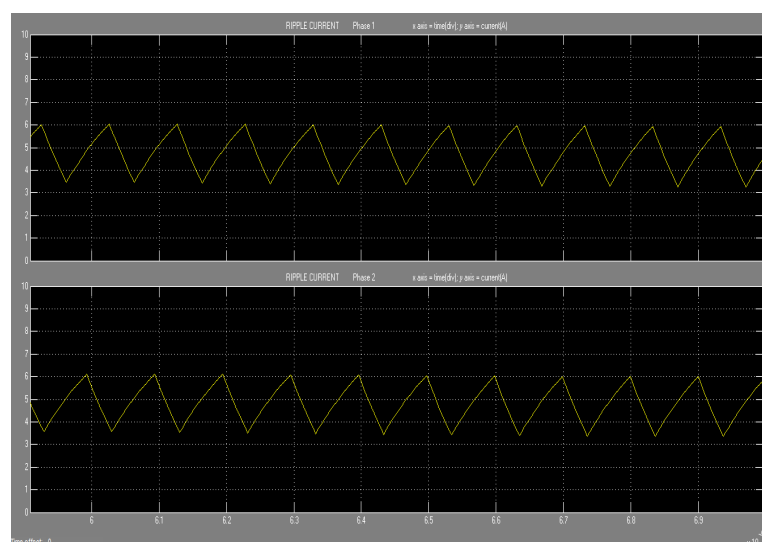


Fig-4.2: Two phase current ripple

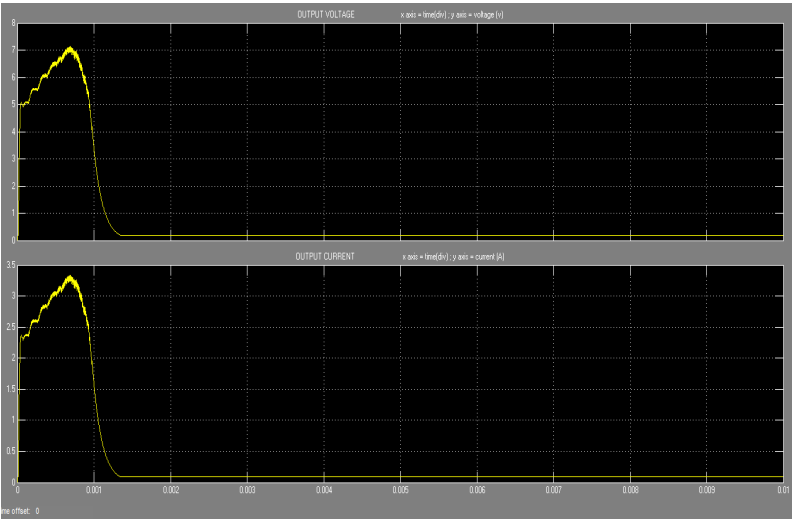


Fig-4.3: Two phase Output voltage and current

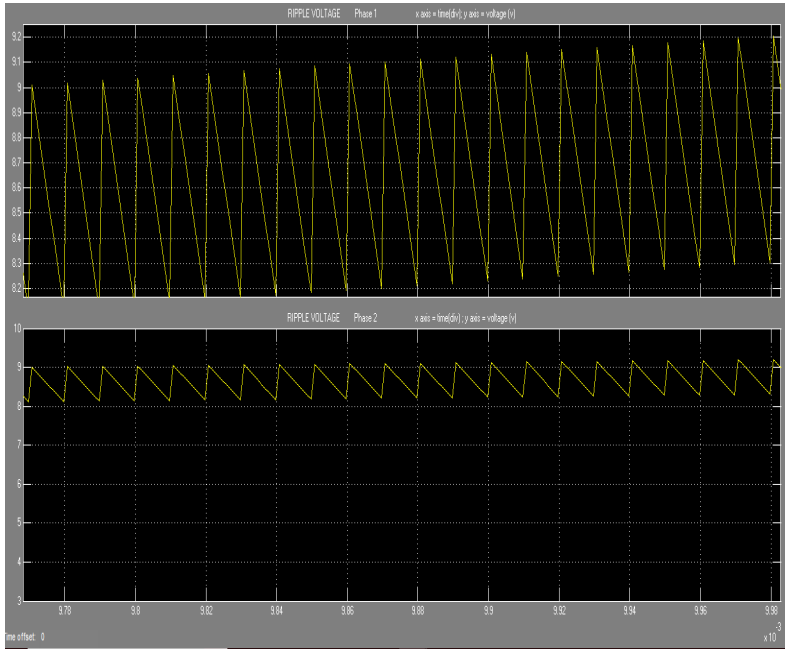


Fig-4.4: Two Phase Ripple Voltage

PROPOSED SIMULINK MODEL

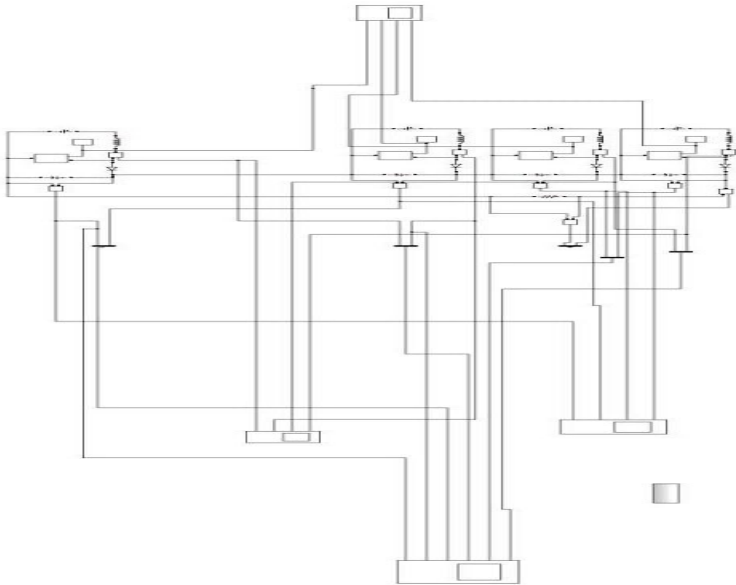


Fig-4.5: Matlab Simulink Model

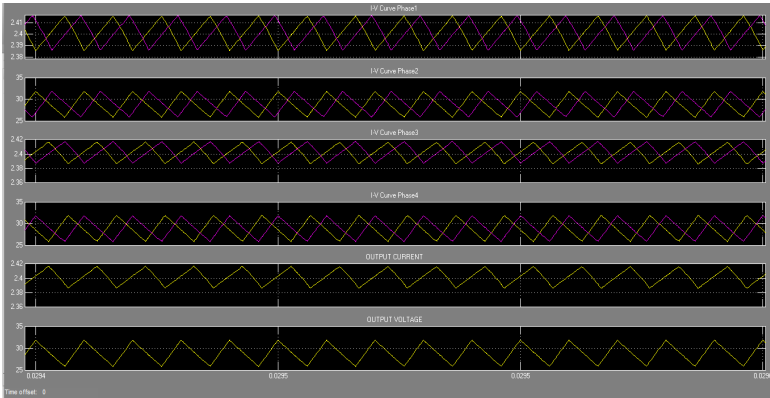


Fig-4.6: Output Voltages and Current Waveform

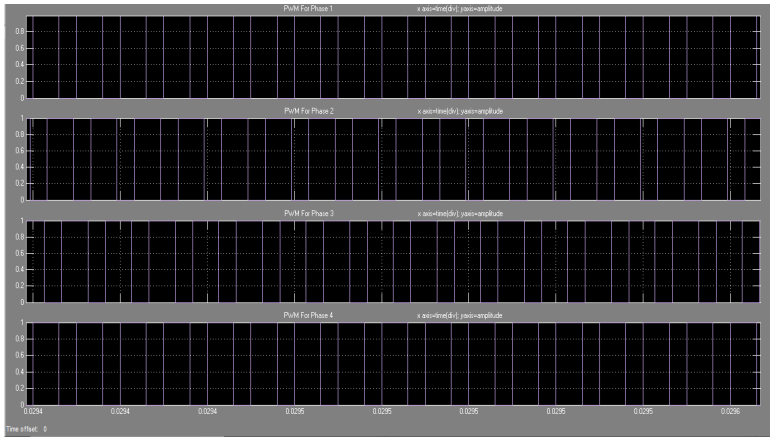


Fig-4.7: PWM Waveform for Four Phases

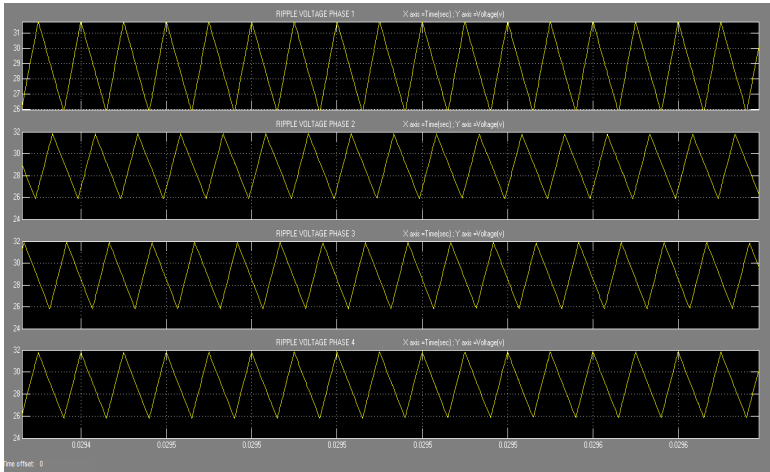


Fig-4.8: Ripple Voltage Waveform

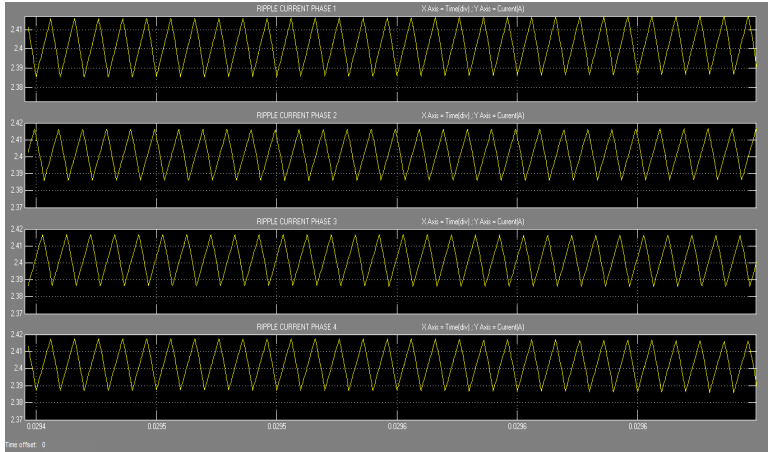


Fig-4.9: Ripple Current Waveform

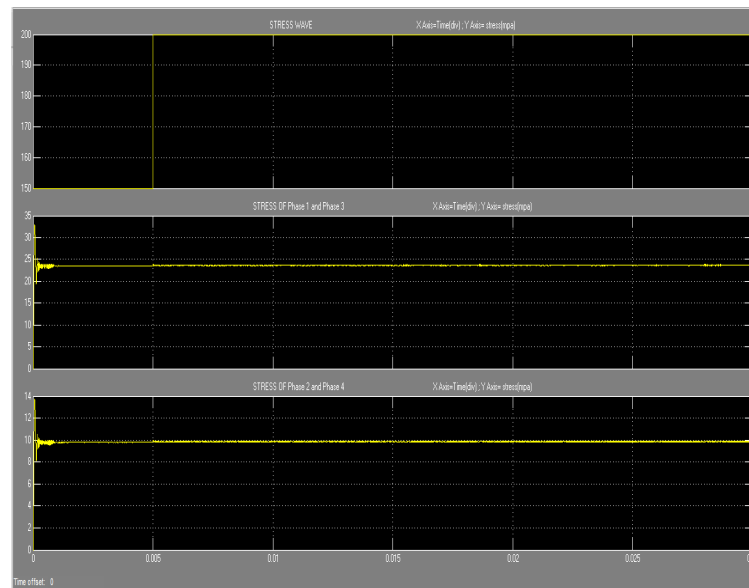


Fig-4.10: Stress Waveform

V CONCLUSION

In this paper, Multiphase Interleaved Boost Converter with higher voltage and reduced current ripples has been successfully developed and which is suitable for low input voltage and high step up conversion applications. The size of Four-boost converters in parallel is almost same as a single boost converter of the same total power because the size of main parts inductors are almost remains same. The simulation result of proposed interleaved boost converters which provide higher voltage and reduced current ripple and voltage ripple compared to conventional interleaved boost converter. Therefore, multiphase interleaved boost converter is suitable for renewable applications.

REFERENCES

1. J.S. Anu Rahavi, T. Kanagapriya, Dr. R. Seyezhai, "Design and Analysis of Interleaved Boost Converter for Renewable Energy Source," in Proc. International Conference on Computing, Electronics and Electrical Technologies, [ICCEET] 2012 IEEE.
2. Y.Ching Hsieh, Te-Chin Hsueh and Hau-Chen Yen, "An Interleaved Boost Converter With Zero-Voltage Transition," IEEE Trans. Power Electron., vol.24, no. 4, April 2009.
3. D. Y. Jung, Y. H. Ji, and S.H. Park, "Interleaved soft-switching boost converter for photovoltaic power-generation system," IEEE Trans. Power Electron., vol.26, no. 4, April 2011.
4. Hosseini, S. H., E. Babaei, and T. Nouri. "An interleaved high step-up DC-DC converter with reduced voltage stress across semiconductors." In Electrical and Computer Engineering (CCECE), 2014 IEEE 27th Canadian Conference on, pp. 1-6. IEEE 2014.
5. Mounica Ganta, Pallamreddy Nirupa, Thimmadi Akshitha and R.Seyezhai (2013), "Design and Simulation of PWM Fed Two-phase Interleaved Boost Converter for Renewable Energy Source", international Journal of Electrical, Electronics and Data Communication, ISSN (p): 2320-2084, Vol. 1, Issue-1, March 2013.
6. Niraj Rana , Mukesh Kumar , Arnab Ghosh and Subrata Banerjee, "A Novel Interleaved Tri-State Boost Converter With Lower Ripple and Improved Dynamic Response," IEEE Trans. Ind. Electron., vol. 67, no. 7, Jul. 2018.
7. Rupesh K C, Naziya Parveen , "Design and Simulation of Interleaved DC-DC Boost Converter for Stand-alone Systems Using Solar Panel," in Proc. International Journal of Innovative Research in Science, Engineering and Technology Vol. 5, Special Issue 9, May 2016.
8. A.Thiyagarajan, S.G Praveen Kumar, A.Nandini, "Analysis and Comparison of Conventional and Interleaved DC/DC boost converter", 2nd International Conference on Current Trends in Engineering and Technology, ICCTET'14.
9. Tian Xue, Zheng Minxin and Yang Songtao, "Maximum Power Point Tracking for Photovoltaic Power Based on the Improved Interleaved Boost Converter," in Proc. IEEE Conference on Industrial Electronics and Applications (ICIEA) 2016.

ELECTRIC VEHICLE CHARGING STATION USING VIENNA RECTIFIER AND 3L DC - DC CONVERTER WITH AN ENERGY STORAGE STAGE

Shree Aasha Lekshman¹, Dr. T. Suresh Padmanabhan² and R. Anandaraj³PG Scholar¹, Professor² and Associate Professor³Department of Electrical and Electronics Engineering, E. G. S. Pillay Engineering College (Autonomous),
Nagapattinam, Tamilnadu

ABSTRACT

This paper proposes a charging station for electric vehicle using Vienna rectifier and 3L dc -dc converter with an energy storage stage (ESS). As in recent times as there is increase in fuel rate so maximum population of the people go in search of electric vehicles. But electric vehicle is not widespread as expected due to some drawback like lack of charging station at a particular distance and long-time charging process. To overcome this drawbacks many systems has been developed in recent times. In this project we use 3 level dc-dc converter for both voltage balancing and to reduce the charging time. In this project we give the input from the ac grid. A Vienna rectifier is proposed to reduce the ac side harmonics, improve the power factor and increase the efficiency as well. During peak hours to balance the demand we are using 12v solar dc output as additional input. In this paper we are taking three loads 1) a resistive load, 2) ESS, 3) dc motor. The output of the project is performed in the mat lab software and simulation are presented in this paper.

Index Terms: Electric Vehicles, Energy storage stage, Fast charger, power balance management, Three-level dc-dc converter, Vienna rectifier.

I. INTRODUCTION

Plug-in electric vehicles, considering under this category to both plug-in hybrid electric and battery electric vehicles, have emerged as the most probable successor for conventional internal combustion engine vehicles. During these last years the sales of these vehicles have been constantly increasing and it is expected to remain in this trend for the upcoming years. Despite of the increasing electric vehicle (EV) fleet, these vehicles still have to solve some shortcomings before becoming a real alternative to transportation. The long recharging process of the batteries, limited mileage capacity (typically below 200 km) and the lack of public fast charging infrastructure are the main barriers to its widespread usage. However, to allow a large-scale penetration of this technology changes are required also from the grid point of view, as the electricity demand will grow accordingly. Nowadays, there is no real threat to the utility grid, as still the automotive industry is mainly sourced by the gasoline supply chain, but this will gradually will shift to a larger electricity consumption with transportation purposes, and if it is not addressed properly, the actual electric system will be unable to satisfy this demand.

In order to address the impacts of large-scale adoption of these vehicles in the utility systems, several studies have been carried out, mostly based on the conventional slow charging process of the batteries. This is mainly because, conventional charging is expected to remain as the preferred charging method, and also the fast charging process of the EV batteries is still not a widespread practice among the owners, due to the lack of facilities and misconceptions regarding the impact of this process to the battery pack. However, fast charging methods are still essential for a largescale adoption of EVs, as it will provide more flexibility to the drivers, occasional longer trips addressing range anxiety. Additionally, in order to reduce power consumption from the utility grid during peak consumption hours, the presence of ESS in these stations is gaining attention.

An alternative to enable fast charging is in the form of fast charging stations, which refers to the concept of having highpower fast chargers installed off-board, similar to gas stations located in public places. The structure of these charging stations can either be with an ac-bus, where each charging unit is fed by its independent ac-dc stage, or each unit connected to a common dc bus enabled by a single ac-dc stage with higher power ratings. Currently, fast charging is only enabled by standalone units, each one with its independent rectifier stage using the ac-bus concept.

We propose a new electric vehicle charging station using Vienna rectifier (refer to fig.1) to reduce the harmonics ,improve the power factor and to increase the efficiency of the system. Input supply is taken from the grid. The ac input is given to the VIENNA rectifier thus it can reduce the harmonics and improve the power factor and increase the efficiency as well.

Nowadays electricity has become very essential for each and every thing we use it may household or in industrial side we are in need of plenty of power to run our electrical and electronic devices.

So to manage the demand of power during peak hours we can additionally add any kind of renewable energy like solar, wind, fuel cell and much more that are available in the universe. In our project we are going to use solar for the additional power supply. PV panel is fixed accordingly to receive the solar energy, the received energy is given to a dc to dc converter. Here we are using MPPT controller for obtaining maximum efficiency.

During these days the petrol and diesel price is increasing high, so many people prefer electric vehicle as it does not need fuel like petrol or diesel also it does not lead to pollution of the atmosphere. Even though many prefer EV it is not spread wide due to some drawbacks like no availability of charging station at a certain distance and even if it is available the time taken for charging is high. So as to overcome such drawbacks a three level dc to dc converter is used for fast charging process is used in our project. Additionally ESS is used for storing the energy as well as it performs the job of voltage balancing of dc bus.

II. CIRCUIT OPERATION

The solar output is efficiently obtained by using converter employed with mppt technique and the 230v ac supply is given from the grid to the Vienna rectifier for reducing the ac side harmonics and improve the power factor for better efficiency.

Now both the dc output is combined balanced and given to the 3L dc-dc converter which gives fast charging technique. And the output can be stored in the ESS for future use also.

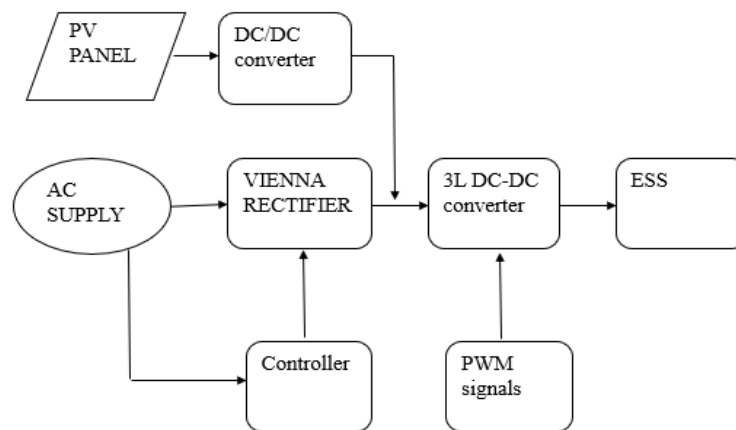


Fig-1: Proposed charging station architecture with balancing ESS

A different dc-bus concept is proposed and validated. The structure is based in the use of a Vienna converter enabling a dc-bus. The use of this dc-bus provides flexibility to the connection of the loads, has higher voltage and power handling capabilities and reduced step-down effort of the dc-dc stages. However, given the adoption of the bipolar structure and the intended application, the balance control becomes essential. In this was done by adding an additional circuit to the system, which enhances the balancing capabilities of the grid-tied converter. The result led to balanced dc voltages even under severe imbalance load conditions. Taking a different approach, this paper proposes a novel balancing method that uses the presence of the existing ESS, regardless of its type, to perform the complementary balancing actions. The idea is to relocate the power consumption of the ESS in order to keep the central converter operating in its balanced zone. This is achieved by the use of a three-level dc-dc interface. As it will be demonstrated, the only requirement of the approach is to meet the minimal balancing power. However, it is important to mention that the presence of this stage is for managing the energy consumption of the charging station, and its operation will be used towards the prevention of drifts in the dc voltages. It will be shown, that the presence of this stationary load in the system can be used to complement the balancing capabilities of the central converter. Moreover, the presence of this stage will allow the use of off the-shelf products for both, the central converter, and the fast charging units. This use of standardized components leads to lower hardware costs, improved system robustness in addition to cost-effective implementation and maintenances.

In the following sections, the inclusion of an energy storage stage in the system will be discussed. This additional stage will perform the tasks of energy buffer and also, perform the complementary balancing of the dc voltages. In order to do so, a dc-dc stage with access to both of the dc buses must be included, to avoid having two batteries in the system, as shown in Fig. 1. To meet this purpose, a three-level dc-dc stage will be featured. A control scheme is developed and proposed, covering the partial and full balancing tasks. The overall performance of the system will be validated both in simulation and experimentally.

III. EXISTING SYSTEM

In the existing system the technique used for voltage balancing and to built a charging station is central neutral point clamped (NPC) converter enabling a bipolar dc-bus fig. 2. The use of this split dc-bus provides flexibility to the connection of the loads, has higher voltage and power handling capabilities and reduced step-down effort of the dc-dc stages. However, given the adoption of the bipolar structure and the intended application, the balance control becomes essential. In this was done by adding an additional circuit to the system, which enhances the balancing capabilities of the grid-tied converter. The result led to balanced dc voltages even under severe imbalance load conditions. Taking a different approach, this paper proposes a novel balancing method that uses the presence of the existing ESS, regardless of its type, to perform the complementary balancing actions. The idea is to relocate the power consumption of the ESS in order to keep the central converter operating in its balanced zone. This is achieved by the use of a three-level dc-dc interface.

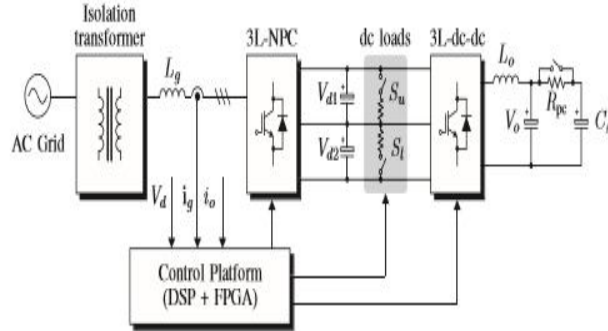


Fig-2: Existing system with 3L-NPC

IV. THREE-LEVEL DC-DC CONVERTER

As stated earlier, in order to perform the balancing complement to the grid-tied converter, the ESS must have access to both dc buses. Considering this requirement, a three level dc-dc converter will be used as the dc-dc stage. This choice is further justified by the reduced voltage stress on the switching devices, allowing the use of conventional low voltage-rated switches; improved output current waveform and improved efficiency in comparison to conventional two-level based topologies. Finally, for this particular application, it will only require the inclusion of a single energy storage stage, as it will be able to compensate currents in both of the dc buses as it will be demonstrated fig.3. The power circuit of the selected topology is presented, where it can be seen that can has three input terminals that can be directly connected to the bipolar charging station. The converter is composed of four switching devices along with their corresponding freewheeling diodes, the input filter capacitors C_{d1} and C_{d2} , and an output inductor L_o and capacitor C_o for filtering purposes. Considering its structure, the basic requirement that $V_{d1} = V_{d2} = V_d$, and the valid combinations of its switching signals, the converter generates four voltage states. Each state results in a different equivalent circuit, as presented in Fig. 3. These states are depicted as follows: when the switches S_{k1} and S_{k4} are turned on, the output voltage V_o is equal to the total input voltage $2V_d$; then when S_{k1} and S_{k3} are on, V_o becomes V_d ; the same output voltage is generated when the switches that are on are S_{k2} and S_{k4} ; finally, when the inner switches S_{k2} and S_{k3} are turned on, the output voltage is equal to zero. Please note that the switching states V_{1P} and V_{1N} generate opposite neutral-point currents, revealing the balancing capabilities of the converter. For the remainder of the paper, these states will be denominated mid-states.

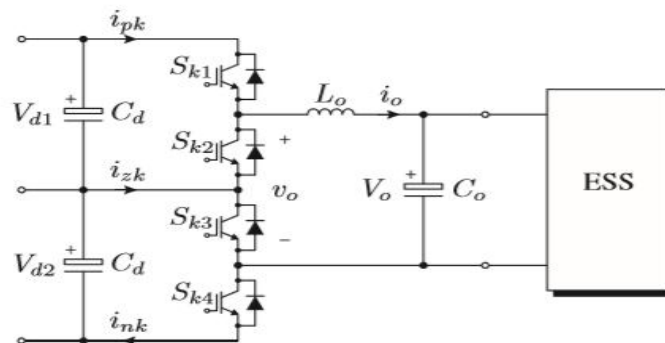


Fig-3: Circuit diagram for the three-level dc-dc stage for the ESS

V. PROPOSED CONTROL SCHEME

Many high power equipment's derive electrical power from three-phase mains, incorporating an active three-phase PFC front end can contribute significantly in improving overall power factor, reducing line pollution, lowering component stresses and reducing component size (e.g. the filter capacitor). Stationary operational behavior of three-phase/switch/level PWM rectifier was analyzed for asymmetrical loading of the output voltages. Maximum admissible load of the neutral point that is capacitive output voltage center point was calculated.

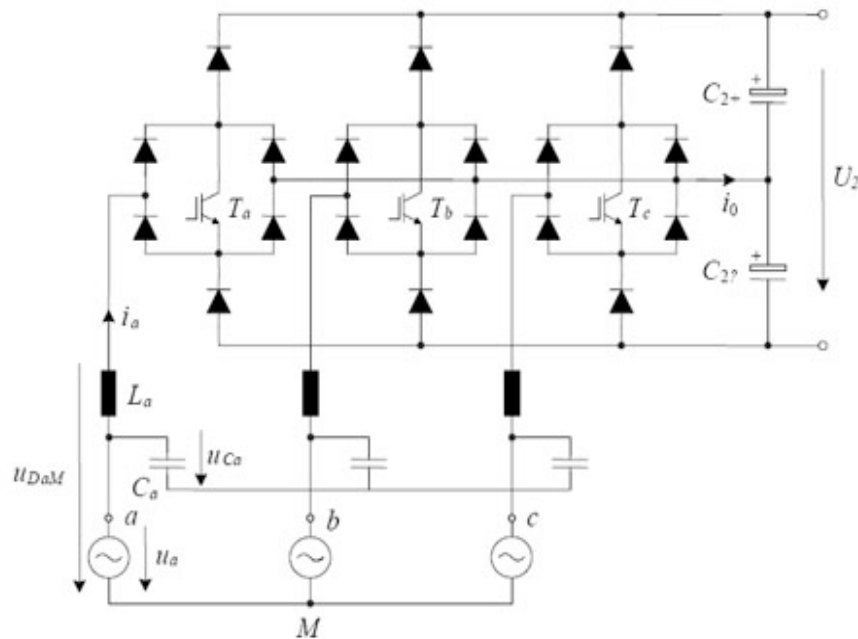


Fig-4: Schematic of a Vienna Rectifier

This topology mentioned known as the VIENNA rectifier and the three-level power structure results in a low blocking voltage stress on the power semiconductors and a small input inductor value and size. Therefore, Vienna is an ideal choice for the implementation of a medium power, unity power factor rectifier that also has a high power density. Three-phase AC to DC diode rectifier with three low-power and low frequency, four quadrant switches, with high power factor was presented. The main features were low cost, small size, high efficiency and simplicity. The high power factor was achieved with three active bidirectional switches rated at a small fraction of the total power, and gated at the line frequency. Application of power module (IXYS VUM25-E) realizing bridge legs of a three phase/switch/level VIENNA rectifier system with low effects on the mains were discussed. This can be a step in the modularization direction. The switching losses and on-state losses of a bridge leg of a rectifier were analyzed to determine the maximum output power. Three-phase diode bridge and DC/DC boost converter combination yielded a three phase/switch/level PWM rectifier [26]. Sinusoidal mains current, controlled output voltage and low blocking voltage stress on the power switches were characterized. Due to high current rate of rise when the phase transistors are turned on the single phase diode bridges in center point legs cannot be realized as mains rectifier. Diodes with short forward recovery time have to be applied to avoid high turn-on losses. Detailed operation and control of VIENNA rectifiers have been reported. Major drawback of the VIENNA topology compared to the full bridge is that it does not allow bi-directional power flow.

The Vienna topology can be implemented with either three switches or six switches. A six switch Vienna Rectifier was selected to lower conduction losses since the phase current flows through only one diode in each phase during the switch conduction and guaranteed to clamp the switch voltage to only half the output voltage. New controller was proposed with one or two integrators and a reset along with several comparators and flip/flops. Control was implemented by sensing either inductor currents or switching currents without multipliers or input voltage sensors.

The system simulation presented. The simulation results, comparison and discussion are presented. Details on the experimental performance, such as the input currents and respective harmonics, output voltage, load current, mid-point voltage and input voltages are given. The overall converter system performances with the synchronous logic control implementation are summarized.

I) Control Scheme

The controls are modeled with functional subsystem blocks. The controls are cascaded and consist of a current loop, a DC center point voltage loop and a DC voltage loop.

The outermost DC voltage loop regulates the sum of the two capacitor voltages using a PI controller. The controller output is the reference for the mains current amplitude i_N^* . This amplitude is multiplied with a three-phase sinusoidal signal which is synchronized with the mains voltages in order to obtain the three-phase mains current reference $i_{N\alpha}^*$. For simplicity, this sinusoidal signal is generated directly from the measured mains voltages.

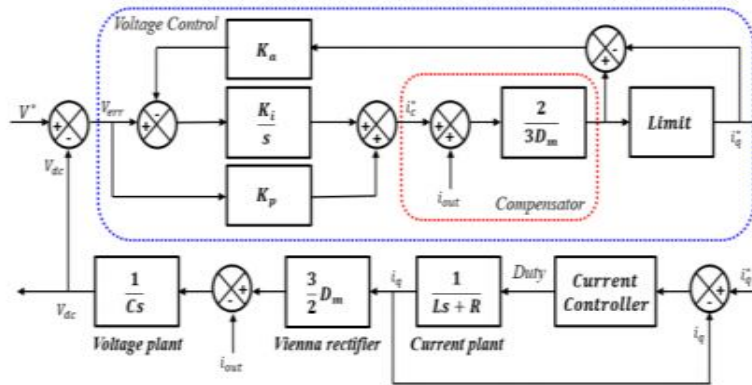


Fig-5: Control Scheme of a Vienna Rectifier

The mains current reference signal is offset by a DC current reference i_N^* . This DC reference is the output of a PI controller regulating the difference of the two capacitor voltages.

Finally, the mains current reference signal is used by the hysteresis current controller to generate the gate signals for the semiconductor switches. Due to the operating principle of the Vienna Rectifier, the gate signal of an individual phase needs to be inverted during the negative half-wave of the corresponding mains phase voltage.

Ii) Proposed Controller for Vienna Rectifier

The controls are modeled with functional subsystem blocks. The controls are cascaded and consist of a current loop, a DC center point voltage loop and a DC voltage loop.

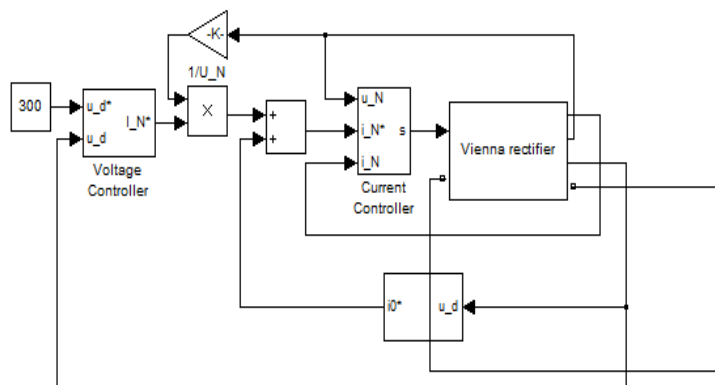
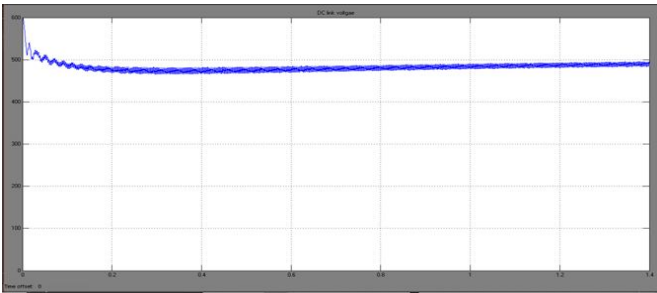


Fig-6: Control Scheme of a Vienna Rectifier

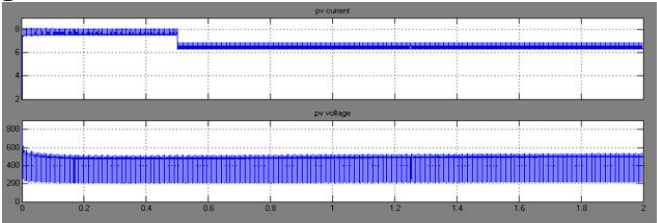
VI. SIMULATION RESULTS

Considering the proposed compensation technique to keep the dc-link voltages balanced, the dynamic performance of the system is validated under several load impacts, simulating the random arrival of vehicles for recharge. In addition, the proposed switching sequence correction is performed in order to keep the ac side currents without even-order harmonics. Here the solar output is 12v this is combined with the Vienna rectifier output 12v and a voltage of 12v is maintained in the dc line. to check the results three different 12v load is connected. the connected three different load are load1-r load, load2-motor and load3-ESS(rechargeable battery). The output waveform of each component and load wave form is given below.

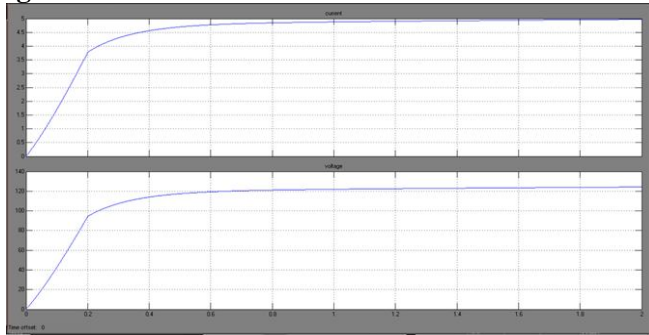
1. Dc Link Voltage



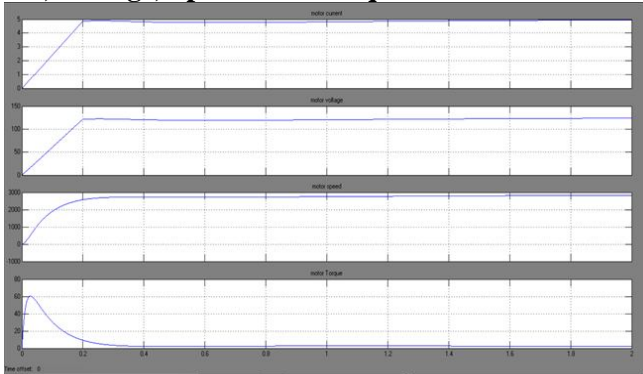
2. Solar current and voltage



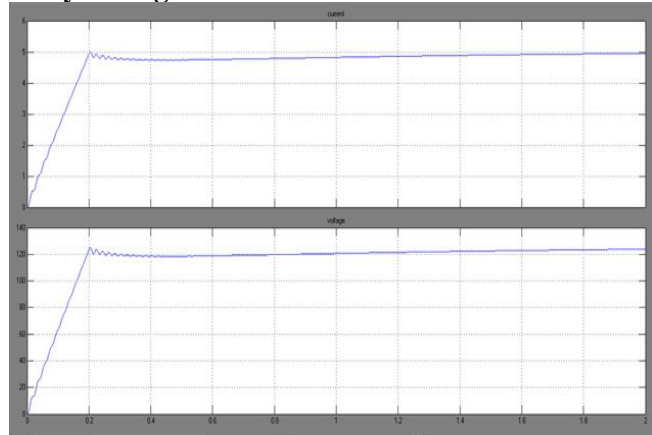
3. Load1-current and voltage



4. Load 2: Dc Motor Current, Voltage, Speed And Torque



5. Load3: Rechargeable Battery Voltage And Current



VII. CONCLUSIONS

Thus an electric vehicle charging station using vienna rectifier and 3level dc-dc converter with ESS is successfully simulated using mat lab software and output waveform has been given above. From the we can conclude that by using vienna rectifier the ac side harmonics has been reduced and power factor has been improved and efficiency of the system is improved. Hence by this system the drawback such as lack of charging station at particular distance as well as lack of fast charging techniques has been overcome. Is important to highlight that despite the ESS converter is providing the additional balancing ability, this does not alter dramatically its operation.

REFERENCES

1. D. Block, J. Harrison, and P. Brooker, "Electric Vehicle Sales for 2014 and Future Projections," Electric Vehicle Transportation Center, March 2015.
2. International Energy Agency, "Hybrid and Electric Vehicles annual report," 2015, available at: <http://www.ieahev.org>, accessed on May. 2015.
3. D. Aggeler, F. Canales, H. Zelaya-De La Parra, A. Coccia, N. Butcher, and O. Apeldoorn, "Ultra-Fast DC-Charge Infrastructures for EV Mobility and Future Smart Grids," in IEEE PES Innov. Smart Grid Technol. Eur. (ISGT), Gothenburg, Sweden, Oct. 2010, pp. 1–8.
4. M. Yilmaz and P. Krein, "Review of Battery Charger Topologies, Charging Power Levels, and Infrastructure for Plug-in Electric and Hybrid Vehicles," IEEE Trans. Power Electron., vol. 28, no. 5, pp. 2151–2169, May. 2013.
5. S. Bai and S. Lukic, "Unified Active Filter and Energy Storage System for an MW Electric Vehicle Charging Station," IEEE Trans. Power Electron., vol. 28, no. 12, pp. 5793–5803, Dec. 2013.
6. L. Dickerman and J. Harrison, "A New Car, a New Grid," IEEE Power Energy Mag., vol. 8, no. 2, pp. 55–61, Mar./Apr. 2010.
7. V. Silva and C. Kieny, "Impacts of EV on Power Systems and Minimal Control Solutions to Mitigate These," Essen, Germany: RWE Deutschland AG, May. 2011, <http://www.g4v.eu/downloads.html>.
8. [8] J. T. Salihi, "Energy Requirements for Electric Cars and Their Impact on Electric Power Generation and Distribution Systems," IEEE Trans. Ind. Appl., vol. IA-9, no. 5, pp. 516–532, Sept 1973.
9. J. Gomez and M. Morcos, "Impact of EV battery chargers on the power quality of distribution systems," IEEE Trans. Power Del., vol. 18, no. 3, pp. 975–981, July 2003.
10. K. Qian, C. Zhou, M. Allan, and Y. Yuan, "Modeling of Load Demand Due to EV Battery Charging in Distribution Systems," IEEE Trans. Power Syst., vol. 26, no. 2, pp. 802–810, May 2011.
11. J. Sexauer, K. McBee, and K. Bloch, "Applications of probability model to analyze the effects of electric vehicle chargers on distribution transformers," IEEE Trans. Power Syst., vol. 28, no. 2, pp. 847–854, May 2013.
12. P. Fan, B. Sainbayar, and S. Ren, "Operation analysis of fast charging stations with energy demand control of electric vehicles," Smart Grid, IEEE Transactions on, vol. PP, no. 99, pp. 1–1, 2015.
13. N. Machiels, N. Leemput, F. Geth, J. Van Roy, J. Buscher, and J. Driesen, "Design criteria for electric vehicle fast charge infrastructure based on flemish mobility behavior," Smart Grid, IEEE Transactions on, vol. 5, no. 1, pp. 320–327, Jan 2014.
14. J. Tant, F. Geth, D. Six, P. Tant, and J. Driesen, "Multiobjective battery storage to improve pv integration in residential distribution grids," Sustainable Energy, IEEE Transactions on, vol. 4, no. 1, pp. 182–191, Jan 2013.
15. International Energy Agency, "Hybrid and Electric Vehicles annual report," 2011, available at: <http://www.ieahev.org>, accessed on Mar. 2015.
16. S. Bae and A. Kwasinski, "Spatial and temporal model of electric vehicle charging demand," Smart Grid, IEEE Transactions on, vol. 3, no. 1, pp. 394–403, March 2012.
17. S. Rivera, B. Wu, S. Kouro, V. Yaramasu, and J. Wang, "Electric Vehicle Charging Station using a Neutral Point Clamped Converter with Bipolar DC Bus," Industrial Electronics, IEEE Transactions on, vol. 62, no. 4, pp. 1999–2009, April 2015.

-
18. ABB. [Online]. Available: <http://new.abb.com/ev-charging>
 19. Blink. [Online]. Available: <http://www.blinknetwork.com/chargers commercial-dc-fast>
 20. Schneider-Electric. [Online]. Available: <http://www.schneiderelectric.com/>
 21. A. Sannino, G. Postiglione, and M. Bollen, "Feasibility of a DC Network for Commercial Facilities," *IEEE Trans. Ind. Appl.*, vol. 39, no. 5, pp. 1499–1507, Sep./Oct. 2003.
 22. Y. Ito, Y. Zhongqing, and H. Akagi, "DC Micro-grid Based Distribution Power Generation System," in *IEEE Int. Power Electron. and Motion Control Conf. (IPEMC)*, vol. 3, Xian, China, Aug. 2004, pp. 1740–1745.
 23. J. Rodriguez, S. Bernet, B. Wu, J. Pontt, and S. Kouro, "Multilevel Voltage-Source-Converter Topologies for Industrial Medium-Voltage Drives," *IEEE Trans. Ind. Electron.*, vol. 54, no. 6, pp. 2930–2945, Dec. 2007.
 24. S. Bai and S. Lukic, "New method to achieve ac harmonic elimination and energy storage integration for 12-pulse diode rectifiers," *IEEE Trans. Ind. Electron.*, vol. 60, no. 7, pp. 2547–2554, July 2013.
 25. P. Grbovic, P. Delarue, P. Le Moigne, and P. Bartholomeus, "A bidirectional three-level dc-dc converter for the ultracapacitor applications," *IEEE Trans. Ind. Electron.*, vol. 57, no. 10, pp. 3415–3430, Oct 2010.
 - [26] L. Tan, B. Wu, S. Rivera, and V. Yaramasu, "Comprehensive dc power balance management in high-power three-level dc-dc converter for electric vehicle fast charging," *IEEE Trans. Power Electron.*, vol. PP, no. 99, pp. 1–1, 2015.

ENHANCEMENT OF PV MODULE BY PARTIAL SHADING DETECTION USING MAXIMUM POWER POINT TRACKING TECHNIQUE

B. S. Umabharathi¹, B. Amalorenaveenantony² and R. Anandaraj³PG Scholar¹, Assistant Professor² and Associate Professor³Department of Electrical and Electronics Engineering, E. G. S. Pillay Engineering College (Autonomous),
Nagapattinam, Tamilnadu

ABSTRACT

The extraction of maximum power is the major requirements in the operation of PV system. Maximum power point tracking techniques will provide a way to enhance the maximum power in the system. So, there is a requirements to a partial shading detection technique identify which incorporate the climate and environmental condition could influence the characteristics of PV arrays. A novel two stage MPPT method is presented to overcome the drawbacks. In first stage, the method is proposed to determine the occurrence of partial shading condition. In the second stage, using a new algorithm that is based on ramp change of the duty cycle and continuous sampling from the PV characteristics of array. It is the present request to stimulate and smooth MPPT technique with partial shading detection of PV arrays with required project result could improve the performance of PV arrays. The performance of the MPPT techniques can be enhanced by using the AT mega microcontroller.

Keywords: Partial shading, MPPT, PV system, microcontroller, perturb and observe.

I INTRODUCTION

Now a days renewable energy sources are used in wide variety. In India solar energy is in vast. But the PV panels have some disturbances like environmental conditions and shading of nearby buildings and trees etc. are reducing the efficiency of the PV panel. So we use the maximum power point tracking techniques.

In this paper we use two MPPT techniques. They are perturb and observe (P&O) and incremental conductance (IC) and short circuit current and open circuit voltage. Therefore, extracting maximum power from a PV system in all operation conditions is the main target of its control. The existing system have some techniques like artificial intelligence, such as fuzzy logic and neural network have more computational load [1].

The entire modules of an array do not receive the same solar irradiance is also called as the partial shading condition PSC. This condition will occur in urban area and moving clouds [2]. If the control system cannot detect and react to this situation, the PV system will be diverted from the optimal operation mode. Bypass diodes are connected parallel in each module there are many peak points in the PV characteristics [3]. In these condition global maximum power point (GMPP) cannot be achieved. If once the PSC is detected, it is based on the open circuit voltage and short circuit current in PV arrays the operating points are converges in the second step [4].

The P&O algorithm and its voltage step size are determined by the dividing rectangles method [5]. This method does not give global maximum power point tracking. The distributed maximum power point tracking in [6] the each module is compensate by regulate in respective maximum power point value by the connection of fly back DC-DC converter in each and every module [7]. This method is based on PV characteristics sampling implementation and integrated circuit. It gives guaranteed performance, high speed and adjustable output [8].

The proposed system having the combination of two algorithm that is perturb and observe and incremental conductance gives the high efficiency and the fast output. It also a low cost in implementation.

II RELATED AND EXISTING WORKS

Most maximum power point tracking (MPPT) techniques based on sliding-mode control (SMC) use another method such as perturb and observe or incremental conductance (IncCond) to provide current or voltage reference which makes the system more complex. To reduce the complexity and to increase the photovoltaic (PV) array efficiency, a direct control high performance MPPT based on improved SMC has been investigated in this study. Using two different step sizes can follow the PV peak power at different operating conditions with rapid convergence and greater accuracy. The new SMC-based MPPT designed for boost-type DC/DC converters is compared with a conventional and modified Incremental Conductance method, and to a classical SMC method which is very similar to that applied by Chu et al.

Solar energy is an interesting alternative to fossil fuel energy. It is one of the quickest increasing renewable energy resources. The direct conversion of the Sun's radiation into electricity is known under the name of

photovoltaic (PV) effect. PV energy is sustainable, clean, without environmental pollution and is of a multidisciplinary nature, involving power systems, power electronics and control theory. PV output power generation is influenced by climatic conditions (e.g. irradiance, panel temperature) and load variation. Therefore, a maximum power point tracking (MPPT) technique intended to control the DC/DC converter duty cycle is required to guarantee an optimal operation of the PV array under different operating conditions.

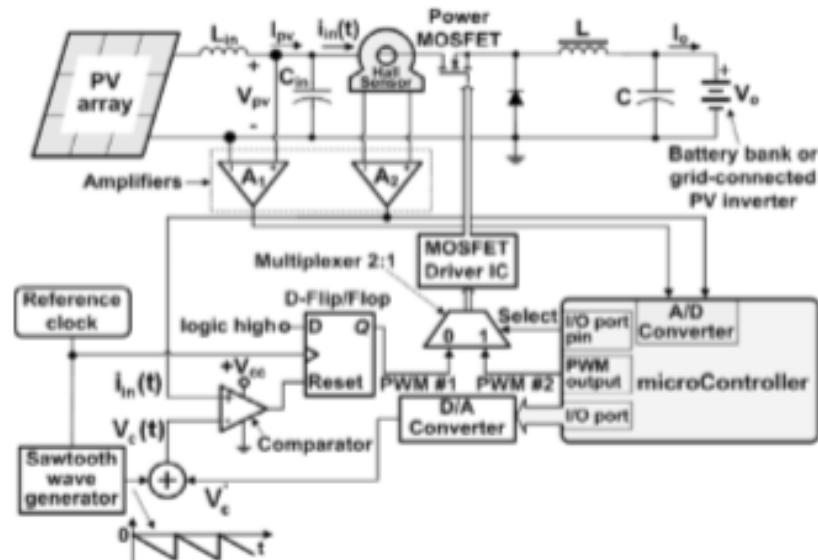


Fig-2.1: Block Diagram

An overview of more than 30 of these MPPTs has been done. Perturb and observe (P&O) and incremental conductance (IC) are widely used in the literature, but they fail under fast-varying climatic conditions. The SMC-based MPPT proposed in this paper is not complex and has the objective of optimising the PV system. This paper may be regarded as an extension of the work of Chu et al. The difference consists of using two different steps and of selecting the sliding surface as a derivative of power to voltage.

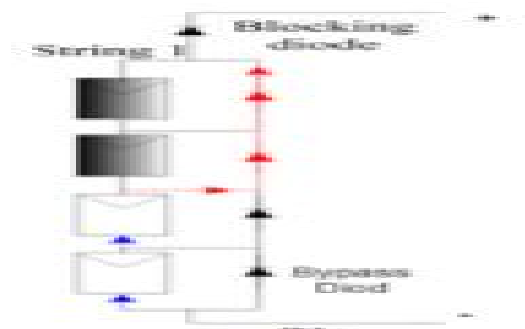


Fig-2.2: Structure of Sample Shading

The proposed method exhibits its best performance in dynamic and steady states. To the best knowledge of the authors, there has been no paper that reports this idea. Another contribution is the using of a stringent irradiance profile as recommended by the EN 50530 which can verify truthfully the effectiveness of the proposed MPPT system. Consequently, this effort is conducted to enhance the dynamic efficiency of PV system with an improved SMC, which can reduce the probability of diverging away from the maximum power.

III PROPOSED SYSTEM

In the last decade, the lack of new conventional energy sources, reveals the significance of the renewable sources. Solar energy is one of the promising renewable types of energy, which is coming from an unlimited solar source – the Sun and can be directly converted to electrical energy by photovoltaic (PV) modules. PV cells have non-linear characteristics which are affected by irradiance level, temperature, total residence etc. Under uniform insolation there is only one maximum point in the $P - V$ curve. Maximum power point trackers (MPPT) in PV systems are responsible for detecting the maximum power point (MPP) and reaching it by the PV modules. Conventional MPPT techniques track well the MPP under zero-shading conditions, however when partial shade condition (PSC) occurs, these methods are trapped at local maximum. During PSC two or more MPP take place in $P - V$ curves, which forces the researchers to find new techniques for MPPTs under PSC.

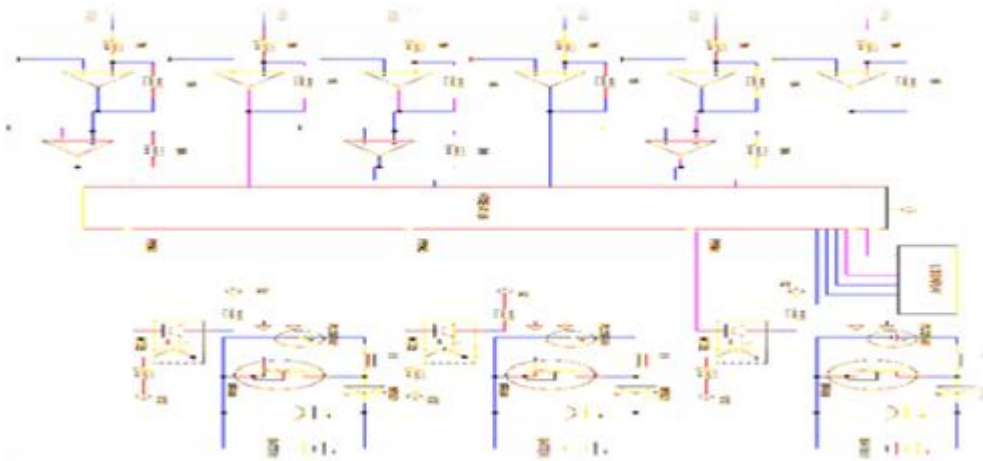


Fig-3.1: Circuit Diagram

The n number of solar panels are connected to the MPPT control which contains the partial shading detection sensor and at mega micro controller. MOSFET driver is connected to the each of the solar panel for sensing the any partial shading is occurred in panel. Boost converter is also connected to the each panel for any PSC occurrence in the panel, the output will be boosted and given to the battery bank.

Here we use two MPPT techniques, they are perturb and observe (P&O) Incremental conductance (IC).

The drawbacks of this proposed DPSO method are listed below

- The array currents in the low and high voltages of the array have big differences.
- To detect PSC the array current samples low and high voltages, cause a big disturbance in the system.
- The comparison curves with conventional PSO method have not been adequately covered, therefore the superiority of the proposed method was not highlighted enough.

Less addressed in the literature is detection of PS occurrence is another issue. It is necessary to detect its incidence before the applying of any process of MPPT in PSC.

IV SIMULATION RESULTS

In simulation results, the simulation results are shown. Here R 2013a is used to show the output of this proposed system. The Simulink model, output power, output voltage, output current, output energy and PSC ranges and normal condition output.

MATLAB RESULT

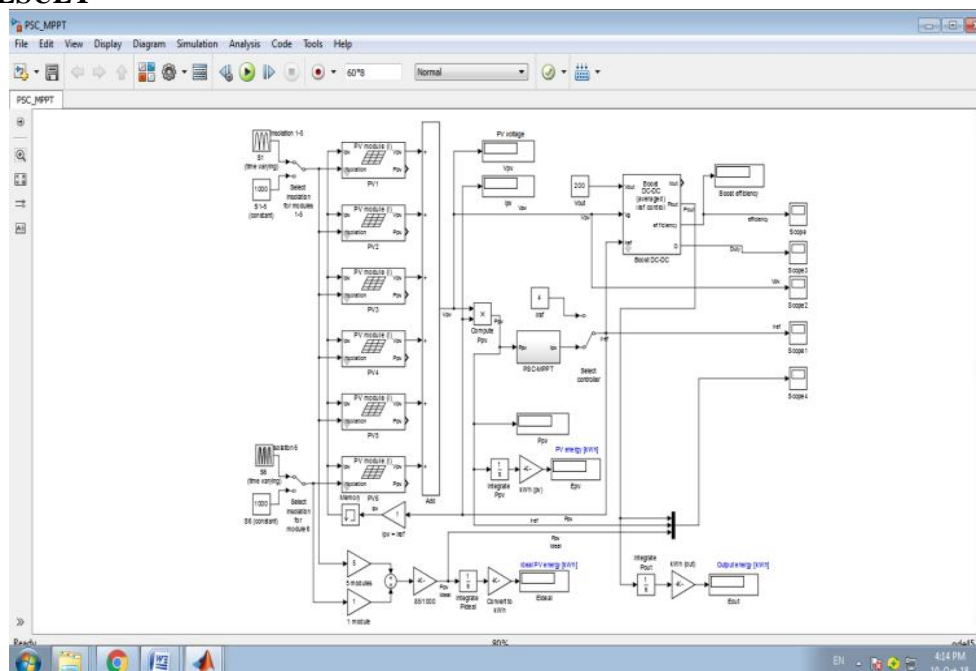
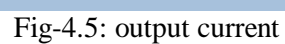
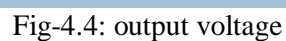


Fig-4.1: Matlab Simulink Model



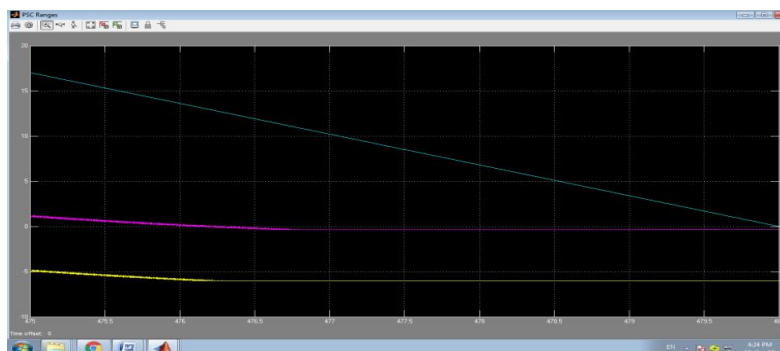


Fig-4.6: PSC ranges

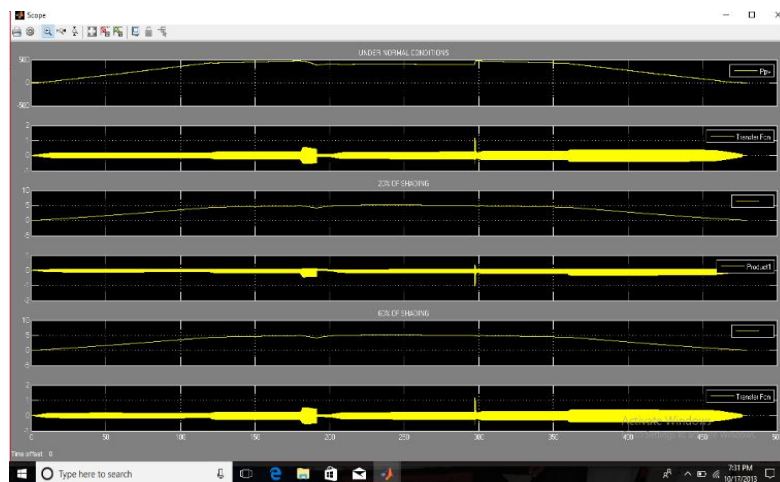


Fig-4.7: under normal condition

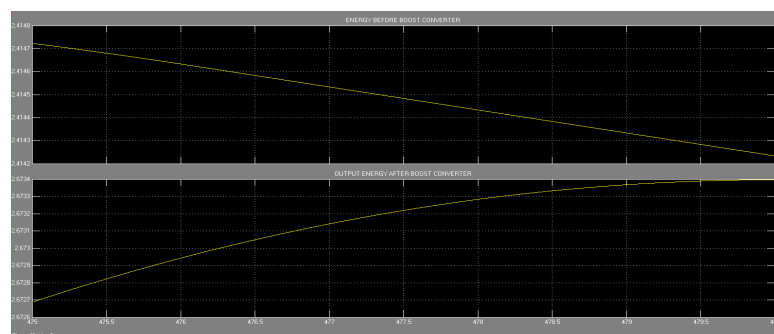


Fig-4.8: compared output

V CONCLUSION

In this paper, the partial shading condition is detected, by using the MPPT techniques in two algorithms. This system determines whether the uniform irradiance occurs or not. This proposed system is operated in simple method and fast algorithm. The perturb and observe, incremental conductance algorithm gives more efficiency than other. This system is based in the ramp change of array voltage sampling of current and voltage continuously. The partial shading condition is detected by using the sensor and it can be corrected. The global maximum power point tracking is easily attained by using this method. The results in simulation shows the increasing efficiency and accuracy of this method. It is high speed, minimum negative impact in while connect to the power system and smooth output.

REFERENCES

1. T. Esmar and P. L. Chapman, "Comparison of Photovoltaic Array Maximum Power Point Tracking Techniques," Energy Conversion, IEEE Transactions on, vol. 22, pp. 439-449, 2007.
2. Y.-J. Wang and P.-C. Hsu, "An investigation on partial shading of PV modules with different connection configurations of PV cells," Energy, vol. 36, pp. 3069-3078, 2011.
3. D. Kun, B. XinGao, L. HaiHao, and P. Tao, "A MATLAB-SimulinkBased PV Module Model and Its Application under Conditions of Nonuniform Irradiance," Energy Conversion, IEEE Transactions on, vol. 27, pp. 864-872, 2012.

-
4. J. Young-Hyok, J. Doo-Yong, K. Jun-Gu, K. Jae-Hyung, L. Tae-Won, and W. Chung-Yuen, "A Real Maximum Power Point Tracking Method for Mismatching Compensation in PV Array Under Partially Shaded Conditions," *Power Electronics, IEEE Transactions on*, vol. 26, pp.
 5. N. Tat Luat and L. Kay-Soon, "A Global Maximum Power Point Tracking Scheme Employing DIRECT Search Algorithm for Photovoltaic Systems," *Industrial Electronics, IEEE Transactions on*, vol. 57, pp. 3456-3467, 2010.
 6. P. Sharma and V. Agarwal, "Exact Maximum Power Point Tracking of Grid-Connected Partially Shaded PV Source Using Current Compensation Concept," *Power Electronics, IEEE Transactions on*, vol. 29, pp. 4684-4692, 2014.
 7. H. Patel and V. Agarwal, "Maximum Power Point Tracking Scheme for PV Systems Operating Under Partially Shaded Conditions," *Industrial Electronics, IEEE Transactions on*, vol. 55, pp. 1689-1698, 2008.
 8. T. Kok Soon and S. Mekhilef, "Modified Incremental Conductance Algorithm for Photovoltaic System Under Partial Shading Conditions and Load Variation," *Industrial Electronics, IEEE Transactions on*, vol. 61, pp. 5384-5392, 2014.
 9. M. Miyatake, M. veerachary, F. Toriumi, N. Fujii, and H. Ko, "Maximum Power Point Tracking of Multiple Photovoltaic Arrays: A PSO Approach," *Aerospace and Electronic Systems, IEEE Transactions on*, vol. 47, pp. 367-380, 2011. K. Sundareswaran, S. Peddapati, and S. Palani, "MPPT of PV Systems Under Partial Shaded Conditions Through a Colony of Flashing Fireflies," *Energy Conversion, IEEE Transactions on*, vol. 29, pp. 463472, 2014.

**INTELLIGENT MPPT CONTROLLER FOR FAST AND EFFICIENT TRACKING UNDER
DIFFERENT ENVIRONMENT CONDITIONS**

M. Sangeetha¹ and S. Latha²PG Scholar¹ and Assistant Professor²Department of Electrical and Electronics Engineering, E. G. S. Pillay Engineering College (Autonomous),
Nagapattinam, Tamilnadu

ABSTRACT

Maximum power point trackers play a major role in obtaining maximum power in photovoltaic (PV) system. The main obstruction in solar energy generation is that power generation is not constant due to environment conditions, so we go for MPPT to obtain Maximum power. MPPT algorithms are necessary in PV applications because the MPP of a solar panel varies with the irradiation and temperature, so the use of MPPT algorithms is required in order to obtain the maximum power from a solar array. The P&O is a standard method which is cheap, easy to implement and has excellent efficiency. The objective is to alleviate the Limitations of conventional P&O method such as non-uniformity of PV Panel temperature, partial shading, steady state oscillation, diverged tracking direction and dust effects. An oscillation detection scheme, boundary condition are used to overcome the above drawbacks. Moreover, this paper presents the intelligent prediction enhanced adaptive P&O method is employed to reduce the non-uniformity of PV panel temperature, dust effect, inability to detect the global peak. The proposed model is verified using MATLAB simulations and the experimental Validation is carried out using boost Converter with AVR microcontroller. The results of proposed method are compared with conventional MPPT techniques and show that the tracking speed and efficiency is highly increased.

Keywords: Maximum Power Point Tracking, PV array, DC-DC Boost converter.

I. INTRODUCTION

Renewable energy is the energy that is obtained from natural resources which is not exhaustible. Now a days, conventional energy resources such as fossil fuels, coal, petroleum and natural gas are depleting so we are in need to switch to renewable energy resources. Renewable energy is extracted from unlimited natural resources such as sunlight, wind, rain, tides, geothermal heat which are obtained in a short period of time. Solar power is one of the best renewable energy sources available because it is one of the cleanest sources of energy. Solar power is energy from the sun that is converted into thermal or electrical energy. Solar technologies can harness this energy for a variety of uses, including generating electricity, providing light and heating water for domestic, commercial, or industrial use. In PV System, there occurs some loss because of continuous changes in temperature and irradiation conditions. Hence, Maximum power point tracking is a technique which is commonly used in photovoltaic system to extract maximum power output. Modelling of photovoltaic Devices and simulating is most important in today's research. The photovoltaic system is the cleanest and most abundant energy resources but this system also has some drawbacks like losses and efficiency. This drawback has been considered and an enhanced way for utilizing solar power is established in this paper. Perturb and observe method is the most commonly used method because of its easy implementation, simple algorithm and highly efficient. However it has some drawbacks. Due to varying environment conditions, the PV panel temperature is not uniform; this non-uniformity leads to some losses in PV panel. During the operation of the PV system, the whole PV array cannot receive uniform radiance, the one module output is vary from another due to clouds, trees, dusts, buildings or various environmental conditions. This is known as partial shading condition. The P&O algorithm oscillates around the MPP which produce some loss in output and due to irradiance the Algorithm losses its tracking direction which leads to energy loss. To overcome these drawbacks we use an enhanced adaptive P&O algorithm using boost converter with intelligent microcontroller AVR is used to solve the non-uniformity in temperature, oscillation, divergence in tracking and partial shading condition. The proposed model is verified using MATLAB simulations and experimental results are verified. Thus the efficiency and tracking speed is increased twice when compared to conventional MPPT technique.

II EXISTING SYSTEM

The basic block diagram of MPPT system is shown in the Fig 2.1. It consists of a PV array, DC-DC Converter, MPPT control unit and a Load. A PV Cell is a semiconductor device that converts solar radiation into DC electricity through the photovoltaic effect (Conversion of solar light energy into electrical energy). When light radiation falls on Solar Cell, it may be reflected, absorbed, or passes right through. Then, the absorbed light generates the electricity. It consists of a very thick n-type crystal covered by a thin n-type layer exposed to the

sun light. It consists of number of individual solar cells are inter connected together and called Module or panel. To get the desired voltage or current, Panels are connected in either series or parallel which is called array. Each PV cell is rated for 0.5 – 0.7 volt and a current of 30mA/cm². In PV System, there occurs some loss because of continuous changes in temperature and irradiation conditions. Hence, Maximum power point tracking is a technique which is commonly used in photovoltaic system to extract maximum power output. The maximum power point tracking is basically a load matching problem. In order to change the input resistance of the panel to match the load resistance (by varying the duty cycle), a DC to DC converter is required. The efficiency of the DC to DC converter is high for boost converter.

Perturb and Observe method is simple and easy to implement. In this we use only one sensor, that is the voltage sensor, to sense the PV array voltage and so the cost of implementation is less and hence easy to implement.

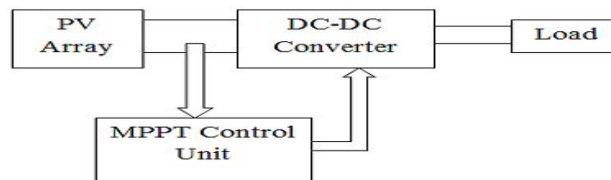


Fig-2.1: Block diagram of MPPT system

The time complexity of this algorithm is very less but on reaching very close to the MPP it doesn't stop at the MPP and keeps on perturbing on both the directions.

In the conventional MPPT Techniques such as Perturb and Observe method (P&O), Hill Climbing (HC), Incremental Conductance (IC). The P&O algorithm continuously oscillates around the MPP, which results in certain amount of power loss. The irradiance increases rapidly causes the P&O to lose its tracking direction which leads to some energy loss. Then, The P&O is not able to track the global peak under partial shading condition. During the operation of the PV system, the whole PV array cannot receive uniform radiance, the one module output is vary from another due to clouds, trees, dusts, buildings or various environmental conditions. This condition is known as partial shading. This reduces the PV panel Output.

In Soft MPPT techniques such as Particle Swarm Optimization (PSO), Differential Evolution (DE), Artificial Neural Network (ANN), Ant Colony Optimization (ACO), Artificial Bee Colony (ABC), Grey Wolf (GW), Fireflies (FF), Cuckoo Search (CS). These soft MPPT techniques has drawbacks such as Implementation Cost, Computational Complexity, Slow tracking speed. To overcome these issues we should go for the proposed Enhanced adaptive P&O MPPT technique using intelligent microcontroller.

III PROPOSED SYSTEM

This paper proposes an intelligent MPPT controller for Fast and efficient tracking under different environment conditions. An enhanced adaptive P&O Algorithm is used in this PV system. The block diagram of proposed system is shown in the Fig 3.1. The no of individual PV cells are connected to form a PV module and the PV module is connected to form the PV array. The sun light falls on the PV array, the solar cells in the array convert the sun light directly into electricity. The output from the array in which the current is increased or decreased with respect to the voltage to get the desired power output. The PV array is then connected to the high performance boost converter. The maximum power point tracking is basically a load matching problem. In order to change the input resistance of the panel to match the load resistance (by varying the duty cycle), a DC to DC converter is required.

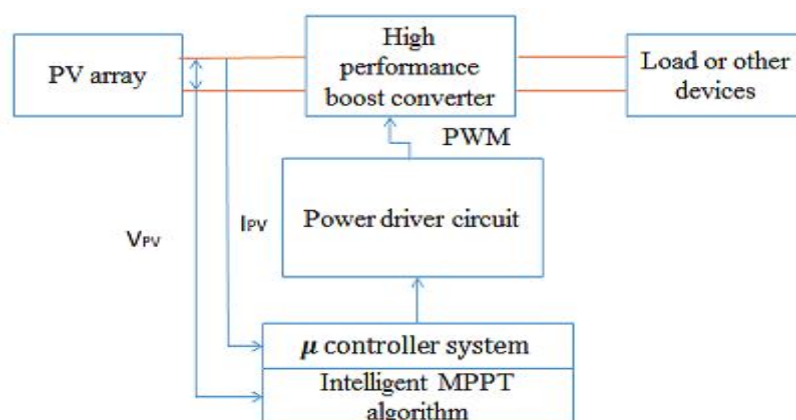


Fig-3.1: Block diagram of proposed system

Then, the voltage is send to the MPPT algorithm. The MPPT is used to extract the maximum available power in the PV module. In this proposed system, an enhanced adaptive P&O method is used to minimize the losses arises during oscillations, diverged tracking direction, dust effect, Non-uniformity of PV panel temperature and inability to detect the global peak under partial shading condition. Adjust the voltage, then the power increases further adjustments are made in that direction until the power no longer increases. This point is called MPP. MPPT requires some samples to obtain the MPP. At this point, the algorithm oscillates around the MPP due to perturbation. The enhanced adaptive P&O detects oscillation by calculating more than three perturbations then minimizes the size of perturbations to mitigate the steady state oscillation. Then the P&O lose its tracking direction and diverged when irradiance increases with time. Thedynamic boundary condition is used to eliminate the diverged tracking direction during irradiation increases and the global peak under partial shading condition is detected by using intelligent prediction method irrespective of dust effects and other environmental conditions. Thus the efficiency and tracking speed is greatly increased. The MOSFET is used as a power driver circuit. PWM allow the control of power supplied to the electrical devices.

A detailed diagram of the proposed global MPPT system is shown in the Fig 3.2. Depending on the PV system application domain, a boost-type dc/dc power converter is used to interface the PV array output power to either a battery bank or a dc/ac inverter connected to the electric grid. Both of these alternative types of dc/dc converter load are represented in Fig by the voltage source V_o .

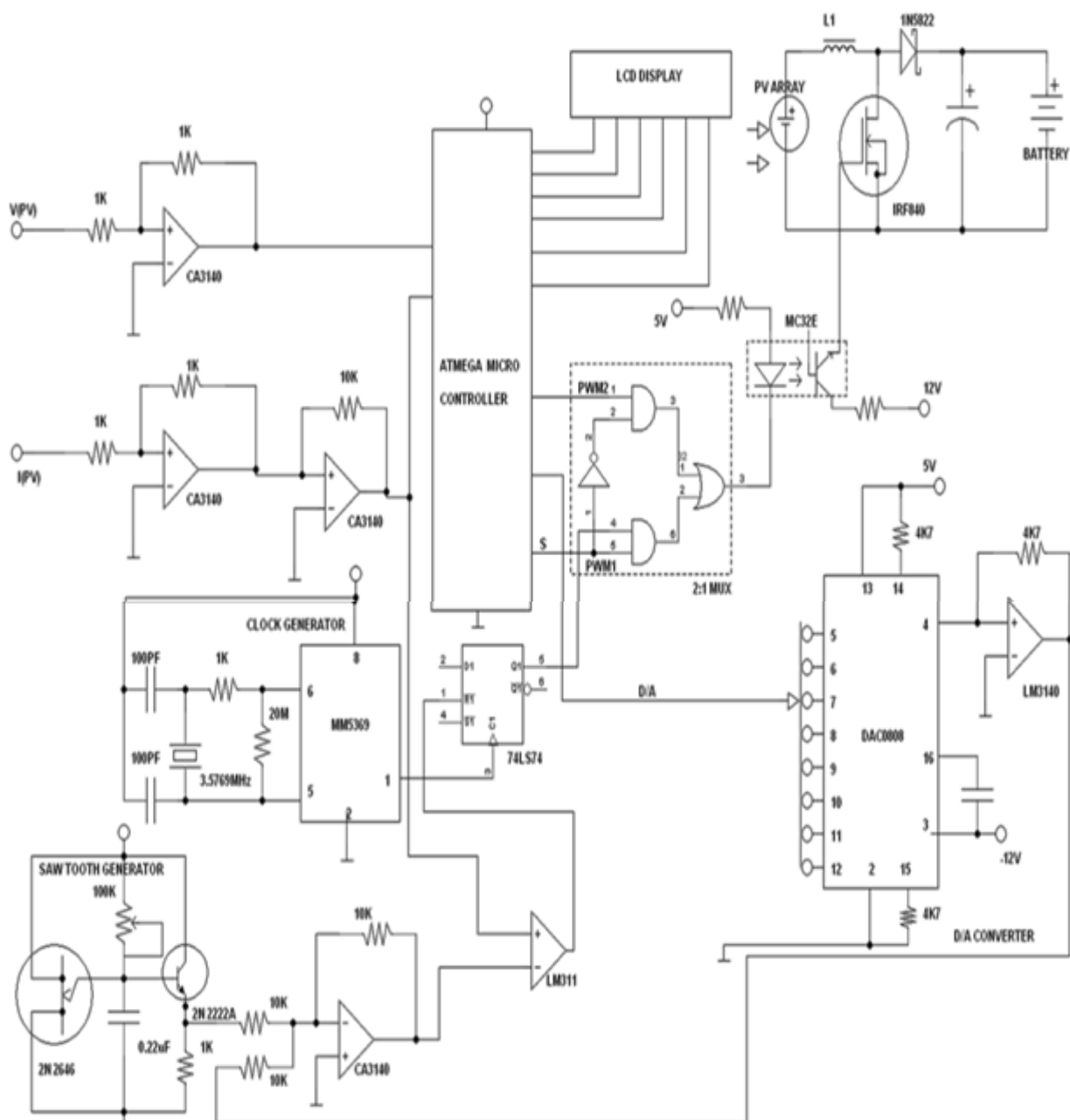


Fig-3.2: circuit diagram of proposed system

The inductance of the cable connecting the PV array to the dc/dc converter L_{in} is considered for stability analysis purposes, as discussed in the following. The inductor L and the input and output filter capacitor values are represented by the letter C_{in} and C respectively, are calculated as described in such that the dc/dc converter operates in continuous conduction mode, and simultaneously, the input and output voltage ripple factors are reduced to an acceptable limit.

The PV array voltage is measured using an operational amplifier-based differential amplifier, and the dc/dc converter input current is measured with a Hall-effect based current sensor. The proposed global MPPT procedure is performed in three consecutive phases: the constant input power, PV array voltage regulation, and P&O stage

In order to execute these processes, the dc/dc power converter is controlled using either the “PWM 1” or the “PWM 2” control signals. The operation of the dc/dc converter in this operating mode constitutes the basis for the detection of the PV array global MPP, according to the proposed global MPPT control algorithm. The “PWM 1” control signal, which is shown in the diagram, is produced by comparing the instantaneous value of the dc/dc converter input current $I(t)$ with the control signal $V_c(t)$ generated by the control unit.

During the P&O MPPT process, the dc/dc converter average input power is calculated by measuring the PV array output voltage and current. The resulting value is compared with the input power measured during the previous iteration of the algorithm. According to the result of the comparison, the duty cycle of the “PWM 2” dc/dc converter PWM control signal.

IV SIMULATION RESULTS

Matlab Simulink Model

The MATLAB Simulink model for enhanced adaptive P&O method is shown in the Fig 4.1. The conventional MPPT algorithm is compared with the enhanced adaptive P&O method.

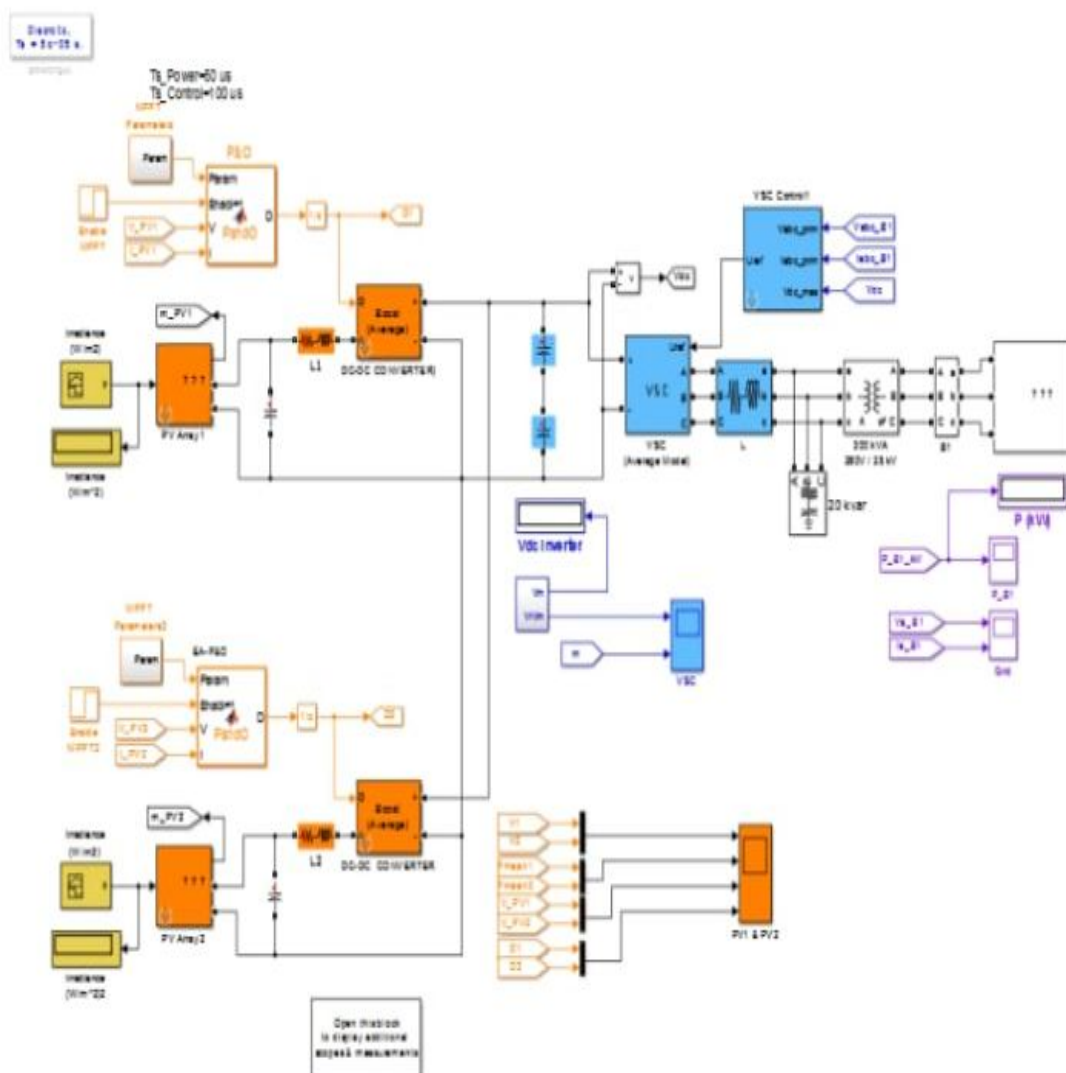


Fig-4.1: MATLAB Simulink model

The output waveform in the Fig 4.2 shows that the irradiance level decreases, the voltage and power value increases. Thus the efficiency and tracking speed is increased greatly.

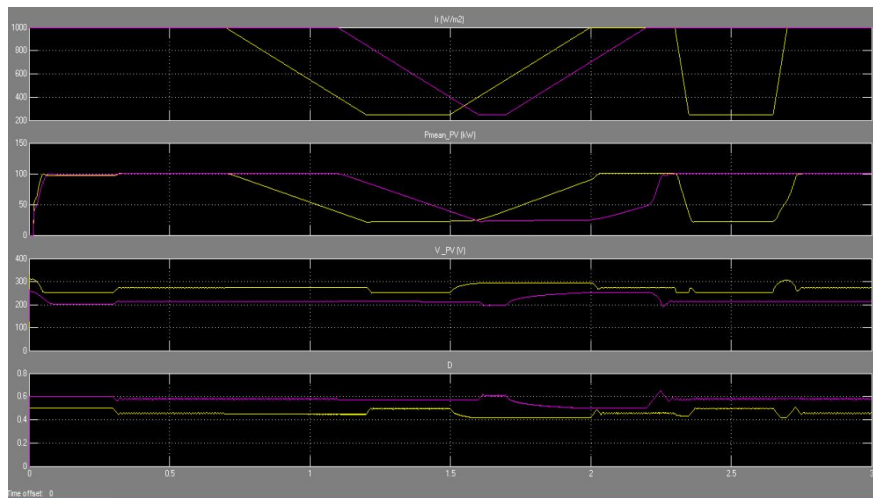


Fig-4.2: comparison of conventional MPPT and enhanced adaptive P&O method waveforms

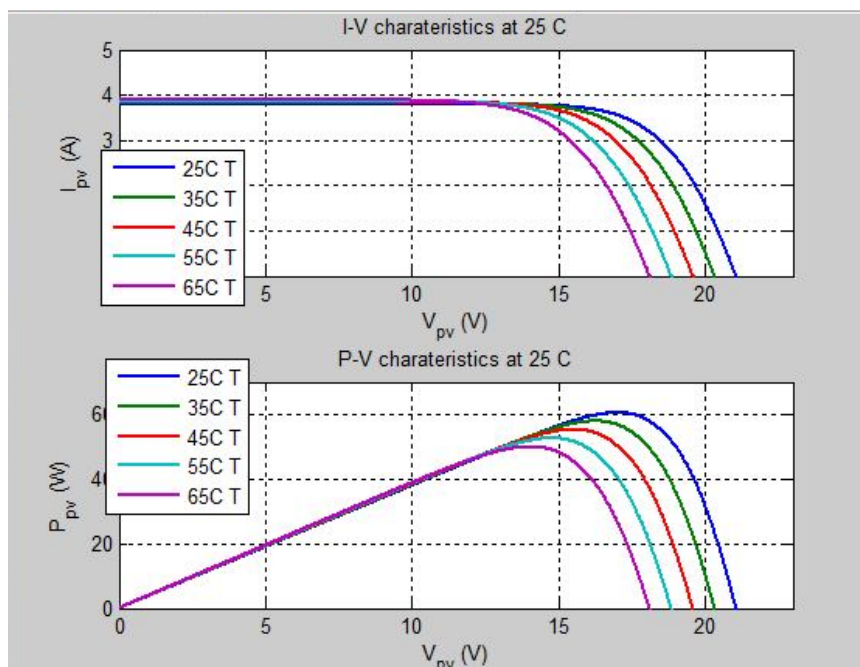


Fig-4.3I: V characteristics and P-V characteristics curve at 25⁰ C at normal temperature

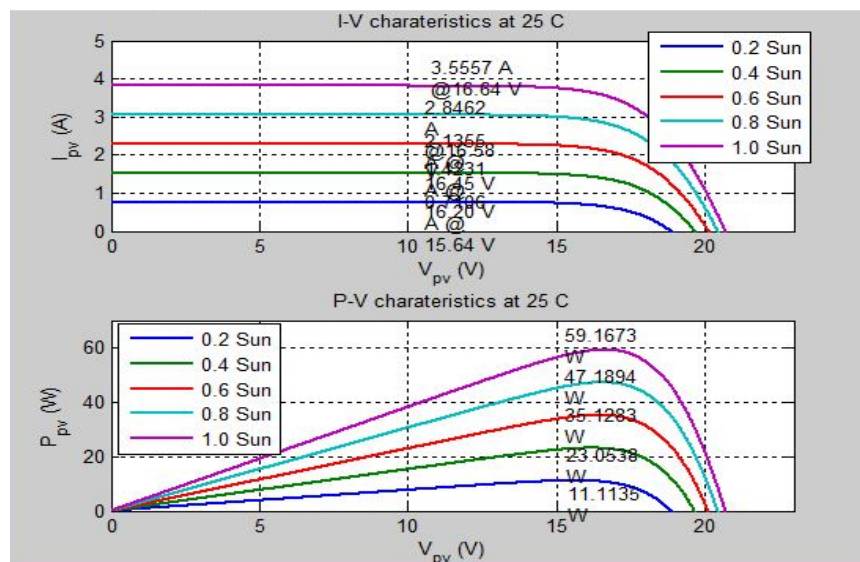


Fig-4.4: I-V characteristics and P-V characteristics curve at 25⁰ C sun temperature

V CONCLUSION

This paper has presented a new MPPT technique called enhanced adaptive perturb & observe algorithm which alleviate all the drawbacks of conventional P&O technique such as steady state oscillation, diverged tracking direction, inability to detect the global peak due to various environmental conditions such as dust effects, non-uniformity of panel temperature and partial shading. The conventional MPPT method is compared with enhanced adaptive P&O method. The simulation results show that the proposed method reduces the losses and increases the efficiency. This work is further extended in phase -2 that the simulation results are then verified by the experimental validation which is carried out using boost converter with microcontroller board. Thus, the simulation results show that the algorithm tracking speed and efficiency is greatly increased irrespective of various environmental conditions.

VI. REFERENCES

1. J. Ahmed and Z. Salam, "A critical evaluation on maximum power point tracking methods for partial shading in PV systems," *Renewable and Sustainable Energy Reviews*, vol. 47, no. 0, pp.933-953, 7// 2015.
2. S. Das, P. K. Sadhu, S. Chakraborty, N. Pal, G. Majumdar, "New Generation Solar PV Powered Sailing Boat Using Boost Chopper", *TELKOMNIKA Indones. J. Electr. Eng*, Vol.12, No. 12, pp.8077–8084, 2014
3. S. Das, P. K. Sadhu, N. Pal, S. Mukherjee, "Single Axis Automatic Solar Tracking System Using Microcontroller", *TELKOMNIKA Indones. J. Electr. Eng*, Vol.12, pp.8028– 8032, 2014
4. D. Dondi, A. Bertacchini, D. Brunelli, L. Larcher , "Modelling and optimization of a solar energy harvester system for self-powered wireless sensor networks", *IEEE Trans Ind Electron*, Vol. 55, pp. 2759–66,2008.
5. K. Ishaque and Z. Salam, "A review of maximum power point tracking techniques of PV system for uniform insolation and partial shading condition," *Renewable and Sustainable Energy Reviews*, vol. 19, no. 0, pp. 475-488, 3// 2013.
6. C. Kai, T. Shulin, C. Yuhua, and B. Libing, "An Improved MPPT Controller for Photovoltaic System under Partial Shading Condition," *Sustainable Energy, IEEE Transactions on*, vol. 5, no.3, pp. 978-985, 2014.
7. S. K. Kollimalla and M. K. Mishra, "A novel adaptive P&O MPPT algorithm considering sudden changes in the irradiance," *Energy Conversion, IEEE Transactions on*, vol. 29, no. 3, pp. 602-610,2014.
8. A. Kouchaki, H. Iman-Eini, and B. Asaei, "A new maximum power point tracking strategy for PV arrays under uniform and non-uniform insolation conditions," *Solar Energy*, vol.91,no.0,pp. 221 -232, 5// 201
9. Y. Li, W. Huang, H. Huang, C. Hewitt, Y. Chen, G. Fang, et al., "Evaluation of methods to extract parameters from current voltage characteristics of solar cells", *Sol Energy*, Vol.90, pp.51– 7,2013
10. P. Maffezzoni, L. Codecasa, D. D'Amore, "Modelling and simulation of a hybrid photovoltaic module equipped with a heat recovery system", *IEEE Trans Ind Electron*, Vol. 56, pp.4311– 8, 2009
11. H.Patel and V.Agarwal, "Maximum Power Point Tracking Scheme for PV Systems Operating Under Partially Shaded conditions," *Industrial Electronics, IEEE Transactions on*,vol.55,no.4,pp.1689-1698,2008.
12. K. Shenai, K. Shah, "Smart DC Micro-grid for Efficient Utilization of Distributed Renewable Energy", *Digest of IEEE Applied Power Electronics Conference and Exposition*, 2011.

WIRELESS POWER TRANSFER BASED ON INTEGRATED HYBRID ENERGY HARVESTING SYSTEM

N. Midula¹ and R. Anandaraj²PG Scholar¹ and Associate Professor²Department of Electrical and Electronics Engineering, E. G. S. Pillay Engineering College (Autonomous),
Nagapattinam, Tamilnadu

ABSTRACT

Solar energy plays an important role in renewable type energy source. By avoiding the quotidian methods of transferring the electrical energy from one place to other place, in which phenomenon is used to transferring the electrical power without the usage of wiring medium based on solar and thermoelectric generation (STEG). When the sunlight falls on the solar panels that converts the light energy into electrical energy. Thermo electric generation is assimilate with solar panels as seeback modules. The heat is evaporated from the panel is highly considered for the thermoelectric generation. Thus, the proposed system simultaneously harvesting both solar and thermal as source, which transmits the energy from transmitter to receiver end.

Keywords: Wireless transfer, Inductive coupling, STEG, Seeback effect.

I INTRODUCTION

In modern power generation harvesting the solar energy requires photovoltaic or installing large scale solar energy. Converting light energy into electrical energy depends on the photovoltaic system through the use of solar cells. Efficiency of a solar panel using the hybrid solar panel. Solar thermal energy is the most readily available source of energy. The solar energy is most important kind of non-conventional source of energy which has been used since ancient times in primitive manner. A thermo electric module is constructed by combining the p-type and n-type semiconductors. This paper will focus on inductively coupled wireless power transfer using renewable source, i.e. solar panels. It gives a efficient, convenient and eco- friendly method of transferring power for remote static devices, or recharging portable devices and the proposed system is reliable, highly proficient and economical when compared to other conventional energy harvesting systems. In hybrid energy harvesting system, the solar panel acts as a main power source. The solar panel is used to convert the incoming light rays into the electrical energy by the process of photo-voltaic generation. The thermo-electric generator is placed on the rear side of solar panel with a proper heat sink, the main function of the heat sink is to convert the waste thermo-electric energy from the solar panel in the form of heat into useful electrical energy by maintaining a suitable temperature gradient across the faces of the thermo-electric generator that is necessary to produce the electrical output. The electrical output characteristics of the solar devices depend upon the luminous intensity of sun as well as on the area exposed to the light rays. This works on the principle of Resonant Magnetic Coupling (RMS) which can be applied to get a maximum power transfer.

II EXISTING SYSTEM

In this project explains the transfer of electrical energy from one place to another place without using the wired medium. The basic principle used here is an inductive coupling. The phenomenon of Inductive coupling brings that by varying the magnetic flux between two inductive coils to transfer energy from the source to load. According to Faraday's Law of electromagnetic induction, it states that — The varying magnetic flux produced by one coil will produce a varying magnetic flux in another induction coil when they are placed in parallel position. The working is similar to the resonant transformer. It consists of two coils primary and secondary coil, which is connected by a LC tank circuit and tuned by a particular frequency. The functioning of these circuits is equivocal and may act as a resonator or an oscillator and multiply the applied frequency or simply escalate it to a large value. Being air core, these transformers possess low coupling coefficient. Most of the energy is transferred through magnetic field. The electric fields are confined within the capacitor. Even though the coupling coefficient being significantly low (i.e. $k < 0.1$) much of the energy from the primary gets transferred to the secondary due to high frequencies (kHz to MHz). MOSFETs are used as a switching device in low power and high frequency switching applications.

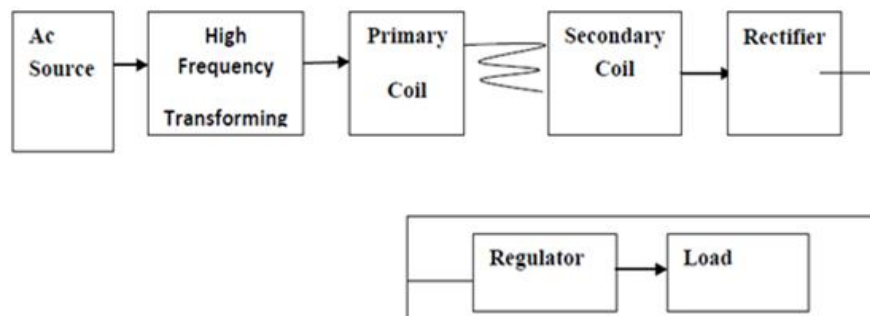


Fig-2.1: Block Diagram

The block diagram consists of primary coil, secondary coil, ac source, regulator, high frequency converter and rectifier. Its schematic can be seen in figure 2.1. The AC source supplies the ac voltage at input of the coil. Then it gets passes to the high frequency transformation is performed by which the frequency is increasing from 50hz to several khz and then it passes to the primary coil. By using the switching devices, the frequency transformation can be done to generate the pulses and given to transmitting inductor in the form of electromagnetic waves then transmitting towards receiving inductor. The receiving inductor is used to receive the electromagnetic waves produced inside the coil in Alternating current form. This voltage gets passed through rectifier which converts the AC voltage in DC voltage. The filter removes the unwanted contents. Its provide smooth DC voltage. The received voltage should be regulated using Voltage regulator so at the output we get regulated DC voltage. This voltage is then given to the load which drives it.

III PROPOSED SYSTEM

In this paper, proposes a simple, convenient, highly proficient, safe and eco-friendly method of transferring power to remote static switching devices. The proposed hybrid energy harvesting system is simultaneously utilizing both solar and thermo-electric energy it makes the system named as hybrid energy harvesting system. An integrated hybrid energy Harvesting system model has been developed in which light energy is converted into electrical energy by using a solar panel. In this paper, TEG is used to retrieve the waste heat and converts the heat energy into electrical energy based on see beck effect. A Small temperature differences and heat sources are suitable for thermoelectric generations. Such generators are used in automotives for waste heat recovery. Solar panel efficiency is improved by using the hybrid solar panel. It is less efficient compared with other heat engines, hence TEG is suitable for small applications. In thermo electric power generation, the temperature gradient is one of the main considerations to generate power.

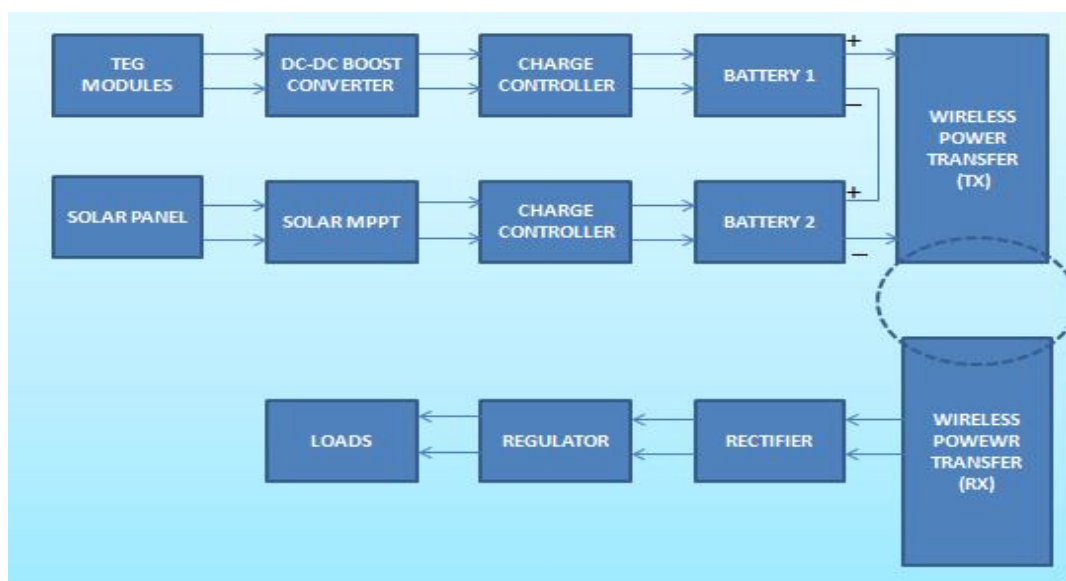


Fig-3.1: Block Diagram of Proposed System

In hybrid energy harvesting system, the solar panels act as a main power source. The purpose of solar panel is used to convert the incoming light rays in the form of solar energy into feasible electrical energy by the process of photo-voltaic generation. The thermo-electric generator is placed on the back side the solar panel with a suitable heat sink, which converts the waste thermo-electric energy from the solar panel in the form of heat into useful electrical energy. The thermo electric generator maintains the temperature gradient to get the efficient electrical output.

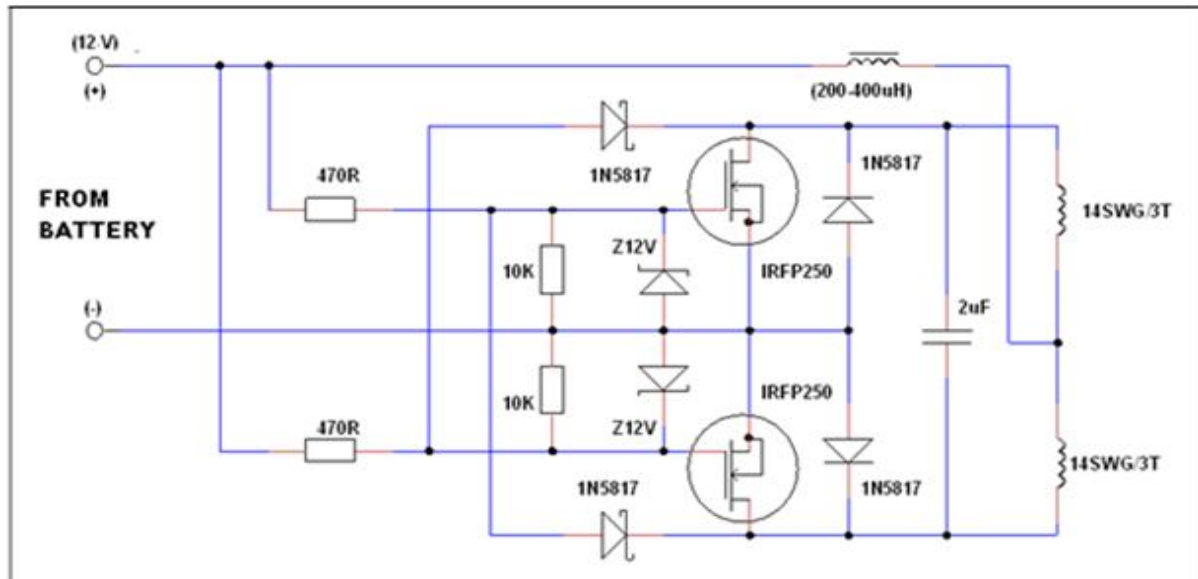


Fig-3.2: Circuit Diagram of Transmitter

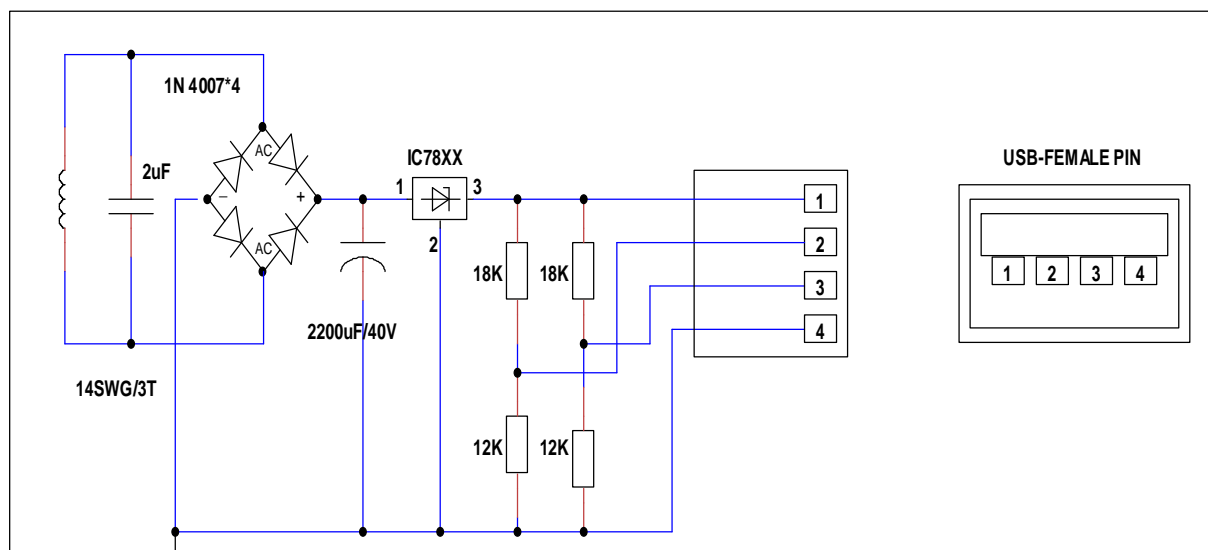


Fig-3.3: Circuit Diagram of Receiver

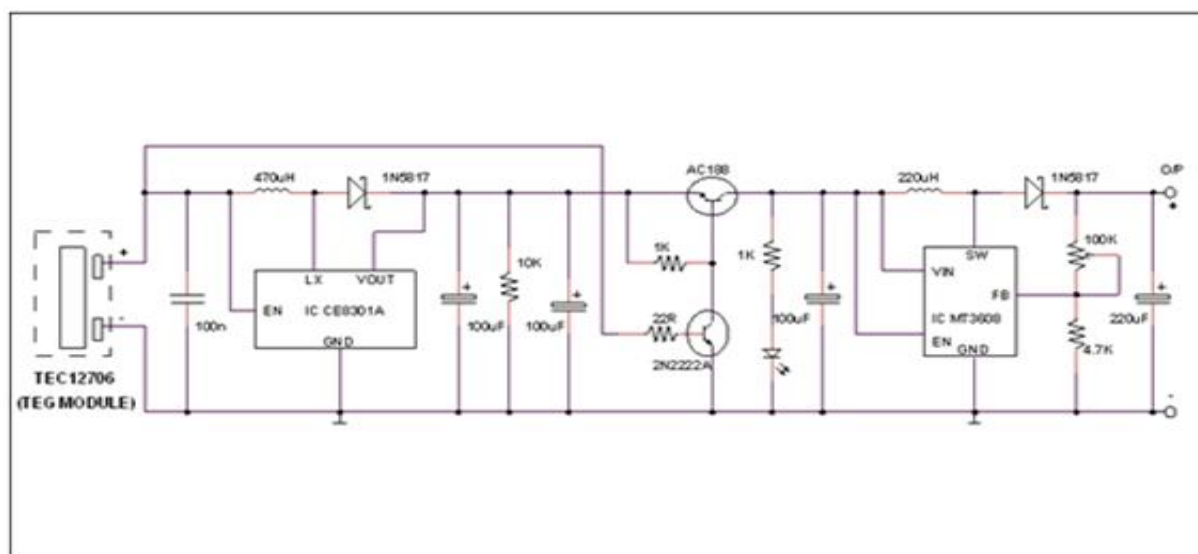


Fig-3.4: circuit diagram of TEG

A PV layer can achieve maximum efficiency about 30%, this is increased by adding TEG layer to convert the waste heat energy to current, thereby increasing the efficiency much better.

IV SIMULATION RESULTS

In this section, the simulation results are shown. Where the output schematics are simulated by the MATLAB 2014Ra and network simulator tool.

Matlab Result

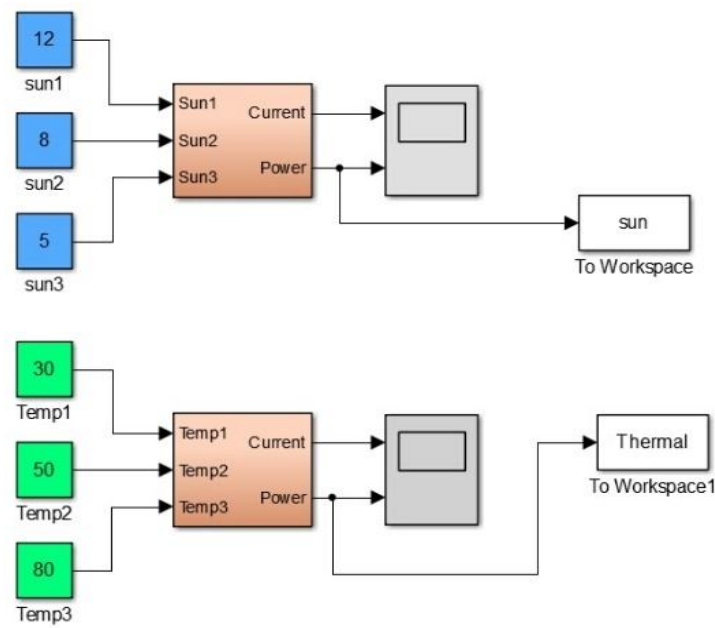


Fig-4.1: MATLAB Simulink Model

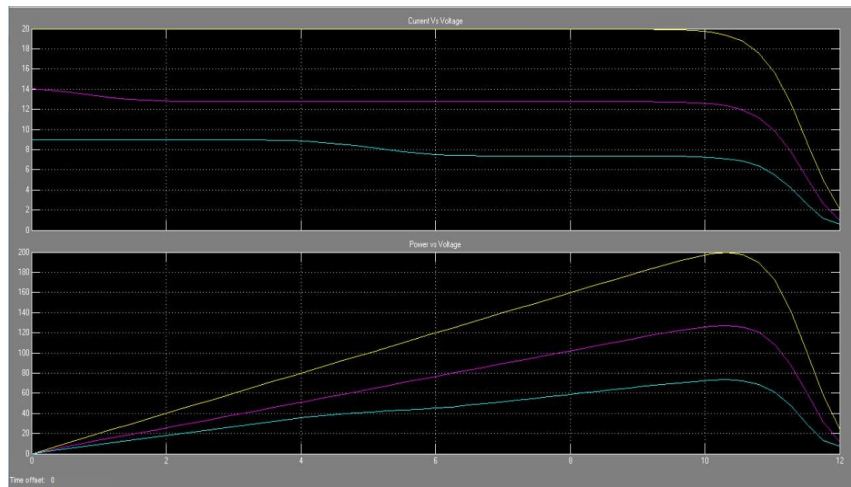


Fig-4.2: Characteristics of Solar energy

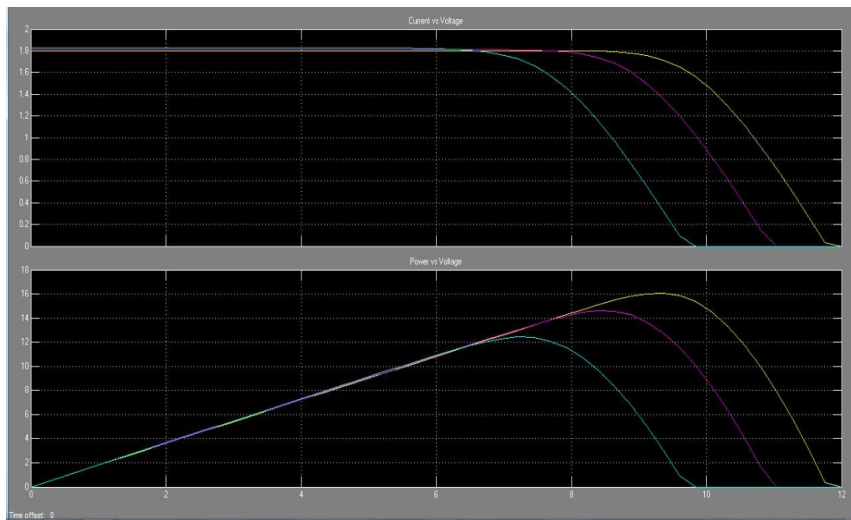


Fig-4.3: Characteristics of Thermal Generation

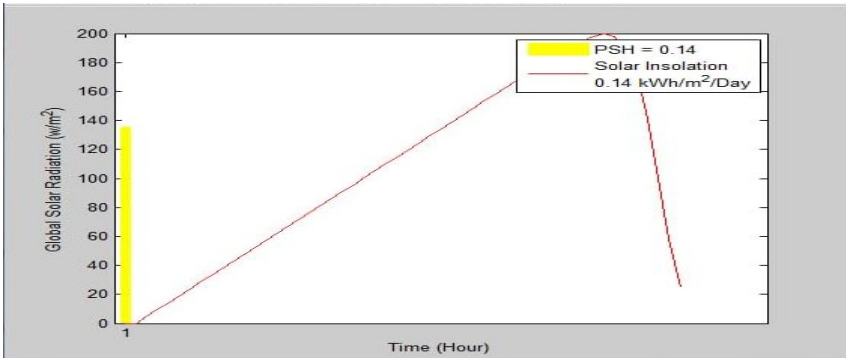


Fig-4.4: Output at Peak Sun Hour

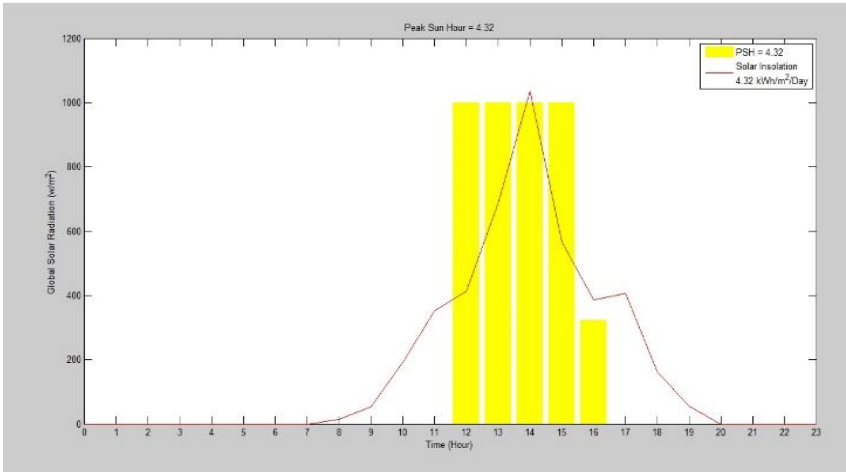


Fig-4.5: Output at Peak Sun Hour

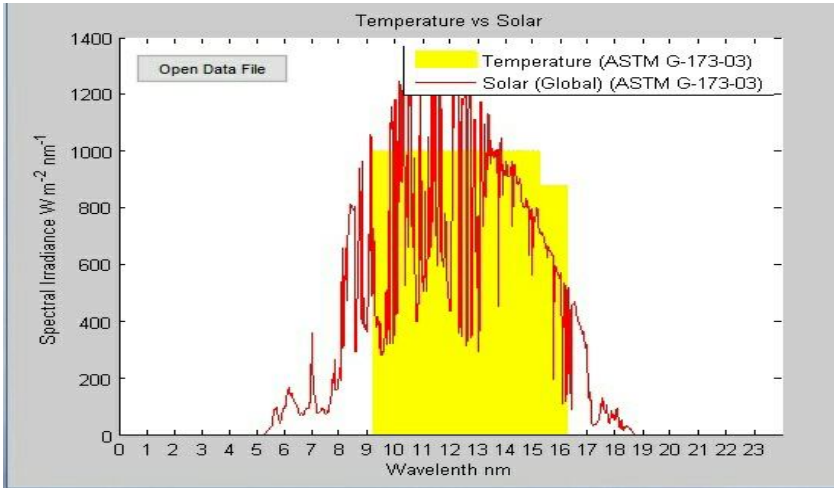


Fig-4.6: Output for Solar and Thermal Generation

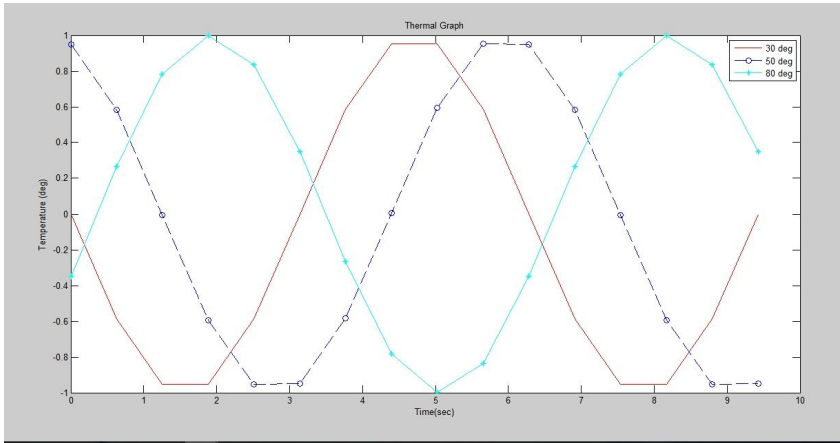


Fig-4.7: Thermal Generation Graph

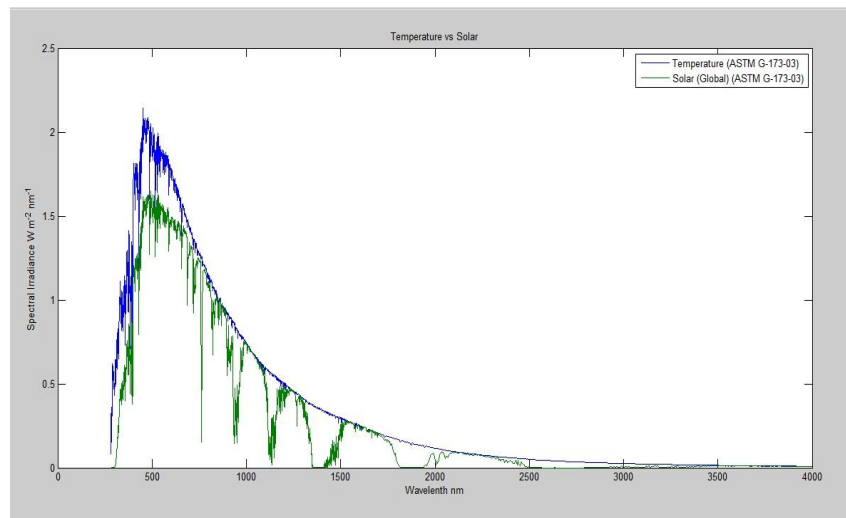


Fig-4.8: Spectral Irradiance For STEG

V CONCLUSION

The power electronic device that transmits power wirelessly and then charging batteries was developed. In this paper, an integrated hybrid model of solar energy was developed with the help of thermo electric generation (TEG). It results have been analyzed and concluded that the proposed hybrid energy harvesting system is effective enough to completely save the electrical power exploit by the solar panel by with the help of TEG. In this work, we have presented solar into electrical conversion using thermoelectric and photovoltaic. The main advantage of this type of technique is that renewable energy is used as source in the form of solar energy. Individuals can be facilitated to charge their electronic device efficiently.

REFERENCES

1. Daniel Kuerschner and Christian Rathge, "Contactless energy transmission systems with improved coil positioning flexibility for high power applications", 39th Power Electronic Specialists Conference (PESC) 2008, Rhodes, Greece, 15. - 19. June 2008, p.4326
2. Maninder Singh, Jaspreet Singh, Anshula, Parth "Efficient Autonomous Solar Panel and Thermo-Electric Generator (TEG) Integrated Hybrid Energy Harvesting System" 2016 Progress in Electromagnetic Research Symposium (PIERS), Shanghai, China, 8-11 August
3. Manikandan, Arun Francis, "Hybrid Solar Energy harvesting system" International Journal of Pure and Applied Mathematics Volume 118 No. 20 2018, 479-484 ISSN: 1311-8080 (printed version); ISSN: 1314-3395 (on-line version)
4. Anand.M, Yogesh Kannan "Wireless Power Transfer by Incorporation of Solar Energy" International Journal of Recent Development in Engineering and Technology, Volume 3, Issue 2, Aug' 2014
5. Vladislav Khayrudinov "Wireless Power Transfer System Development and Their Implementation," Thesis, Dept Electron Eng., Helsinki Metropolia University of Applied Sciences, Helsinki, Finland, 2015.
6. Luciano Mescia et al, "Innovative Materials and Systems for Energy Harvesting Applications", Hershey PA: IGI Global, 2015.
7. Saurabh Deshmukh, Ameya Kulkarni "Solar Power Generation and Wireless Power Transmission System" "IOSR Journal of Electrical and Electronics Engineering (IOSR-JEEE) e-ISSN: 2278-1676, p-ISSN: 2320-3331, Volume 9, Issue 4 Ver. II (Jul - Aug. 2014), PP 14-18.
8. Yongliang Li et al., "Wide spectrum solar energy harvesting through an integrated photovoltaic and thermoelectric system", ELSEVIER, 2014, pp. 39-44.
9. J. Hirai, T-W. Kim, A. Kawamura-"Study on intelligent battery charging using inductive transmission of power and information"

A DESIGN OF SELECTIVE HARMONIC MITIGATION BASED SELF-ELIMINATION OF TRIPLEN HARMONICS FOR SINGLE-PHASE SEVEN-LEVEL INVERTERS**N. Saraswathi**

PG Scholar

Department of Electrical and Electronics Engineering, E. G. S. Pillay Engineering College (Autonomous),
Nagapattinam, Tamilnadu**ABSTRACT**

In this paper all triplen harmonic orders are eliminated through a modified selective harmonic mitigation-pulse amplitude modulation (SHM-PAM) technique and it is suitable for single phase seven level voltage source inverter. The regular operation of the proposed SHM-PAM technique eliminate the fifth and seventh harmonic orders. It is also shown that the planned technique is extendible to fully completely different construction voltage waveforms and a flow sheet of self-elimination of all triplen harmonics has been given. Then, it's incontestable that the most range of harmonic orders would be controlled with the minimum range of accessible angles during a low switch frequency voltage wave shape.

Keywords: SHM-PAM, triplen harmonic elimination, multilevel inverter (MLI).

I INTRODUCTION

The motor that energies the wheels generally uses AC power, therefore there should be a conversion from DC to AC by a power converter, inverter is used for this conversion. Inverter classified into current source inverter (CSI) and voltage source inverter (VSI). Multilevel Voltage Source Inverters (VSIs) are used in high power applications using average-voltage switches. Cascaded H-bridge inverter is one of the most popular topologies which has modular structure producing high number of voltage levels that is appealing for industries. The highest power rating reported for a manufactured CHB is reported up to 120MW [1]. Although several multilevel inverter topologies have been projected by the investigators, CHB inverters have expanded much more popularity due to flexible organization, feasible, trustworthy and humble control approach. Various switching methods have been executed on the CHB inverter with sinusoidal pulse width modulation (SPWM), Hysteresis, etc, while the high switching frequency is the strongest limit to use them in high power applications such as high power uninterrupted power supply (UPS) or motor drives[4].

Furthermore, this condition would be poorer if the switching frequency is limited below 1 kHz meanwhile low order harmonics are projecting in Fast Fourier Analysis (FFT) of the output voltage/current wave shapes. Modulation is the method of switching the semiconductor device in a power converter in accordance with some switching function [6]-[8]. With the increased topological advances of MLIs, the modulation techniques have also grown over the years. It reviewed various types of MLI topologies, control techniques, applications and also recent advances in MLIs.

Performance of switching strategies in an inverter, can be related to the harmonic contents of its output voltage. To destroy extreme number of harmonics amplitudes in single-phase inverters using smallest imaginable number of angles an improved SHM-PAM technique is presented in this paper. All triplen harmonics are also excluded without adding extra pulses [1]-[4]. Harmonics are integral multiples of some fundamental frequency that, when added together, result in a distorted waveform shown in fig.1.

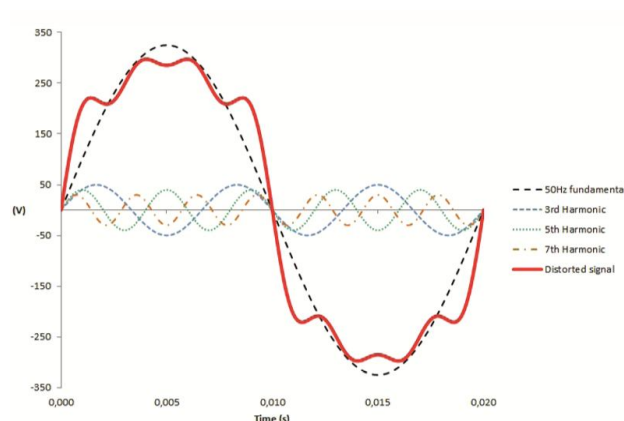


Fig-1: Decomposition example of a complex distorted signal, as addition of 50Hz fundamental and 3rd, 5th and 7th harmonics (150Hz, 250Hz, 350Hz respectively).

A. SELECTIVE HARMONIC MITIGATION PULSE AMPLITUDE MODULATION (SHM-PAM)

Selective Harmonic Elimination or Mitigation (SHE or SHM) modulation techniques have been offered as a solution in several literatures to eliminate or mitigate the of lower order harmonics amplitude in low switching frequency. In both control approaches, firing pulses for power switches are obtained. However, Selective Harmonic Mitigation technique can act more flexible than Selective Harmonic Elimination in terms of more number of harmonics components reduction and voltage controlling. This excellence is because of the statistic that the non-eliminated harmonics in the SHE are left uncontrolled [1]-[2].

The Fourier decomposition of voltage waveform is

$$V_{out} = \sum_{n=1,3,5,\dots}^{\infty} (H_n \sin(n\omega t)) \quad (1)$$

Where H_n specifies amplitude of n -th voltage harmonic order:

$$H_n = \frac{4}{n\pi} \sum_{i=1}^m (V_i \cos(n\alpha_i)) \quad (2)$$

$n = 1, 3, 5, \dots$

For a typical low frequency voltage the conventional SHM equations is expressed as,

$$\begin{cases} F_1 = \frac{4}{\pi} \sum_{i=1}^m (V_i \cos(\alpha_i)) = m_a \\ F_n = \frac{4}{\pi} \sum_{i=1}^m (V_i \cos(n\alpha_i)) \leq m_a L_n \quad \forall n = 5, 7, \dots, 49 \end{cases} \quad (3)$$

According to Eq. (3), all non-triplen harmonics up to 49th order are considered in the SHM equations to obtain more flexible results than the SHE technique. To assign suitable coefficient for each sub-function the SHM formula requires to redefine as an objective function (OF) as the following

$$OF(\alpha_1, \dots, \alpha_m, V_1, \dots, V_m) = \sum_{n=1,5,7,\dots,49} C_n (F_n^2) + C_{THD} THD \quad (4)$$

The coefficients in SHM's OF (C_n) are assumed as

$$C_1 > C_3 > \dots > C_{49} \quad (5)$$

In the proposed SHM formula, the values of DC sources are assumed to change linearly with respect to m_a while switching angles are kept constant. The relationship between the DC sources voltage and m_a must be as follow:

$$V_i = A_i m_a \quad (6)$$

so as to mitigate more amplitude of harmonics, the following criteria should be met.

$$0 < A_i < 1 \quad (7)$$

m_a will be unconcerned from equations by replacing Eq. (6) into the conventional SHM equations Eq.(3) and the SHM-PAM equation will be achieved as:

$$\begin{cases} F_{new1} = \sum_{i=1}^m (A_i \cos(\alpha_i)) = \frac{\pi}{4} \\ F_{newn} = \sum_{i=1}^m (A_i \cos(n\alpha_i)) \leq \frac{n\pi}{4} L_n \quad \forall n = 5, 7, \dots, 49 \end{cases} \quad (8)$$

B. TOTAL HARMONIC DISTORTION (THD)

The THD is an effective index to evaluate the status of harmonic contents in any staircase voltage waveform. Moreover, the THD is a criterion to indicate that how the waveform is similar and close to the sine wave. THD value in SHM-PAM technique shown in fig.2. Thus, the THD's formula is computed by [2]:

$$THD = \frac{\sqrt{\sum_{n=3,5,7,\dots,49} H_n^2}}{H_1} \quad (9)$$

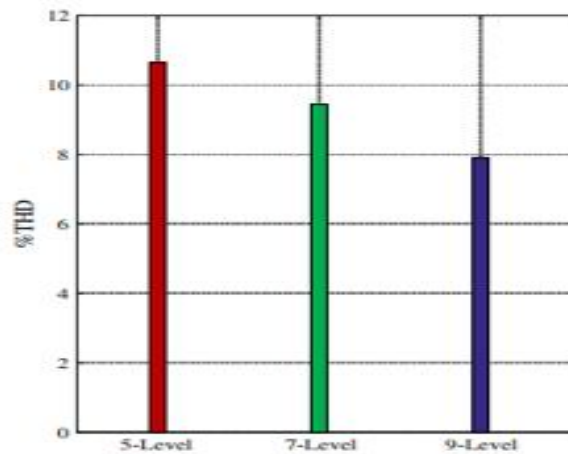


Fig-2: THD value in SHM-PAM technique

II SINGLE PHASE FIVE LEVEL CASCADED H-BRIDGE INVERTER

The Existing System, SHM-PAM algorithm on a 2-cell single-phase Cascaded H-Bridge (CHB) inverter as a typical five level configuration shown in fig.3 dealing with linear and nonlinear loads. Then, it is demonstrated that the maximum number of harmonic orders would be controlled with the minimum number of available angles in a low switching frequency voltage waveform.

Existing construction carrier-based pulse width modulation (PWM) methods don't have any special provisions once inverters operate at low modulation indices. Construction sub harmonic PWM developed by Carrara and change frequency optimum PWM developed by steinke. The modulation wave shape within the carrier bands and a few levels go unused in each these strategies at low modulation indices. The house vector technique developed by liu for low modulation index regions was due to the utilization of slow-switching thyristors and not as a method to maximize device utilization.

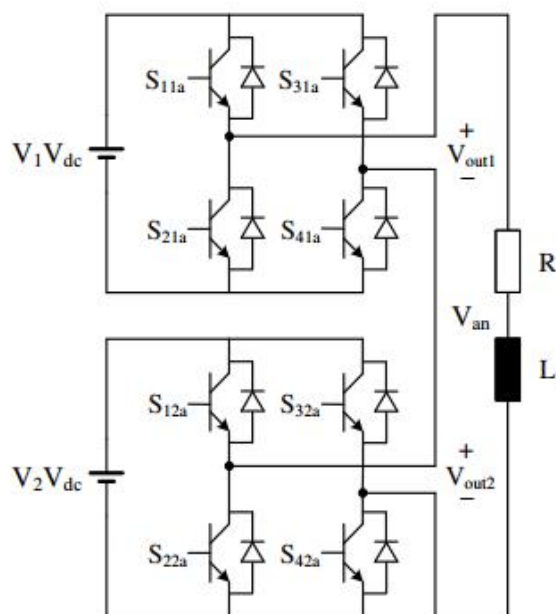


Fig-3: Single phase five level cascaded H-Bridge inverter

III SINGLE PHASE SEVEN LEVEL CASCADED H-BRIDGE INVERTER

The SHM-PAM rule on a 3-cell single-phase Cascaded H-Bridge (CHB) electrical converter as a typical 7 level configuration shown in fig.4 managing linear and nonlinear loads. The corresponding output waveform for seven level inverter shown in fig.6. Then, it's incontestable that the variety of harmonic orders would be controlled with the minimum variety of obtainable angles in a very low switch frequency voltage modulation. The single phase H-bridge cell, which is the building block for the cascaded H-bridge inverter is associated with separate dc sources. The inverter dc bus voltage V_{dc} is usually fixed, while its ac output voltage V_{ab} can be adjusted by either bipolar or unipolar modulation schemes. With different combinations of four switches, S_1 to S_4 , each inverter level can generate three different voltages at the output $+V_{dc}$, $-V_{dc}$ and 0.

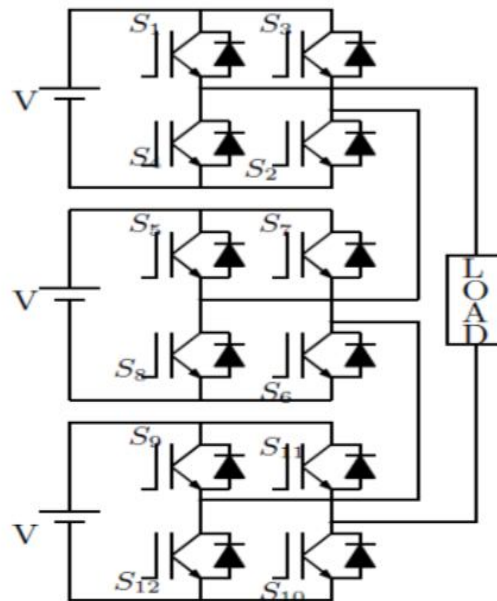


Fig-4: Single phase seven level cascaded H-Bridge inverter

One of the foremost challenges in single-phase structures is mitigation of triplen harmonics at intervals the output energy to beat this balk the number of shift transitions ought to be inflated but it ends up in higher shift loss and lower efficiency. Throughout this paper a modified strategy is introduced to mitigate triplen harmonics in single-phase structures whereas the shift frequency is unbroken low.

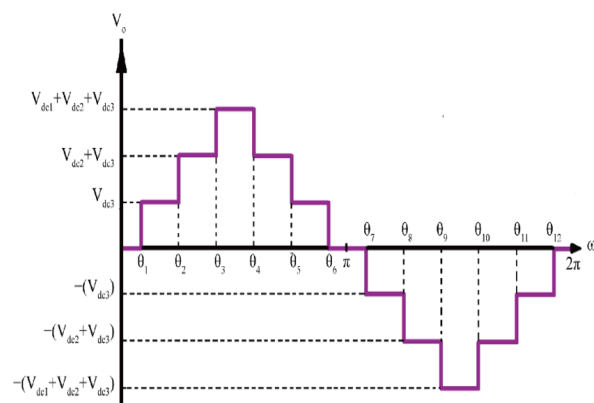


Fig-5: Output waveform

IV RESULTS OF SIMULATION

Some simulation tests have been carried out using MATLAB/Simulink for single phase seven-level CHB inverter to evaluate the feasibility of the SHM-PAM technique and the obtained results. The parameters used in the simulation are: the nominal voltage for each separated DC sources, $V_{dc}=100$ V, the output R-L load, $R=40\ \Omega$ & $L=20$ mH. As well, the frequency of output voltage is 50 Hz. The simulation results have been presented for to prove that the pulses width are constants while the value of ma changes. Simulation circuit for seven level CHB and corresponding output shown in fig.6-9.

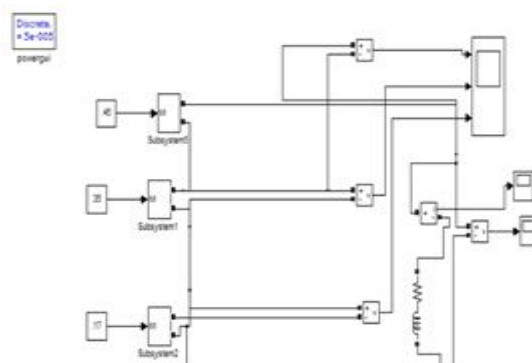


Fig-6: Simulink circuit of single phase seven level cascaded H-Bridge inverter

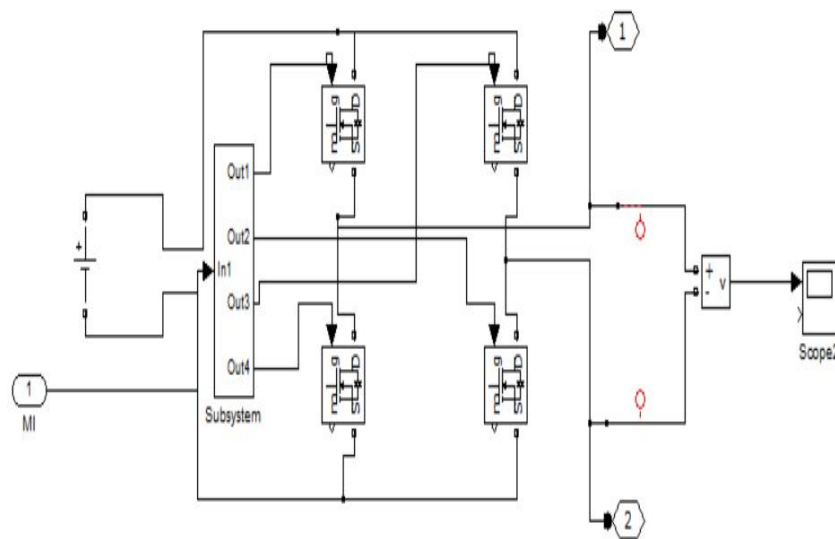


Fig-7: Simulation circuit of cell 1 of CHB inverter

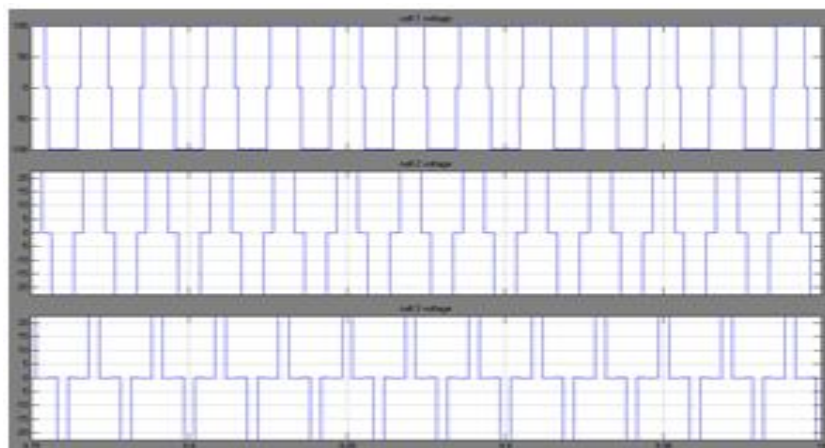


Fig-8: Output voltage of inverter

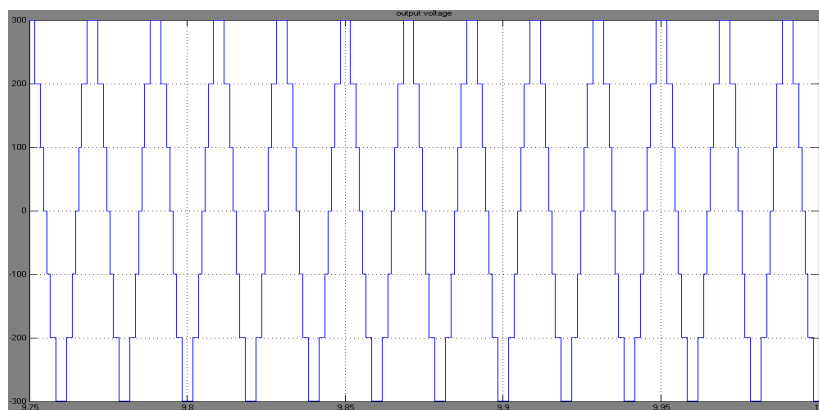


Fig-9: Output voltage of load

V CONCLUSION

In order to eliminate all triplen harmonics a novel state for two angles in seven-level low switching frequency voltage waveform has been projected to change conventional SHM-PAM equations. The normal SHM relations mitigate 5th and 7th harmonic orders without considering added pulses. The advantage of it is controlling maximum number of harmonics amplitudes with minimum number of variables in single-phase inverter where both triplen and non-triplen order have to be considered in the equations. All triplen harmonics are eliminated. Hereafter, compared to conventional SHM-PAM technique the modified SHM-PAM technique has fewer number of equations while more harmonics could be controlled. The offered method has been applied on single-phase seven-level CHB inverter and verified below both linear and nonlinear loads. It will be suitable for single-phase UPS application that must supply these type of loads in real-world conditions.

REFERENCES

1. Mohammad Sharifzadeh, Hani Vahedi, Ramon Portillo, Leopoldo Garcia Franquelo, Kamal Al-Haddad, "Selective Harmonic Mitigation Based Self-Elimination of Triplen Harmonics for Single-Phase Five-Level Inverters" 2018
2. J. Nápoles Luengo, A. Watson, J. J. Padilla, L. Galván, J. Ignacio, L. García Franquelo, et al., "Selective Harmonic Mitigation Technique for Cascaded H-Bridge Converters With Nonequal DC Link Voltages," 2013.
3. S. K. Sahoo and T. Bhattacharya, "Phase-Shifted Carrier-Based Synchronized Sinusoidal PWM Techniques for a Cascaded H-Bridge Multilevel Inverter," IEEE Transactions on Power Electronics, vol. 33, pp. 513-524, 2018.
4. L. G. Franquelo, J. Napoles, R. C. P. Guisado, J. I. León, and M. A. Aguirre, "A flexible selective harmonic mitigation technique to meet grid codes in three-level PWM converters," IEEE Transactions on Industrial Electronics, vol. 54, pp. 3022-3029, 2007.
5. J. Napoles, J. I. Leon, R. Portillo, L. G. Franquelo, and M. A. Aguirre, "Selective harmonic mitigation technique for high-power converters," IEEE Transactions on Industrial electronics, vol. 57, pp. 2315-2323, 2010.
6. J. Pontt, J. Rodríguez, and R. Huerta, "Mitigation of Noneliminated Harmonics of SHEPWM Three-Level Multipulse Three-Phase Active Front End Converters With Low Switching Frequency for Meeting Standard IEEE-519-92," IEEE Transactions on Power Electronics, vol. 19, pp. 1594-1600, 2004.
7. A. Moeini, H. Zhao, and S. Wang, "A Current Reference based Selective Harmonic Current Mitigation PWM Technique to Improve the Performance of Cascaded H-bridge Multilevel Active Rectifiers," IEEE Transactions on Industrial Electronics, vol. PP, pp. 1 - 1, 2016.
8. L. M. Tolbert, F. Z. Peng, and T. G. Habetler, "Multilevel PWM methods at low modulation indices," IEEE Transaction on Power Electronics, vol. 15, no. 4, pp. 719-725, Jul. 2000.
9. M. S. Dahidah, G. Konstantinou, and V. G. Agelidis, "A review of multilevel selective harmonic elimination PWM: formulations, solving algorithms, implementation and applications," IEEE Transactions on Power Electronics, vol. 30, pp. 4091-4106, 2015.
10. J. Li, S. Bhattacharya, and A. Q. Huang, "A new nine-level active NPC (ANPC) converter for grid connection of large wind turbines for distributed generation," IEEE Transaction on Power Electronics, vol. 26, no. 3, pp. 961-972, Mar. 2011.

SINGLE-STAGE SWITCHED-BOOST INVERTER WITH FOUR SWITCHES FOR AC/DC APPLICATION

J. Jayasri

PG Scholar

Department of Electrical and Electronics Engineering, E. G. S. Pillay Engineering College (Autonomous),
Nagapattinam, Tamilnadu

ABSTRACT

This paper intends a recent single-phase single-stage switched-boost device among four switches for ac and dc application. The same as the quasi-z-source device QZSI and quasi-switched boost device QSBI the planned device have the foremost selections as incessant input current buck/boost voltage with single-stage alteration and shoot-through imperviousness. Compared to the QSBI the planned device relates an additional condenser and removes one diode and one a smaller amount control. This paper presents the operational principles PWM management policy restriction vogue tips and simulation results for the planned device. To authenticate the routine of the planned device associate 100 w example be designed by associate a 230V/50 cycle output voltage in complete and grid-connected method. By using this system we get dual output (AC & DC) without affecting the output voltage. Compared to the previous system this inverter has low input voltage but to gain high output voltage. It shares the total voltage in both AC and DC applications. The simulation and experimental results harmonized those of the theoretical analysis.

Keywords: Switched boost inverter, Quasi-Z-source, shoot-through resistance.

I. INTRODUCTION

High gain inverters realize wide selection of applications in trade like renewable force systems/distributed production systems engineering drives ups classification electrical vehicles etc. [2]. Inverters for renewable or ups applications need high voltage boosting action attributable to the low-voltage output nature of the renewable cause and storage space systems like star PV fuel cells batteries etc. [3]. (VSI) voltage source inverter is thus not appropriate for this sort of applications because it will solely manufacture associate degree ac output voltage under its dc put. Boost feature is typically additional to VSI by inserting a lift primarily based convertor in cascade [1]-[3]. These inverters but suffer from the subsequent disadvantages: the boost quantitative relation of the standard boost convertors restricted due to the circuit non-idealities. This prevents operation of the system at terribly high boost mode viz. achieving 110/220 v r.m.s. ac from 24/48 v dc input. Because the convertor structure contains a VSI connected at the dc link the convertor is susceptible to get broken thanks to electromagnetic interference (EMI) [4]-[9]. EMI will cause spurious turn-on of prime and bottom switches of any electrical converter leg inflicting the dc link electrical device or dc supply to short which may harm the switches. Thanks to the worldwide force challenge grid-tied inverters for the renewable power cause have become wide used today's. They'll be divided into voltage-source inverters and current-source inverters [11] wherever the VSI is that the dominant convertor. One amongst explanations is that the VSI doesn't want an oversized electrical device because the energy storage space part whereas the (CSI) current source inverter ought to adopt a bigger electrical device so as to stay the dc current constant for a correct modulation. The analysis associated with CSI in the main specializes in the management [12]. So far a way to decrease the whole dc-link inductance for CSI may be a challenge particularly within the low voltage and three-phase application space. A boost device modify of degree device may well be a dc-to-dc power device alongside connect output rule larger than its input rule. It's a class of switched-mode management provide switched mode power supply (SMPS) surround a minimum of 2semiconductors a diode and a joint semiconductor and a minimum of one energy storage a tool inductance or the 2semiconductors on. To diminish the size, heaviness and price of the power inverters, a switched-boost inverter (SBI) is proposed. Filters mass-produced from capacitors typically alongside inductors are typically further to the output of the machine to cut back output power ripple.

II. SINGLE PHASE SINGLE STAGE SWITCHED BOOST INVERTER WITH FOUR SWITCHES

The circuit schematic of improved inverter [4]-[9] is shown in fig. 1. It achieves high boost by utilizing the force transfer through the device action of the coupled device l1 and l2 among turns-ratio one the planned convertor contains of a filled with life confrontation network which contains coupled device l1, l2 among n1primary and n2 secondary turns capacitance co controlled switch s two diodes prosecuting attorney that precedes the sole section converter bridge. The secondary winding type of turns n2 is typically unbroken however primary type of turns n1 for proper converter operation.

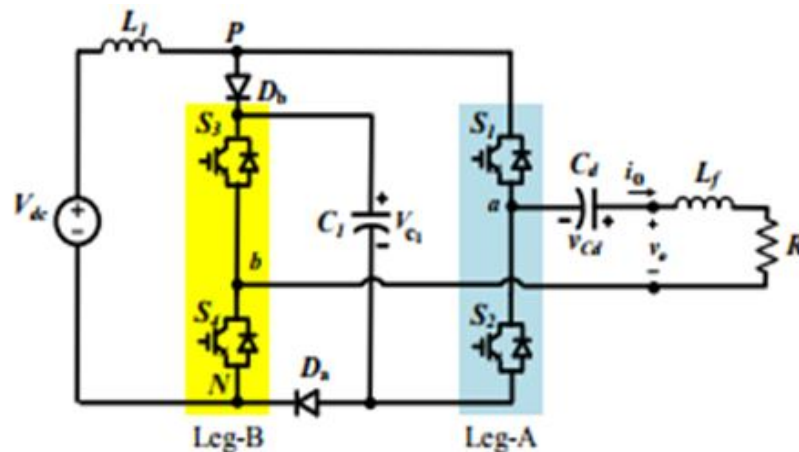


Figure-1: Single Phase Switched Boost Inverter Circuit Diagram

In fig. 1 switch s and converter bridge switches unit of measurement shown victimization they're going to even be accomplished victimization of MOSFETS. As active devices within the main represent the resistance network among the planned converter it'll be thought of as a filled with life resistance network. This will get on the contrary to the quality resistance provide network thought where passive parts kind most an area of this network planned converter operates during an extremely in a very shoot-through duty interval or d interval and b non-shoot-through interval or $1-d$ interval in an exceedingly switch cycle. The shoot-through state is achieved by turning on every switches of any converter leg s_1-s_4 or s_3-s_2 along with switch s . In non-shoot-through state switch s is turned off whereas diodes prosecuting attorney and enter conduction; the converter bridge are going to be either in power state s_1-s_2 or s_3-s_4 turned on or in free-wheeling state s_1-s_3 or s_2-s_4 turned on. So the planned converter has six permissible operative states: I two shoot-through interval or duty d interval II two non-shoot-through active or power intervals and III two non-shoot-through zero or free-wheeling interval. The planned converter among the three operative states is shown from fig. 1 a severally. In this system the input voltage is given by regulated power supply only. Because 19v battery is not available in market. This inverter has some disadvantages are easily component failure, lower efficiency and increased voltage stress and also produced single output only.

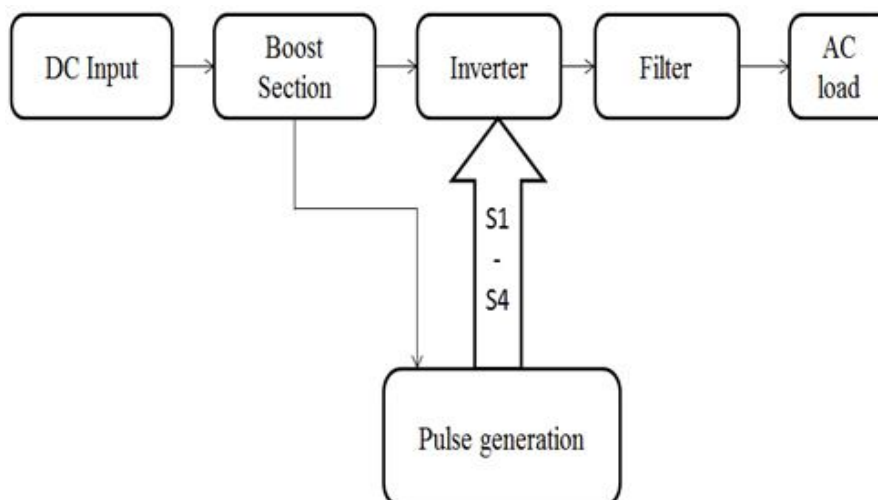


Figure-2: Boost Inverter with Four Switches

III. SINGLE-STAGE SWITCHED-BOOST INVERTER WITH FOUR SWITCHES FOR AC/DC APPLICATION

Single-stage switched-boost inverter with four switches for ac/dc application represents for the dc contribution supply sent during the boost converter this converter is use single inductance and single diode in improve operation. In this system input voltage is given by power supply or else also given by renewable energy like solar, wind. After that output is given this technique is that the electrical converter or ac output. The filters employed for this course is purpose of separate out the unwanted noise and can gets dual outputs at the same time. By using this system we produced dual output (AC & DC) without affecting output voltage. It shares the total voltage in both applications. The simulation and ground breaking results counterpart those of the theoretical analysis is shown below. Compared to the previous system the proposed inverter has benefits like low cost, reduced component counts, high efficiency and increased voltage gain.

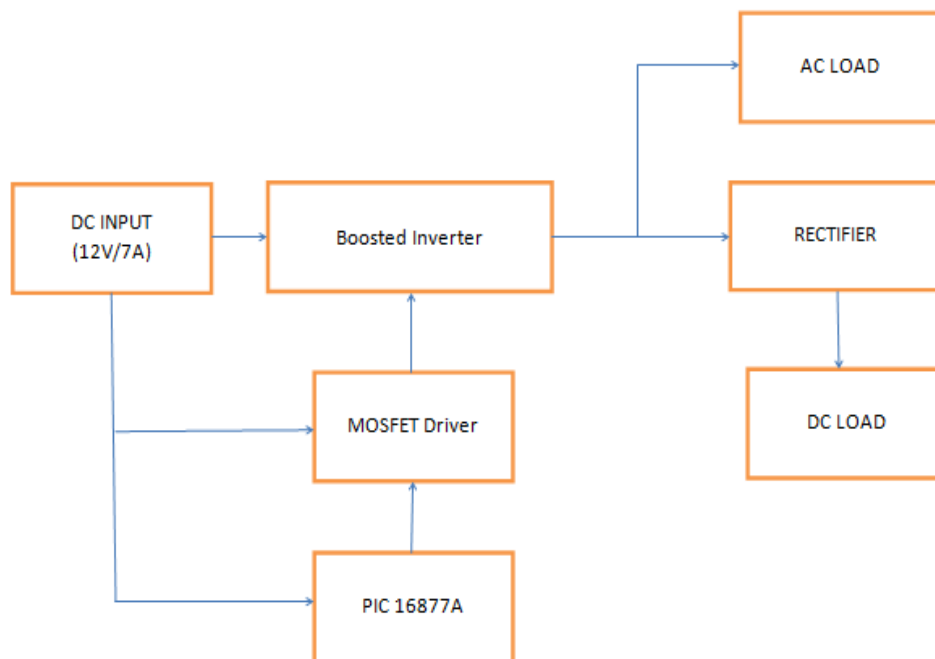


Figure-3: Single-Stage Switched-Boost Inverter with Four Switches for AC/DC Application Block Diagram

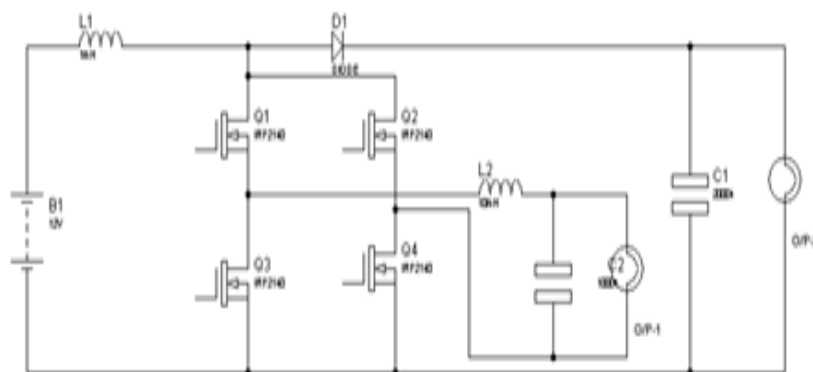


Figure-4: Single-Stage Switched-Boost Inverter with Four Switches for AC/DC Application

A MODES OF OPERATION

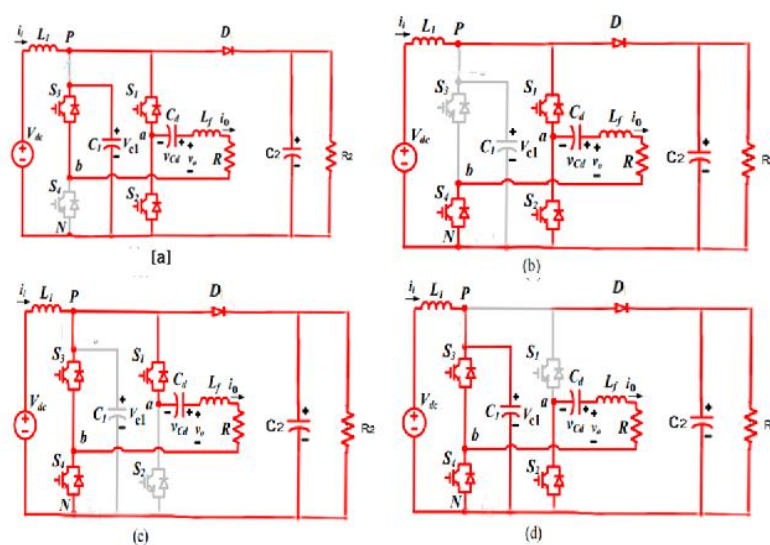


Figure-5: Shoot through Modes

- a) MODE 1
- c) MODE 3

- b) MODE 2
- d) MODE 4

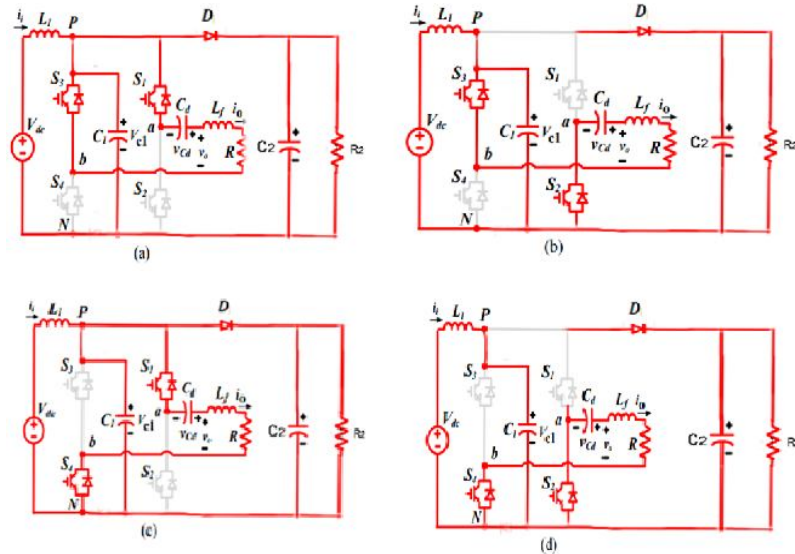


Figure-6: Non Shoot through Modes

- a) MODE 5 b) MODE 6
b) MODE7 d) MODE 8

IV. MATLAB RESULTS

MATLAB is a high-performance language for technical computing MATLABR2009b. It integrates computation, visualization, and programming in an easy-to-use environment where problems and solutions are expressed in familiar mathematical notation. Typical uses include,

- Math and computation
- Algorithm development
- Modeling, simulation, and prototyping
- Data analysis, exploration, and visualization
- Scientific and engineering graphics
- Application development, including Graphical User Interface building

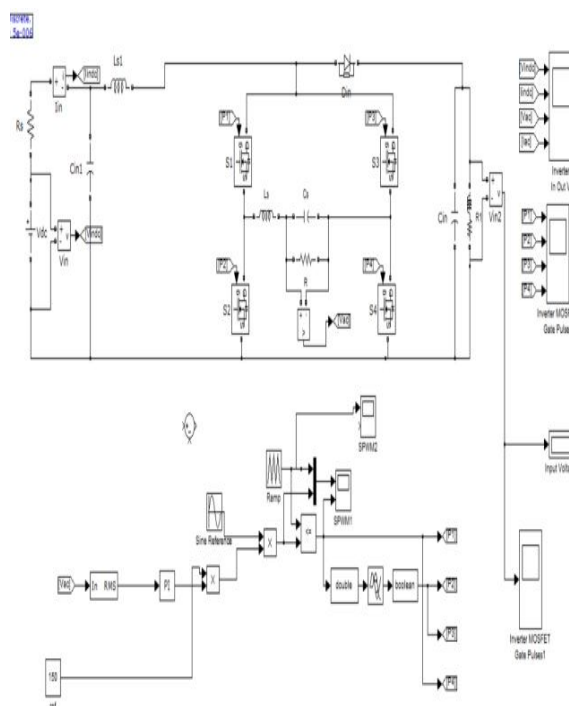


Figure-7: Simulation Circuit of Single-Stage Switched-Boost Inverter with Four Switches for AC/DC Application.

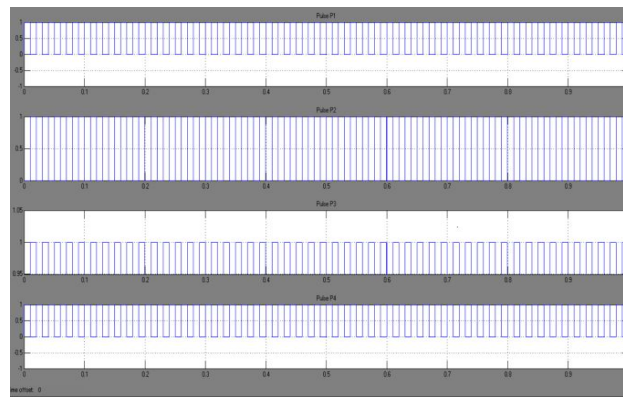


Figure-8: Pulse Generation of MOSFETS

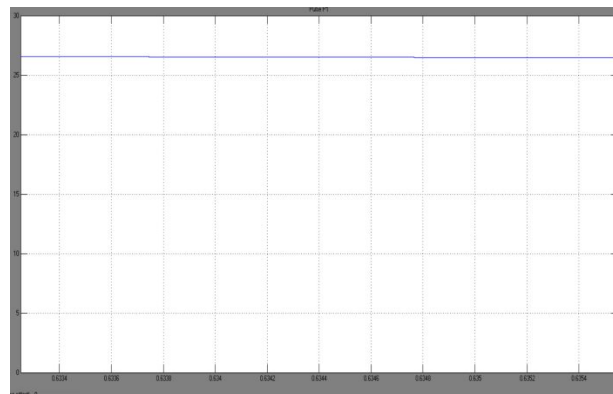


Figure-9: DC output voltage

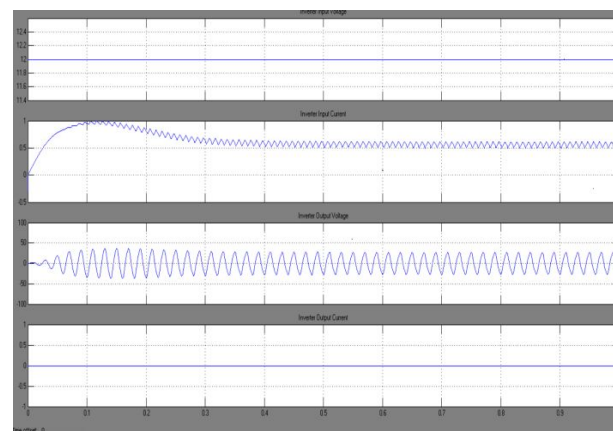


Figure-10: Output and Input of Voltage & Current Waveform for Single-Stage Switched-Boost Inverter with Four Switches for AC/DC Application

V. CONCLUSION

Single-Stage switched-boost inverter with four switches for ac/dc application was projected throughout this paper. The projected convertor contains a high responsibility as a result of it resists every shoot-through and open circuit development. By victimization this concept we tend to urge twin output voltage i.e. ac and dc output voltage that output voltage is equally distributed. To boost the ac output voltage of the projected converter is higher or below the dc input voltage. As results of the dc capacitance filter is utilized to urge obviate dc part of the output voltage the projected convertor cannot operate with the physical phenomena load that the capacitance and device connected asynchronous. A try of qsbi has an additional active switch than zs/qzsi; this rating on each the switches and diodes for qsbi can be a smaller amount than those for qzsi. Operational principles analysis PWM management theme parameter vogue pointers and simulation results are given. The laboratory example was designed to verify the operational theory of the projected convertor in complete and grid-connected modes. The input voltage of the projected convertor is 12v and produces the output of 24v ac and 24v dc is shown above in fig. 9 and 10. Using this system we get dual output (AC & DC) without affecting output voltage. It shares the total voltage in both applications. A bit like the quality boost convertor the projected convertor introduces a low frequency current at the input. Further analysis got to be administered to eliminate the low frequency input current of the projected convertor.

VI REFERENCE

1. Y. Xue, L. Chang, "Topologies of single-phase inverters for small distributed power generators: an overview," *IEEE Transactions on Power Electronics*, vol. 19, no. 5, pp. 1305–1314, Sept. 2004.
2. S. Dasgupta, S. K. Sahoo, and S. K. Panda, "Single-phase inverter control techniques for interfacing renewable energy sources with microgrid—part I: parallel-connected inverter topology with active and reactive power flow control along with grid current shaping," *IEEE Transactions on Power Electronics*, vol. 26, no. 3, pp. 717–731, March 2011.
3. Tan Kheng Suan Freddy, N. A. Rahim, "Comparison and analysis of single-phase transformerless grid-connected PV inverters," *IEEE Transactions on Power Electronics*, vol. 29, no. 10, pp. 5358–5369, Oct. 2014.
4. R. O. Caceres, and I. Barbi, "A boost DC-AC converter: analysis, design, and experimentation," *IEEE Transactions on Power Electronics*, vol. 14, no. 1, pp.134–141, Jan. 1999.
5. P. Sanchis, A. Ursæa, E. Gubía, and L. Marroyo "Boost DC-AC inverter: a new control strategy," *IEEE Transactions on Power Electronics*, vol. 20, no. 2, pp. 343–353, March 2005.
6. D. B. W. Abeywardana, "A rule-based controller to mitigate dc-side second-order harmonic current in a single-phase boost inverter," *IEEE Transactions on Power Electronics*, vol. 31, no. 2, pp. 1665–1679, Feb. 2016.
7. D. B. W. Abeywardana, B. Hredzak, and V. G. Agelidis, "An input current feedback method to mitigate the dc-side low-frequency ripple current in a single-phase boost inverter," *IEEE Transactions on Power Electronics*, vol. 31, no. 6, pp. 4594–4603, June 2016.
8. J. Kan, S. Xie, Y. Wu, Y. Tang, Z. Yao, and R. Chen "Single-stage and boost-voltage grid-connected inverter for fuel-cell generation system," *IEEE Transaction on Power Electronics*, vol. 62, no. 9, pp. 5480–5490, Sept. 2015.
9. H. Ribeiro, A. Pinto, and B. Borges, "Single-stage DC-AC converter for photovoltaic systems," in *Proc. IEEE Energy Conversion Congress and Exposition*, 2010, pp. 604–610.
10. B. Ge, Y. Liu, H. Abu-Rub, "An active filter method to eliminate dc-side low-frequency power for a single phase quasi-z-source inverter," *IEEE Transaction on Ind. Electronics*, vol. 63, no. 8, pp. 4838-4848, Aug 2016.
11. B. N. Alajmi, K. H. Ahmed, G. P. Adam, and B. W. Williams, "Single-phase single-stage transformer less grid-connected PV system," *IEEE Transaction on Power Electronics*, vol. 28, no. 6. pp. 2664-2676, June 2013.
12. Sorrel Alistair Shield Grogan, D. G. Holmes, and B. P. McGrath, "High-performance voltage regulation of current source inverters," *IEEE Transaction on Power Electronics.*, vol. 26, no. 9, pp. 2439–2448, Sept. 2011.
13. Minh-Khai Nguyen, "Trans-switched boost inverters," *IET Power Electronics.*, vol. 9, no. 5, pp. 1065–1073, April 2016.
14. S. S. Nag, and S. Mishra, "A coupled inductor based high boost inverter with sub-unity turns-ratio range," *IEEE Transaction on Power Electronics*, vol. 31, no. 11, pp. 7534–7543, Nov. 2016.
15. Minh-Khai Nguyen, "A comparison between single-phase quasi-Z-source and quasi-switched boost inverters," *IEEE Transaction on Power Electronics*, vol. 62, no. 10, pp. 6336 - 6344, Oct. 2015.

A COMPARATIVE ANALYSIS OF CLASSICAL THREE PHASE MULTILEVEL (FIVE LEVEL) INVERTER TOPOLOGIES

K. Kalaivanan¹ and K. Nandakumar²

PG Scholar¹ and Assistant Professor²

Department of Electrical and Electronics Engineering, E. G. S. Pillay Engineering College (Autonomous),
Nagapattinam, Tamilnadu

ABSTRACT

Multilevel inverters are an attractive choice for multi mega-watt industrial drive applications. In comparison with conventional two level voltage source inverter this technology gives quality performance. In this paper comparison of three classical topologies of three phase multilevel inverter is presented. The multi level inverters analyzed using MATLAB-Simulink software are Neutral Point- Clamped or Diode Clamped Multilevel Inverter (NPCMLI or DC-MLI) Flying Capacitor Multilevel Inverter (FCMLI) and Cascaded H-Bridge Multilevel Inverter (CHBMLI). The comparison is based on output voltage quality and power circuit complexity. Each inverter is controlled by the multi-carrier sinusoidal pulse width modulation (MCSPWM).

Keywords: Multilevel inverters, multi-carrier sinusoidal pulse width modulation, Battery.

I INTRODUCTION

Present day world is facing enormous increase in energy consumption. Multilevel inverter is an important technology in the field of power electronics. For industrial applications multi level inverter fed a.c. drive gives quality performance and is best option for energy saving. Multilevel inverter uses medium voltage semiconductor devices, sources and produces high output power. Sources like batteries, super capacitors, solar panels can be used as medium voltage sources. This technology is showing popularity for multi mega watt industrial drive application. As compared to conventional two level inverter, in which harmonic contents can be reduced by raising switching frequency, multilevel inverter has many advantages such as output voltage waveform can be generated at low switching frequencies thereby reducing switching losses, more efficiency, low harmonic distortion and near sinusoidal output. There are less voltage stresses on power switches and low electromagnetic interference. However, this multi level technology requires more number of switches which makes the control circuitry complicated. Recently, some new multi level inverter topologies have been presented. It includes asymmetric and/or hybrid inverters. In asymmetric topology unequal d.c. source magnitudes are used while hybrid inverters are designed by using different topologies, applying different modulation techniques or semiconductor technologies. The main objective of recent novel topologies is to reduce number of components required as compared to classical topologies. In recently introduced and updated topologies are reviewed. However the novel topologies have some drawbacks such as loss of modularity, problems with switching frequencies and restrictions on the modulation and control method. To control multilevel inverters there exist different modulation methods. They are sinusoidal pulse width modulation (SPWM), selective harmonic elimination (SHE-PWM), space vector modulation (SVM) etc. These methods can be classified according to switching frequencies used.

In industrial applications the SPWM control method is very popular. Based on the classical SPWM, for multilevel technology various multi-carrier techniques have been developed. They are helpful to reduce the harmonics in the output waveforms. Fundamental switching frequency can be used for SVM and SHE-PWM methods. Commutations of the power switches take place once or twice during one cycle of the output voltages to generate a staircase waveform. Comparative analysis of MATLAB simulated models of three classical topologies is carried out in this paper by using MC-SPWM.

II EXISTING METHOD

Neutral Point Clamped Multilevel Inverter (NPCMLI) is also known as Diode Clamped Multilevel Inverter (DC-MLI), proposed by Nabae et al., in 1981. This was the first generation of multilevel technology which was basically a three level inverter. Researchers' efforts made this topology known as state-of-the-art of multilevel technology.

A d.c. link is divided into four capacitors C1, C2, C3 and C4 and connects to switches in series through clamping diodes. Due to this arrangement one capacitor voltage will appear across each switch. If d.c. link voltage is V_{dc} , then voltage across each capacitor will be $V_{dc}/4$. This topology requires $(n-1) \times (n-2)$ clamping/blocking diodes per phase, if each diode has voltage rating same as active device voltage rating. Here n is number of inverter output voltage levels. Means, requirement of clamping diodes increases with increase in n , which makes the topology bulky and impractical.

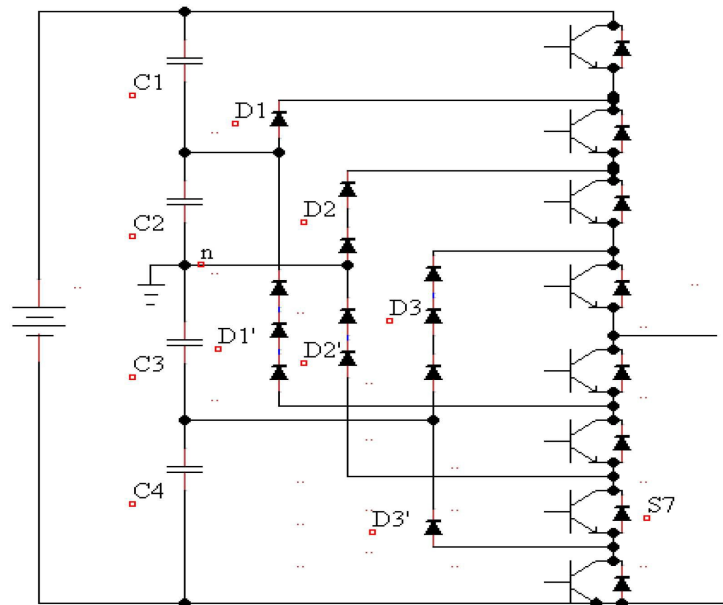


Fig-1: Single Phase FiveLevel NPC-MLI

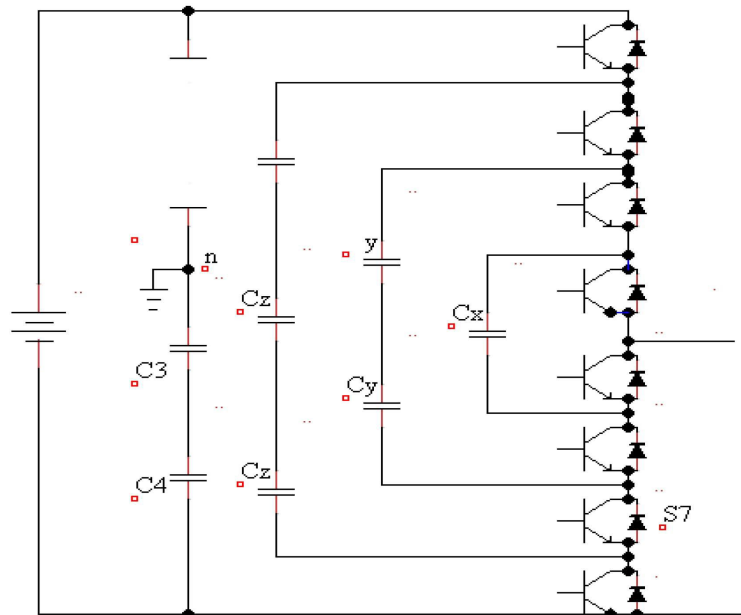


Fig-2: Single Phase Five Level FC-MLI

III PROPOSED SYSTEM

1. Working Principle

In conventional multilevel converters, the power semiconductor switches are combined to produce a high-frequency waveform in positive and negative polarities. However, there is no need to utilize all the switches for generating bipolar levels. This idea has been put into practice by the new topology. This topology is a hybrid multilevel topology which separates the output voltage into two parts. One part is named level generation part and is responsible for level generating in positive polarity. This part requires high frequency switches to generate the required levels. The switches in this part should have high-switching frequency capability the other part is called polarity generation part and is responsible for generating the polarity of the output voltage which is the low-frequency part operating at line frequency. The topology combines the two parts (high frequency and low frequency) to generate the multilevel voltage output. In order to generate a complete multilevel output, the positive Levels are generated by the high-frequency part (level generation), and then, this part is fed to a full-bridge inverter (polarity generation), which will generate the required polarity for the output. This will eliminate many of the semiconductor switches which were responsible to generate the output voltage levels in positive and negative polarities. The RV topology in seven levels is shown in Fig. 1. As can be seen, it requires ten switches and three isolated sources. The principal idea of this topology as a multilevel inverter is that the left stage in Fig. 1 generates the required output levels (without polarity) and the right circuit (full-bridge converter) decides about the polarity of the output voltage.

2. BLOCK DIAGRAM

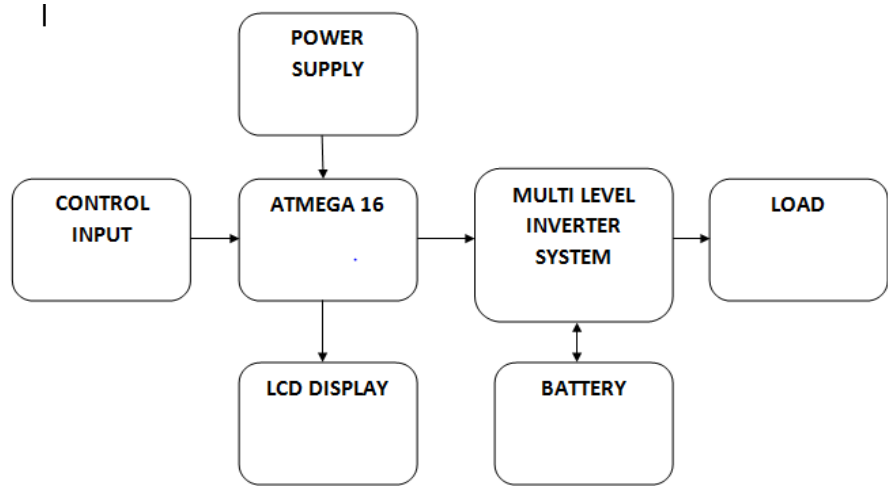


Fig-3: Block Diagram of Proposed System

3. CIRCUIT DIAGRAM

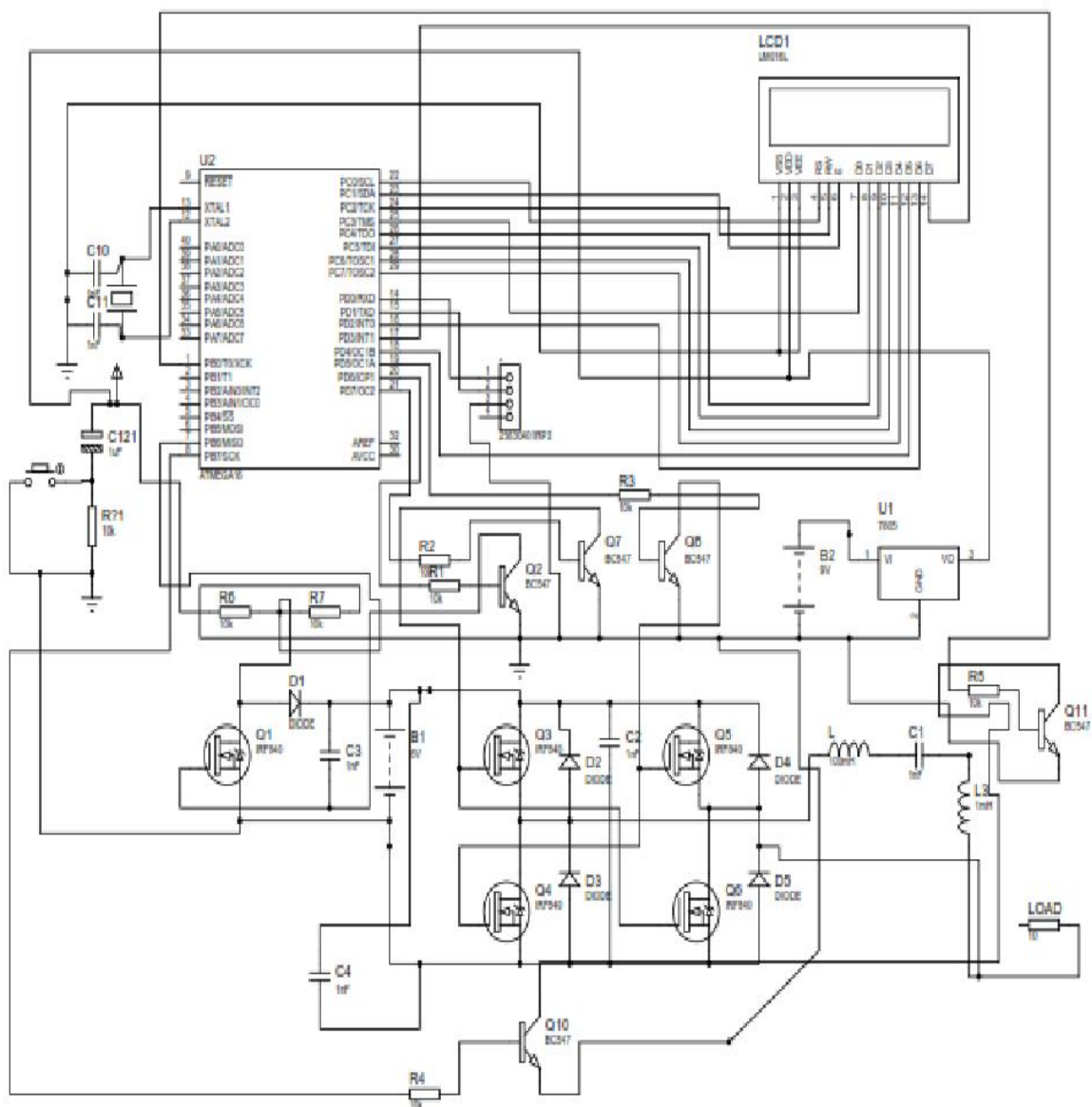


Fig-4: Circuit Diagram of Proposed System

IV MATLAB RESULT

1. SIMULINK DIAGRAM

Fig 11. Simulation Diagram of Proposed system

2. INPUT

i) Input Voltage

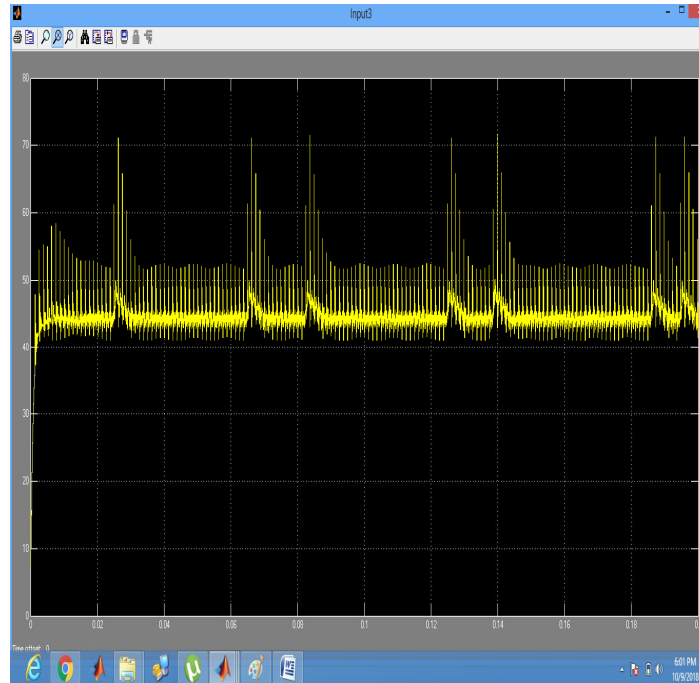


Fig-12: Input Voltage

ii) Input voltage and current from source

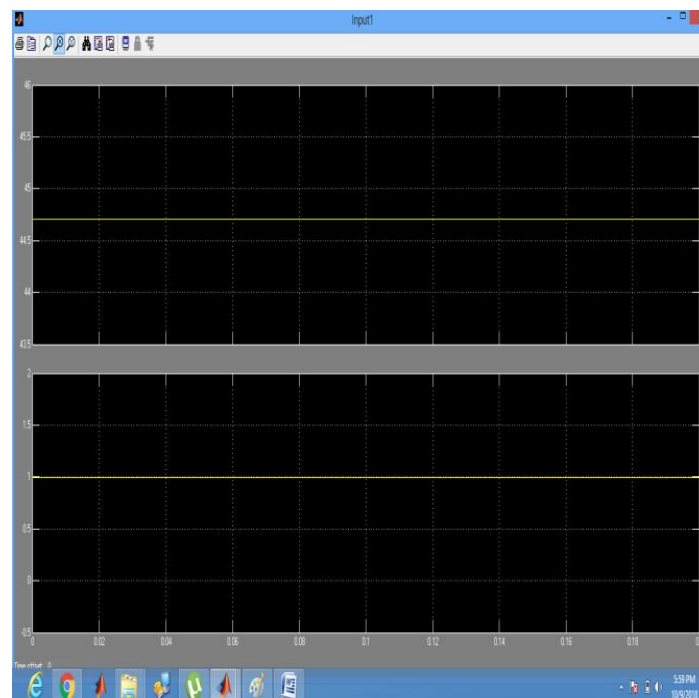


Fig-13: Input Voltage and current from source

V CONCLUSION

This paper presents comparison of three classical topologies (NPC-MLI, FC-MLI, CHB-MLI) of three phase five level inverter. MATLAB-Simulink models are developed for all the three topologies. Using PD-PWM a novel pulse generation circuit is designed. From simulation results it is observed that the generated voltage spectrum is very much improved for five level inverter topologies. Among three topologies the CHB topology requires least number of components and minimum harmonics in the output voltage.

VI REFERENCE

1. Franquelo, L. G., J. Rodn'guez, J. I. Leon, S. Kouro, R. Portillo, and M. A M. Prats, "The age of multi level converters arrives", IEEE Ind. Electron. Mag., pp. 28-39, Jun. 2008.
2. Jih-Sheng Lai, Fang Cheng Peng " Multi level converters-A newbreed of power converters", IEEE transactions on industryapplications, vol. 32, no. 3, may June 1996.
3. L. Tolbert, F.-Z. Peng, and T. Habetier, "Multilevel converters forlarge electric drives, " IEEE Trans. Ind. Applicat., vol. 35, pp. 36-44, Jan./Feb. 1999.
4. J. Rodriguez, Jih-Sheng Lai, Fang Cheng Peng "Multilevel inverters:A survey of topologies, control, and applications, " IEEETrans. Ind. Electronics, vol. 49, no. 4, pp. 724-738, Aug. 2002
5. ANabae, I. Takahashi, H.Akagi "A new neutral-point clampedPWM inverter" IEEE Trans. On Ind. App. Vol. IA-I7, No.5,September/October 198 I, pp 5 I 8-52
6. F. Z. Peng and J. S. Lai, "Multilevel cascade voltage-sourceinverter with separate DC source, " U.S. Patent 5 642 275, June 24,1997.
7. T. A Meynard, H. Foch, "Multilevel conversion: High voltagechoppers and voltage source inverters, " IEEE-PESC ConferenceRecord, pp.397-403, 1992.
8. P. W. Hammond, "A new approach to enhance power quality formedium voltage AC drives, " IEEE Trans. Ind. Appl., vol. 33, no.I, pp. 202-208, Jan./Feb. 1997.

CONTROL AND OPERATION OF A DC GRID-BASED WIND POWER GENERATION SYSTEM IN A MICROGRID

D. Senthilkumar¹ and R. Anandaraj²PG Scholar¹ and Associate Professor²Department of Electrical and Electronics Engineering, E. G. S. Pillay Engineering College (Autonomous),
Nagapattinam, Tamilnadu

ABSTRACT

This paper presents the design of a dc grid-based wind power generation system in a poultry farm. The proposed system allows flexible operation of multiple parallel-connected wind generators by eliminating the need for voltage and frequency synchronization. A model predictive control algorithm that offers better transient response with respect to the changes in the operating conditions is proposed for the control of the inverters. The design concept is verified through various test scenarios to demonstrate the operational capability of the proposed microgrid when it operates connected to and islanded from the distribution grid, and the results obtained are discussed.

Index Terms: Wind power generation, dc grid, energy management, model predictive control.

I. INTRODUCTION

POULTRY farming is the raising of domesticated birds such as chickens and ducks for the purpose of farming meat or eggs for food. To ensure that the poultries remain productive, the poultry farms in Singapore are required to be maintained at a comfortable temperature. Cooling fans, with power ratings of tens of kilowatts, are usually installed to regulate the temperature in the farms [1]–[3]. Besides cooling the farms, the wind energy produced by the cooling fans can be harnessed using wind turbines (WTs) to reduce the farms' demand on the grid. The Singapore government is actively promoting this new concept of harvesting wind energy from electric ventilation fans in poultry farms which has been implemented in many countries around the world [4]. The major difference between the situation in poultry farms and common wind farms is in the wind speed variability. The variability of wind speed in wind farms directly depends on the environmental and weather conditions while the wind speed in poultry farms is generally stable as it is generated by constant-speed ventilation fans. Thus, the generation intermittency issues that affect the reliability of electricity supply and power balance are not prevalent in poultry farm wind energy systems.

Many research works on dc microgrids have been conducted to facilitate the integration of various DERs and energy storage systems. In [5], [6], a dc microgrid based wind farm architecture in which each wind energy conversion unit consisting of a matrix converter, a high frequency transformer and a single-phase ac/dc converter is proposed. However, the proposed architecture increases the system complexity as three stages of conversion are required. In [7], a dc microgrid based wind farm architecture in which the WTs are clustered into groups of four with each group connected to a converter is proposed. However, with the proposed architecture, the failure of one converter will result in all four WTs of the same group to be out of service. The research works conducted in [8]–[10] are focused on the development of different distributed control strategies to coordinate the operation of various DERs and energy storage systems in dc microgrids. These research works aim to overcome the challenge of achieving a decentralized control operation using only local variables. However, the DERs in dc microgrids are strongly coupled to each other and there must be a minimum level of coordination between the DERs and the controllers. In [11], [12], a hybrid ac/dc grid architecture that consists of both ac and dc networks connected together by a bidirectional converter is proposed. Hierarchical control algorithms are incorporated to ensure smooth power transfer between the ac microgrid and the dc microgrid under various operating conditions. However, failure of the bidirectional converter will result in the isolation of the dc microgrid from the ac microgrid.

Many research works on designing the controllers for the control of inverters in a microgrid during grid-connected and islanded operations is conducted in [13]–[15]. A commonly adopted control scheme which is detailed in [13], [14] contains an inner voltage and current loop and an external power loop to regulate the output voltage and the power flow of the inverters. In [15], a control scheme which uses separate controllers for the inverters during grid-connected and islanded operations is proposed. Although there are a lot of research works being conducted on the development of primary control strategies for DG units, there are many areas that require further improvement and research attention. These areas include improving the robustness of the controllers to topological and parametric uncertainties, and improving the transient response of the controllers.

A. System Description

The overall configuration of the proposed dc grid based wind power generation system for the poultry farm is shown in Fig. 1. The system can operate either connected to or islanded from the distribution grid and consists of four 10 kW permanent magnet synchronous generators (PMSGs) which are driven by the variable speed WT. The PMSG is considered in this paper because it does not require a dc excitation system that will increase the design complexity of the control hardware. The three-phase output of each PMSG is connected to a three-phase converter (i.e., converters A, B, C and D), which operates as a rectifier to regulate the dc output voltage of each PMSG to the desired level at the dc grid. The aggregated power at the dc grid is inverted by two inverters (i.e., inverters 1 and 2) with each rated at 40 kW.

The coordination of the converters and inverters is achieved through a centralized energy management system (EMS). The EMS controls and monitors the power dispatch by each WG and the load power consumption in the microgrid through a centralized server. To prevent excessive circulating currents between the inverters, the inverter output voltages of inverters 1 and 2 are regulated to the same voltage. Through the EMS, the output voltages of inverters 1 and 2 are continuously monitored to ensure that the inverters maintain the same output voltages. The centralized EMS is also responsible for other aspects of power management such as load forecasting, unit commitment, economic dispatch and optimum power flow. Important information such as field measurements from smart meters, transformer tap positions and circuit breaker status are all sent to the centralized server for processing through wireline/wireless communication. During normal operation, the two inverters will share the maximum output from the PMSGs (i.e., each inverter shares 20 kW).

The maximum power generated by each WT is estimated from the optimal wind power $P_{w, opt}$ as follows [23]:

$$P_{w, opt} = \frac{1}{2} C_{p, opt} \rho A \lambda_{opt}^3 \omega_{r, opt}^3 \quad (1)$$

$$C_{p, opt} = \frac{1}{2} C_{p, opt} \rho A \lambda_{opt}^3 \quad (2)$$

$$\omega_{r, opt} = \frac{\lambda_{opt}}{R} v \quad (3)$$

where k_{opt} is the optimized constant, $\omega_{r, opt}$ is the WT speed for optimum power generation, $C_{p, opt}$ is the optimum power coefficient of the turbine, ρ is the air density, A is the area swept by the rotor blades, λ_{opt} is the optimum tip speed ratio, v is the wind speed and R is the radius of the blade. When one inverter fails to operate or is under maintenance, the other inverter can handle the maximum power output of 40 kW from the PMSGs. Thus the proposed topology offers increased reliability and ensures continuous operation of the wind power generation system when either inverter 1 or inverter 2 is disconnected from operation. An 80 Ah storage battery (SB), which is sized according to [24], is connected to the dc grid through a 40 kW bidirectional dc/dc buck-boost converter to facilitate the charging and discharging operations when the microgrid operates connected to or islanded from the grid. The energy constraints of the SB in the proposed dc grid are determined based on the system-on-a-chip (SOC) limits given by

$$SOC_{min} < SOC \leq SOC_{max} \quad (4)$$

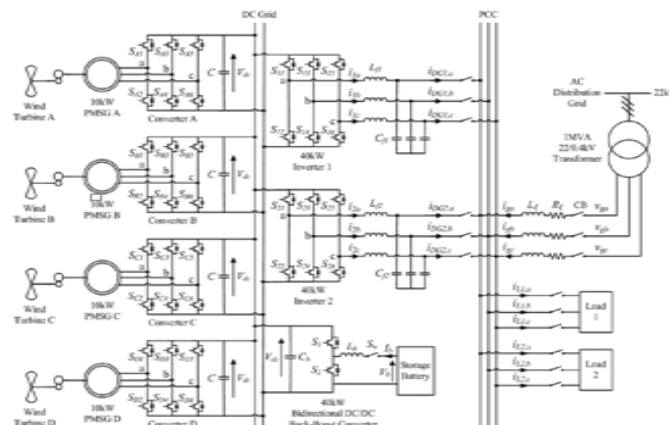


Figure-1: Overall configuration of the proposed dc grid based wind power generation system in a micro grid.

System Operation

When the microgrid is operating connected to the distribution grid, the WTs in the microgrid are responsible for providing local power support to the loads, thus reducing the burden of power delivered from the grid. The SB can be controlled to achieve different demand side management functions such as peak shaving and valley filling depending on the time-of-use of electricity and SOC of the SB [27]–[29].

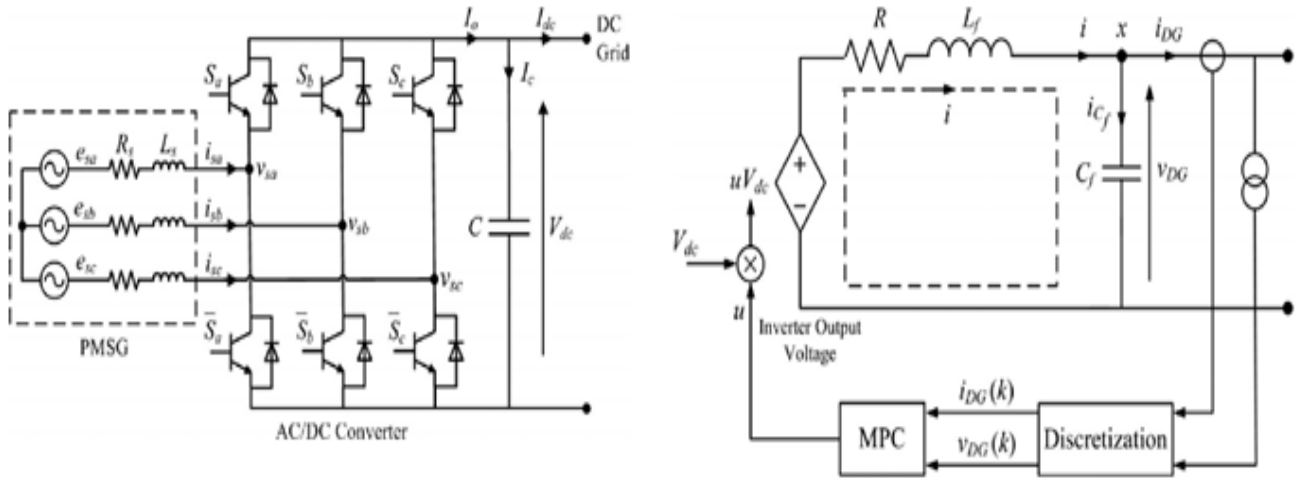
During islanded operation where the CBs disconnect the microgrid from the distribution grid, the WTs and the SB are only available sources to supply the load demand. The SB can supply for the deficit in real power to maintain the power balance of the microgrid as follows:

$$P_{wt} + P_{sb} = P_{loss} + P_l \quad (5)$$

where P_{wt} is the real power generated by the WTs, P_{sb} is the real power supplied by SB which is subjected to the constraint of the SB maximum power $P_{sb, max}$ that can be delivered during discharging and is given by

$$P_{sb} \leq P_{sb, max} \quad (6)$$

P_{loss} is the system loss, and P_l is the real power that is supplied to the loads.



AC/DC Converter Modeling

Fig. 2 shows the power circuit consisting of a PMSG which is connected to an ac/dc voltage source converter. The PMSG is modeled as a balanced three-phase ac voltage source e_{sa} , e_{sb} , e_{sc} with series resistance R_s and inductance L_s [30], [31]. As shown in [32], the state equations for the PMSG currents i_{sa} , i_{sb} , i_{sc} and the dc output voltage V_{dc} of the converter can be expressed as follows:

$$\begin{aligned} L_s \frac{di_s}{dt} &= -R_s i_s + e_s - K S V_{dc} \quad (7) \\ \frac{dV_{dc}}{dt} &= i_s^T S - I_{dc} \quad (8) \end{aligned}$$

where

$$i_s = [i_{sa} \ i_{sb} \ i_{sc}]^T, e_s = [e_{sa} \ e_{sb} \ e_{sc}]^T$$

$$K = \begin{bmatrix} 2/3 & -1/3 & -1/3 \\ -1/3 & 2/3 & -1/3 \\ 1/3 & 1/3 & 2/3 \end{bmatrix}$$

$$S =$$

$$S = \begin{bmatrix} S_a & S_b & S_c \\ S_a & S_b & S_c \\ S_a & S_b & S_c \end{bmatrix}$$

is the ac/dc converter switching

$S = S_a \ S_b \ S_c$ T functions

which are defined as

$$S_j = \begin{cases} 1, & S_j \text{ is ON} \\ 0, & S_j \text{ is OFF} \end{cases} \quad \text{for } j = a, b, c \quad (9)$$

DC/AC Inverter Modeling

The 40 kW three-phase dc/ac inverters which connect the dc grid to the point of common coupling (PCC) are identical, and the single phase representation of the three phase dc/ac inverter.

MATLAB / Simulink. The effectiveness of the proposed design concept is evaluated under different operating conditions when the microgrid is operating in the grid-connected or islanded mode of operation. The system parameters are given in Table I. The impedances of the distribution line are obtained from [34]. In practical implementations, the values of the converter and inverter loss resistance are not precisely known. Therefore, these values have been coarsely estimated.

A. Test Case 1: Failure of One Inverter During Grid-Connected Operation

When the microgrid is operating in the grid-connected mode of operation, the proposed wind power generation system will supply power to meet part of the load demand. Under normal operating condition, the total power generated by the PMSGs at the dc grid is converted by inverters 1 and 2 which will share the total power supplied to the loads. When one of the inverters fails to operate and needs to be disconnected from the dc grid, the other inverter is required to handle all the power about 22 kW which is converted by inverters 1 and 2 into 20 kW and 8 kVAR of real and reactive power respectively. Figs. 5 and 6 show the wave-forms of the real and reactive power delivered by inverters 1 and 2 for $0 \leq t < 0.4$ s respectively. For $0 \leq t < 0.2$ s, both inverters 1 and 2 are in operation and each inverter delivers about 10 kW of real power and 4 kVAR of reactive power to the loads. The remaining real and reactive power that is demanded by the loads is supplied by the grid which is shown in Fig. 7. It can be seen from Fig. 7 that the grid delivers 40 kW of real power and 4 kVAR of reactive power to the loads for $0 \leq t < 0.2$ s. The total real and reactive power supplied to the loads is about 60 kW and 12 kVAR as shown in the power waveforms of Fig. 8.

The unsteady measurements observed in the power waveforms for $0 \leq t < 0.08$ s are because the controller requires a pe-riod of about four cycles to track the power references during the initialization period. As compared to conventional control strategies, it can be observed that the proposed MPC algorithm is able to quickly track and settle to the power reference. This is attributed to the optimization of the inverters through the generated by the PMSGs. In this test case, an analysis on the microgrid operation when one of the inverters is disconnected from operation is conducted.

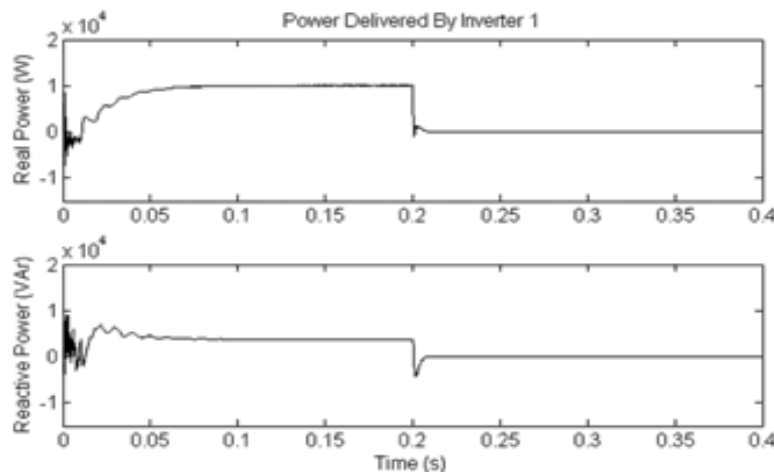


Fig-5: Real (top) and reactive (bottom) power delivered by inverter 1

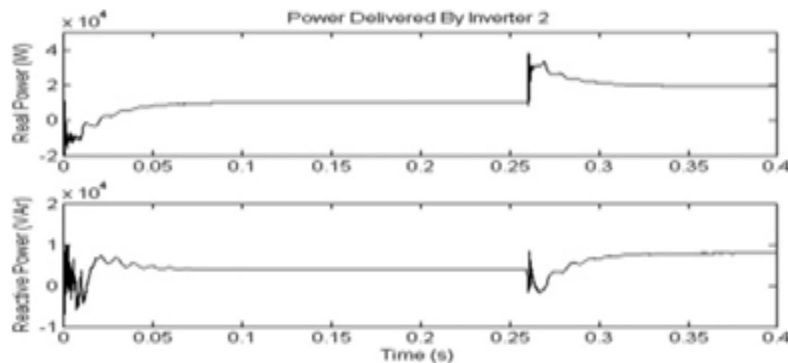


Fig-6: Real (top) and reactive (bottom) power delivered by inverter 2.

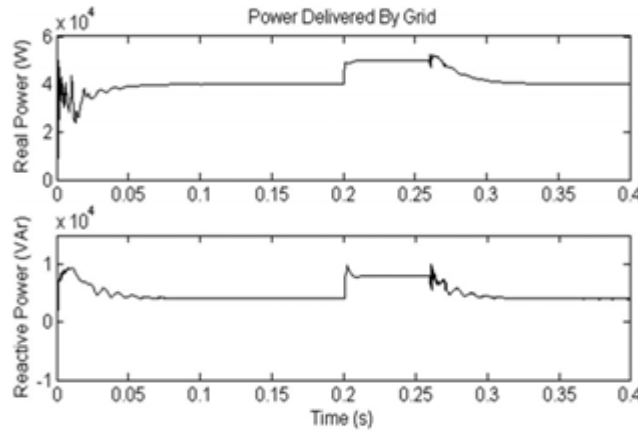


Fig-7: Real (top) and reactive (bottom) power delivered by the grid.

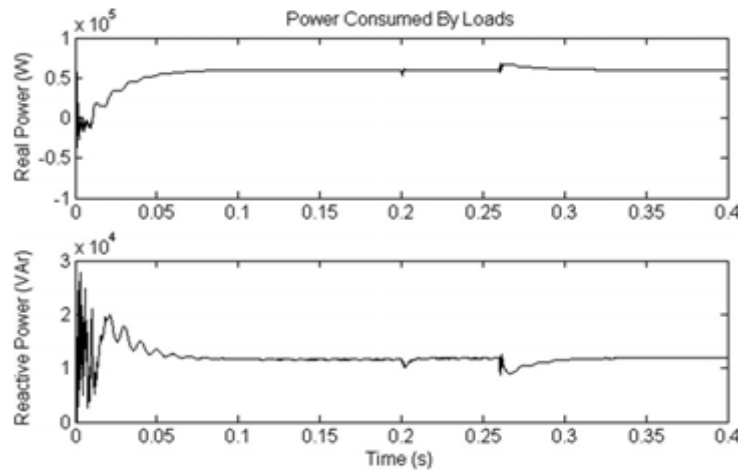


Fig-8: Real (top) and reactive (bottom) power consumed by the loads.

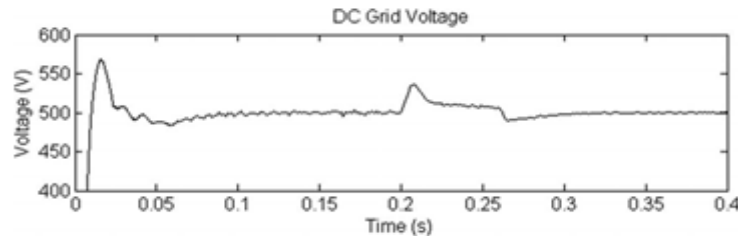
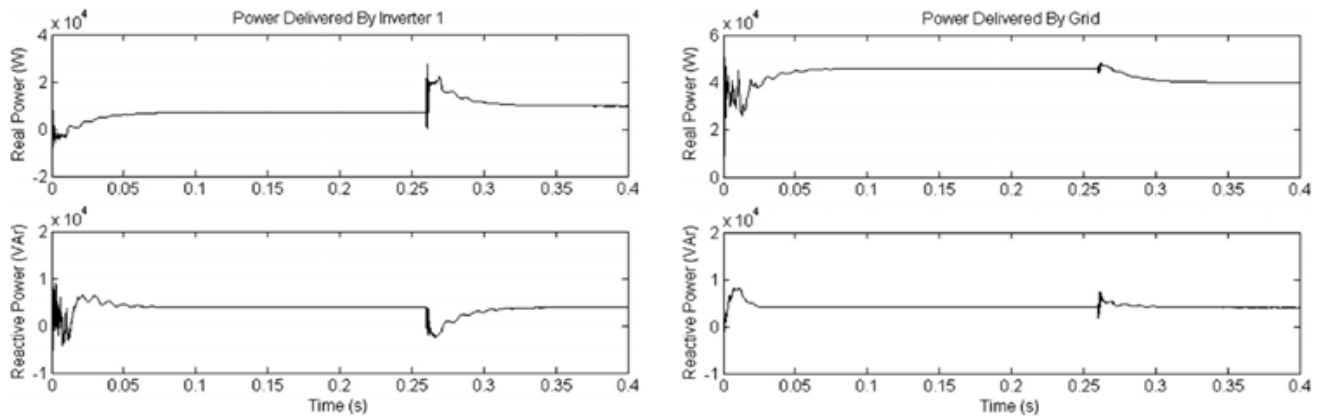


Fig-9: DC grid voltage.

With each PMSG generating about 5.5 kW of real power, the total power generated by the four PMSGs is model-based MPC control. Essentially, model-based control schemes are able to take into account the system parameters such that the overall performance can be optimized. At $t = 0.2$ s, inverter 1 fails to operate and is disconnected from the micro grid, resulting in a loss of 10 kW of real power and 4 kVAr of reactive power supplied to the loads. As shown in Fig. 5, the real and reactive power supplied by inverter 1 is decreased to zero in about half a cycle after inverter 1 is disconnected.

This undelivered power causes a sudden power surge in the dc grid which corresponds to a voltage rise at $t = 0.2$ s as shown in Fig. 9. To ensure that the load demand is met, the grid automatically increases its real and reactive power generation to 50 kW and 8 kVAr respectively at $t = 0.2$ s, as shown in Fig. 7. At $t = 0.26$ s, the EMS of the micro grid increases the reference real and reactive power supplied by inverter 2 to 20 kW and 8 kVAr respectively. A delay of three cycles is introduced to cater for the response time of the EMS to the loss of inverter. As shown in Fig. 6, inverter 2 manages to increase its real and reactive power supplied to the loads to 20 kW and 8 kVAr for $0.26 \leq t < 0.4$ s. At the same time, the grid decreases its real and reactive power back to 40 kW and 4 kVAr as shown in Fig. 7 respectively. The power balance in the micro grid is restored after three cycles from $t = 0.26$ s. It is observed from Fig. 9 that the voltage at the dc grid corresponds to a voltage dip at $t = 0.26$ s due to the increase in power drawn by inverter 2 and then returns to its nominal value of 500 V for $0.26 \leq t < 0.4$ s. As observed in Fig. 8, at $t = 0.26$ s, the changes in power delivered by inverter 2 and the grid also cause a transient in the load power.



B. Test Case 2: Connection of AC/DC Converter During Grid-Connected Operation

The most significant advantage of the proposed dc grid based wind power generation system is that it facilitates the connection of any PMSGs to the micro grid without the need to synchronize their voltage and frequency. This capability is demonstrated in this case study. The microgrid operates connected to the grid and PMSG A is disconnected from the dc grid for $0 \leq t < 0.2$ s as shown in Fig. 1. The real power generated from each of the remaining three PMSGs is maintained at 5.5 kW and their aggregated real power of 16.5 kW at the dc grid is converted by inverters 1 and 2 into 14 kW of real power and 8 kVAr of reactive power. As shown in Figs. 10 and 11, each inverter delivers real and reactive power of 7 kW and 4 kVAr to the loads respectively. The rest of the real and reactive power demand of the loads is supplied by the grid as shown in Fig. 12. It can be seen from Fig. 12 that the grid delivers 46 kW of real power and 4 kVAr of reactive power to the loads.

At $t = 0.2$ s, PMSG A which generates real power of 5.5 kW is connected to the dc grid. This causes a sudden power surge at the dc grid and results in a voltage rise at $t = 0.2$ s as shown in the voltage waveform of Fig. 13. At $t = 0.26$ s, the EMS increases the real delivered by each inverter to 10 kW while the reactive power supplied by each inverter remains unchanged at 4 kVAr as shown in Figs. 10 and 11. These causes a momentarily

V. CONCLUSION

In this paper, the design of a dc grid based wind power generation system in a microgrid that enables parallel operation of several WGs in a poultry farm has been presented. As compared to conventional wind power generation systems, the proposed microgrid architecture eliminates the need for voltage and frequency synchronization, thus allowing the WGs to be switched on or off with minimal disturbances to the microgrid operation. The design concept has been verified through various test scenarios to demonstrate the operational capability of the proposed microgrid and the simulation results has shown that the proposed design concept is able to offer increased flexibility and reliability to the operation of the microgrid. However, the proposed control design still requires further experimental validation because measurement errors due to inaccuracies of the voltage and current sensors, and modeling errors due to variations in actual system parameters such as distribution line and transformer impedances will affect the performance of the controller in practical implementation. In addition, MPC relies on the accuracy of model establishment, hence further research on improving the controller robustness to modeling inaccuracy is required. The simulation results obtained and the analysis performed in this paper serve as a basis for the design of a dc grid based wind power generation system in a micro grid.

REFERENCES

1. M. Czarick and J. Worley, "Wind turbines and tunnel fans," *Poultry Housing Tips*, vol. 22, no. 7, pp. 1–2, Jun. 2010.
2. The poultry guide: Environmentally control poultry farm ventilation systems for broiler, layer, breeders and top suppliers. [Online]. Available: <http://thepoultryguide.com/poultry-ventilation/>
3. Livestock and climate change. [Online]. Available: <http://www.worldwatch.org/files/pdf/Livestock%20and%20Climate%20Change.pdf>.
4. Farm Energy: Energy efficient fans for poultry production. [Online]. Available: <http://farmenergy.exnet.iastate.edu>.
5. A. Mogstad, M. Molinas, P. Olsen, and R. Nilsen, "A power conversion system for offshore wind parks," in *Proc. 34th IEEE Ind. Electron.*, 2008, 2106–2112.

-
6. A. Mogstad and M. Molinas, "Power collection and integration on the electric grid from offshore wind parks," in *Proc. Nordic Workshop Power Ind. Electron.*, 2008, pp. 1–8.
 7. D. Jovic, "Offshore wind farm with a series multiterminal CSI HVDC," *Elect. Power Syst. Res.*, vol. 78, no. 4, pp. 747–755, Apr. 2008.
 8. X. Lu, J. M. Guerrero, K. Sun, and J. C Vasquez "An improved droop control method for DC microgrids based on low bandwidth communication with DC bus voltage restoration and enhanced current sharing accuracy," *IEEE Trans. Power Electron.*, vol. 29, no. 4, pp. 1800–1812, Apr. 2014.
 9. T. Dragicevi, J. M. Guerrero, and J. C Vasquez, "A distributed control strategy for coordination of an autonomous LVDC microgrid based on power-line signaling," *IEEE Trans. Ind. Electron.*, vol. 61, no. 7, 3313–3326, Jul. 2014.
 10. N. L. Diaz, T. Dragicevi, J. C. Vasquez, and J. M. Guerrero, "Intelligent distributed generation and storage units for DC microgrids—A new concept on cooperative control without communications beyond droop control," *IEEE Trans. Smart Grid*, vol. 5, no. 5, pp. 2476–2485, Sep. 2014.
-

EXPERIMENTAL STUDY ON STRENGTH AND DURABILITY PROPERTIES OF GGBS BASED CONCRETE IN SEA WATER

P. Malliga¹ and Dr. B. VidiVELLI²Associate Professor¹, Department of Civil Engineering, E. G. S.Pillay Engineering College (Autonomous), Nagapattinam, TamilnaduProfessor², Department of Civil and Structural Engineering, Annamalai University, Chidambaram

ABSTRACT

Concrete made with Portland cement has been a popular construction material in the world for the past 170 years or more. The major causes in our construction industry is emission of carbon dioxide and solid waste disposal problem. However, reduction of cement consumption by partial replacement of ordinary Portland cement by industrial wastes or by-products. This paper presents investigation on different levels of ground granulated blast furnace slag as a partial replacement of cement to study durability properties of concrete. Ground granulated blast furnace slag is by-product and is obtained by quenching molten iron slag from a blast furnace in water or steam, to produce a glassy, granular product that is then dried and ground into a fine powder. These materials when combined with calcium hydroxide, exhibits cementations property. Partial replacement of ground granulated blast furnace slag 20%, 40% and 70% replacement will increase strength of 13.36%, 8.5% and 7.8% in 28 days of curing in potable water, sea water and H_2SO_4 acid respectively than the conventional concrete. The water to cement ratio is 0.5 for all mixes and mix proportion of M_{20} grade was found to be 1:1.4:2.61. Ground granulated blast furnace slag serves as an eco friendly way of utilizing the product without dumping it on earth's surface.

Keywords: Ground granulated blast furnace slag (GGBS), sea water, H_2SO_4 acid.

1. INTRODUCTION

Concrete is one of the important construction material used in the world in all engineering works including the infrastructure development at all stages. Cement is second most used material in the world. But this rapid production of cement creates two big environmental problems for which we have to find out civil engineering solutions. First environmental problem is emission of CO_2 in the production process of the cement. One tonne of carbon dioxide is estimated to be released to the atmosphere when one tonne of ordinary Portland cement is manufactured. The use of waste material having cementitious properties as a replacement of cement in concrete. The main focus now a days is on search of waste material or by product from manufacturing processes, which can be used as partial replacement of cement in concrete, without compromising on its desired strength. Ground Granulated Blast Furnace Slag has been constantly in use as cementations replacement for sustainable infrastructure. Ground-granulated blast-furnace slag (GGBS or GGBFS) is a by-product of iron manufacturing industry. Iron ore, coke and limestone are fed into the furnace, and the resulting molten slag floats above the molten iron at a temperature of about $1500^\circ C$ to $1600^\circ C$. The molten slag has a composition of 30% to 40% silicon dioxide (SiO_2) and approximately 40% CaO , which is close to the chemical composition of Portland cement. After the molten iron is tapped off, the remaining molten slag, which mainly consists of siliceous and aluminous residues, is then rapidly water- quenched, resulting in the formation of a glassy granulate. This glassy granulate is dried and ground to the required size which is known as ground granulated blast furnace slag (GGBS). The production of GGBS requires little additional energy compared with the energy required for the production of Portland cement. The replacement of Portland cement with GGBS will lead to a significant reduction of carbon dioxide gas emission. GGBS is therefore an environmentally friendly construction material. It can be used to replace as much as 80% of the Portland cement when used in concrete. GGBS concrete has less water permeability.

2. LITERATURE REVIEW

A. Syed Asif Ali^[1] "Experimental study on partial replacement of cement by fly ash and GGBS " .The partial replacement of cement by 9% of ground granulated blast furnace slag and 40% fly ash will improve the compressive strength, split tensile strength and flexural strength. Mix proportion of M_{25} grade was found to be 1:1.36:2.71. the compressive strength was found to be in 7 days and 28 days of curing are $31.59 N/mm^2$ and $45.47 N/mm^2$ respectively. The split tensile strength was found to be $12.78 N/mm^2$ at 28 days of curing. The flexural strength was found to be $8.81 N/mm^2$ at 28 days of curing. **B. Yogendra O.Patil^[2] "GGBS as partial replacement of OPC in cement concrete- An experimental study"**. This paper presents an experimental study of compressive and flexural strength of concrete prepared with ordinary Portland. Cement, partially replaced by ground granulated blast furnace slag in different proportions varying from 0% to 40%. It is observed

from the investigation that the strength of concrete is inversely proportional to the % of replacement of cement with ground granulated blast furnace slag. It is concluded that the 20% replacement of cement is possible without compromising the strength with 90 days curing. The replacement of ordinary Portland cement by GGBS up to 20% shows the marginal reduction of 4% to 6 % in compressive and flexural strength for 90 days curing, however beyond 20% replacement by GGBS the reduction in strength is substantial. The reduction in the cost of concrete at the current market rate is 14%, in the case of GGBS as replacement of ordinary Portland cement by 20%. The partial replacement of ordinary Portland cement by GGBS, not only provides the economy in the construction but it also facilitates environmental friendly disposal of waste slag. **C. Swaroop^[3] “Durability studies on concrete with fly ash & GGBS”**. Study is mainly confined to evaluation of changes in both compressive strength and weight reduction in five different mixes of M30 grade namely conventional aggregate concrete (CAC), concrete made by replacing 20% of cement by fly ash (FAC₁), concrete made by replacing 40% of cement by fly ash (FAC₂), concrete made by replacing 20% replacement of cement by GGBS (GAC₁) and concrete made by replacing 40% replacement of cement by GGBS (GAC₂). **D. Tanveer Asif zardi^[4] “Suitability & Performance of concrete with the addition of GGBS as partial replacement of cement”**. This article represents an study of compressive strength of concrete prepared with ordinary Portland cement 53 grade, partially replaced by GGBS in different proportions varying from 0%, 10%, 20% and 30%. The increase in percentage of GGBS results in decrease in strength of concrete. But at 20% GGBS the compressive strength is nearer to plain concrete mix, at the age of 28 days curing. The reduction in the cost of concrete at the current market rate is 14% in the case of GGBS as replacement of ordinary Portland cement by 30%. **E. Suresh^[5] “Ground granulated blast slag (GGBS) in concrete- a review”**. The present technical report focuses on investigating characteristics of concrete with partial replacement of cement with ground granulated blast furnace slag (GGBS). The topic deals with the usage of GGBS and advantages as well as disadvantages in using it in concrete. This usage of GGBS serves as replacement to already depleting conventional building materials and the recent years and also as being a byproduct it serves as an eco friendly way of utilizing the product without dumping it on ground. The movement of moisture of GGBS mixes, probably due to the dense and strong microstructure of the interfacial aggregate/binder transition zone are probably responsible for the high resistance of GGBS mixes to attack in aggressive environments such as silage pits. The mineral composition cement paste of GGBS probably contributes to this resistance. **F. Amit gaval^[6] “Experimental study on ground granulated blast furnace slag in concrete”**. Use of GGBS improves the quality of concrete. GGBS concrete is characterized by high strength, lower heat of hydration, and resistance to chemical corrosion. In recent years GGBS when replaced with cement has emerged as a major alternative to conventional concrete and has rapidly drawn the concrete industry attention due to its cement savings, energy savings, and cost savings, environmental and socio-economic benefits. The optimum GGBS replacement as cementitious material is characterized by high compressive strength, low heat of hydration, resistance to chemical attack, better workability, and good durability and cost effective. The flexural strength was maximum at 40% replacement of GGBS. To increase in the GGBS replacement level workability of concrete increase. Use M40 grade of concrete the compressive strength increase when the cement is replaced by GGBS. At 40% replacement of cement by GGBS the concrete attained maximum compressive strength. **G. Mohd majiduddin^[7] “Experimental investigation on the effect of physical, chemical and mechanical properties of fly ash and ground granulated blast furnace slag (GGBS) on concrete”**. This experiment study aimed to investigate the physical, chemical and mechanical property of fly ash and blast furnace slag cement concrete. Compressive strength of fly ash obtained for 5% replacement of cement has shown significant improvement in various properties at the age of 28 days indicated by 13% increase in compressive strength and in GGBS, 40% replacements shown significant improvement in various properties at the age of 28 days indicated by 85% increase in compressive strength. Highest flexural strength in fly ash is obtained for 20% replacement and strength is 5.43N/mm² and in GGBS 30% replacements have got highest flexural strength and the strength is 3.54N/mm². The advantage of the use of fly ash and GGBS in concrete is the flexibility that it allows with the selection of the mixture proportions. The sub grade of the road infrastructures can consume the slag produced or stored with significant quantities. Slag is an insensitive material with water, quality which is suitable for the use of sub-grade. The insensitivity is due primarily to its cleanliness and its small percentage of slag is at lower than 80µm. this slag has a very tight grain-size distribution, which decreases the aptitude for the compaction, and this will be necessary thus to carry out a correction with other material. **H. Yasutaka sagawa^[8] “ Properties of concrete with GGBS and its applications for bridge superstructures”**. This paper deals with the chloride diffusion coefficient of the concrete mixed with ground granulated blast furnace slag was investigated. As the results, GGBS reduced the effective diffusion coefficient of chloride ion by from 1/5 to 1/10. Also, GGBS with specific surface area of 6000 cm²/g improved the chloride resistance of concrete when water to binder ratio (W/B) was smaller than 45%. In addition, GGBS with specific surface area of 6000cm²/g was applied to

prestressed concrete bridge. The effective diffusion coefficient of the concrete used for bridge superstructure showed the lower value. As the results of simple simulation by using fick's second law, it is expected that steel bars in concrete will not occur corrosion for 100 years. **I. Sonali^[9] "To study the partial replacement of cement by GGBS & RHA and natural sand by quarry sand in concrete"**. Good compressive strength is obtained when 22.5% GGBS + 7.5% Rice husk ash is replaced with cement and natural sand is replaced by 60% quarry sand for M40 grade of concrete. Permeable voids are decreases with the age of curing and the combination of ground granulated blast furnace slag and rice husk ash and quarry sand will be more durable. **J. Vignesh^[10] "An experimental investigation on strength parameters of fly ash based geo polymer concrete with GGBS"**. In this paper an attempt is made to study strength properties of geo polymer concrete using low calcium fly ash replacing with slag in 5 different percentages. Sodium silicate (103 kg/m^3) and sodium hydroxide of 8 molarities (41 kg/m^3) solutions were used as alkaline solution in all 5 different mixes. Fly ash is replaced by GGBS for reducing green house gases and emission of CO_2 . Water absorption property is lesser than the normal concrete. The optimum replacement level of fly ash by GGBS in geo polymer concrete will achieve more strength in short time (i.e., 70% of the compressive strength in first 4 hours of setting). **K. Santosh Kumar karri^[11] "Strength and Durability studies on GGBS concrete"**. The present paper focuses on investigating characteristics of M20 and M40 grade concrete with partial replacement of cement with ground granulated blast furnace slag by replacing cement via 30%, 40%, 50%. Workability of concrete increases with the increase percentage of GGBS. The compressive strength values of acid effected concrete decreases than normal concrete but effect of acid on concrete decreases with increase of percentage of GGBS. The effect of Hcl on strength of concrete is lower than the effect of H_2SO_4 on strength of concrete.

3. MATERIAL & ITS PROPERTY

A. Cement

Cement in general can be defined as a material which possesses very good adhesive and cohesive properties which make it possible to bond with other materials to form compact mass. Ordinary Portland cement of 43 grade (SUPER) was used in this investigation. The physical properties of the cement tested according to Indian standards procedure confirms to the requirements of IS 10262- 2009 and the physical properties are given in table 1.

PROPERTIES	RESULT OBTAINED
Specific gravity	3.12
Soundness	8
Fineness	8%
Initial setting time	34mins
Final setting time	540mins
Consistency	31%

Table -1: Properties of cement

B. FINE AGGREGATE

The fine aggregate used in the project was locally supplied and conformed to grading zone II as per IS: 383:1970. It was first sieved through 4.75mm sieve to remove any particles greater than 4.75mm. Properties of the fine aggregate are tabulated below in Table 2.

PROPERTIES	RESULT OBTAINED
Specific gravity	2.64
Bulk density	1668 kg/m^3
Fineness modulus	2.75
Grading zone	Zone II
Water absorption ratio	1%

Table – 2: Properties of Fine Aggregate

C. COARSE AGGREGATE

Locally available coarse aggregate having the maximum size of (10 - 20mm) were used in this project. Coarse aggregate confirming to IS 383:1970. Properties of the coarse aggregate are tabulated in Table 3.

PROPERTIES	RESULT OBTAINED
Specific gravity	2.84
Bulk density	1765 kg/m ³
Fineness modulus	6.45
Maximum size	20mm
Water absorption ratio	0.5%

Table – 3: Properties of coarse aggregate

D. GROUND GRANULATED BLAST FURNACE SLAG

In the present investigation GGBS marketed by Astra chemicals, Chennai is used. The results furnished by the manufacturer are presented in Table 4.

Chemical Composition		Physical Properties	
Calcium oxide	33.2%	Colour	Off-white
Silica	34.4%	Specific gravity	2.9
Alumina	21.5%	Bulk density	1200 kg/m ³
Magnesia	9.5%	Fineness	>350 m ² /kg
Iron oxide	0.2%	Particle size	40 microns

Table -4: Properties of GGBS

E. POTABLE WATER

Potable Water used for mixing and curing is clean and free from injurious amount of oils, acids, alkalis, salts, sugar, organic materials or other substances that may be deleterious to concrete. Potable water is used for mixing concrete. The pH value of water lies between 6 and 8 that indicate the water is free from organic matters.

F. SEA WATER

Sea water used for curing the concrete cubes and cylinder for 7 days, 14 days, 28 days and 60 days for identifying alkali aggregate expansion. PH value of sea water lies between 7.5 to 8.4, the average value in equilibrium with the atmospheric CO₂ being 8.2.

G. H₂SO₄ ACID SOLUTION

Concrete cubes are cured in H₂SO₄ acid for 7 days, 14 days, 28 days, 60 days in 5ml H₂SO₄ acid of 1 litre of potable water for studying durability properties of concrete. Most soils contain some sulphate in the form of calcium, sodium, potassium and magnesium. They occur in soil or ground water. Because of solubility of calcium sulphate is low; ground waters contain more of other sulphates and less of calcium sulphate. Ammonium sulphate is frequently present in agricultural soil and water from the use of fertilizers or from sewage and industrial effluents. Decay of organic matters in marshy land, shallow lakes often leads to the formation of H₂S, in which can be transformed into sulphuric acid by bacterial action. A characteristic whitish appearance is the indication of sulphate attack.

4. RESULTS**a. Compressive strength test results**

Sl.No	% OF GGBS	Compressive Strength In N/mm ²			
		7 days	14 days	28 days	60 days
1	0	13.33	20.84	28.35	37.30
2	20	13.25	21.13	30.98	38.54
3	40	14.34	21.95	32.70	39.31
4	70	14.17	20.99	31.42	38.36

Table – 5: Comparison of compressive strengths of various cubes cured in potable water

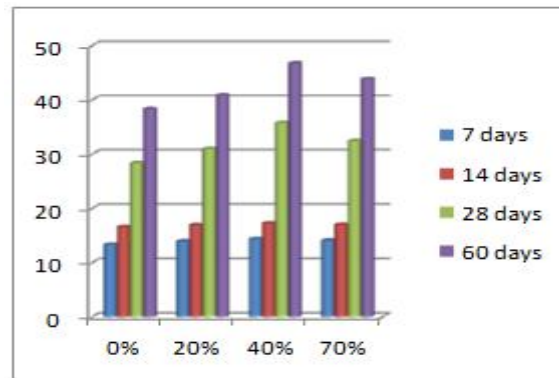


Figure – 1: Comparison of compressive strengths of various cubes cured in potable water

SLNO	% OF GGBS	Compressive Strength N/mm ²			
		7 days	14 days	28 days	60 days
1	0	11.80	16.96	21.92	32.25
2	20	12.31	17.23	22.56	33.81
3	40	12.43	17.88	23.24	34.13
4	70	13.75	17.67	23.15	33.58

Table - 6 : Comparison of compressive strengths of various cubes cured in sea water

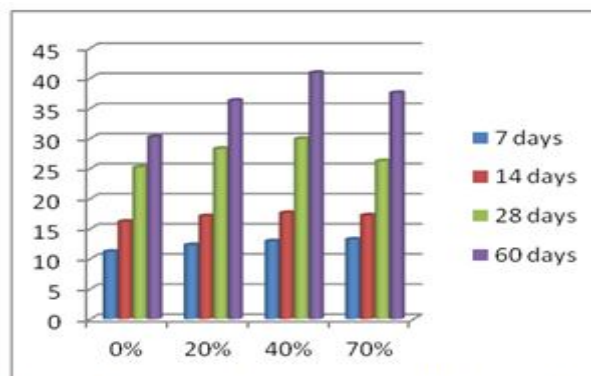


Figure - 2 : Comparison of compressive strengths of various cubes cured in sea water

SLN O	% OF GGBS	Compressive Strength N/mm ²			
		7 days	14 days	28 days	60 days
1	0	9.90	14.02	19.83	30.60
2	20	10.28	14.63	19.98	31.08
3	40	10.64	14.79	20.12	31.65
4	70	10.91	15.02	20.53	32.04

Table – 7: Comparison of compressive strengths of various cubes cured in H₂SO₄ acid solution

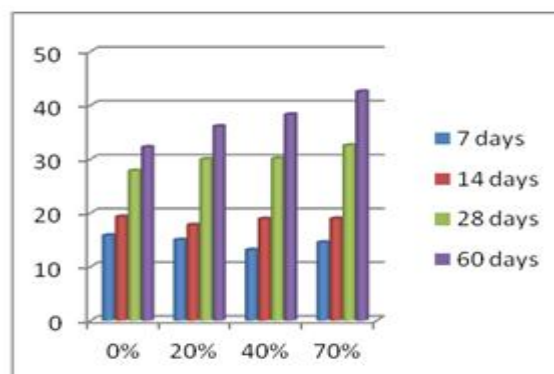


Figure – 3: Comparison of compressive strengths of various cubes cured in H₂SO₄ acid solution

b. Split Tensile Strength Test Results

SI. NO	% OF GGBS	Split Tensile Strength N/mm ²		
		7 days	14 days	28 days
1	0	0.89	1.79	2.69
2	20	0.95	1.9	2.85
3	40	1.06	2.13	3.20
4	70	0.90	1.81	2.72

Table – 8: Split tensile strength test results

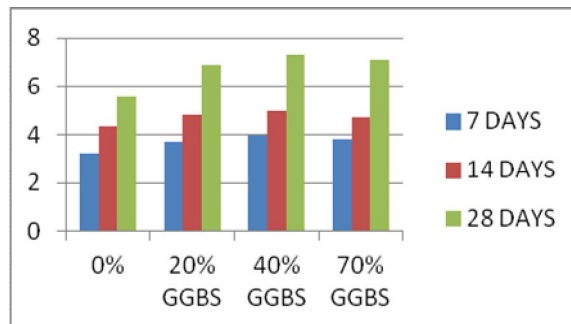


Figure – 4: Split tensile strength test results

c. Flexural Strength Test Result

SI.NO	% OF GGBS	Flexural Strength in 28 days N/mm ²
1.	0%GGBS	3.21
2.	20% GGBS	3.33
3	40%GGBS	3.54
4	70%GGBS	3.30

Table – 9: Flexural strength test result

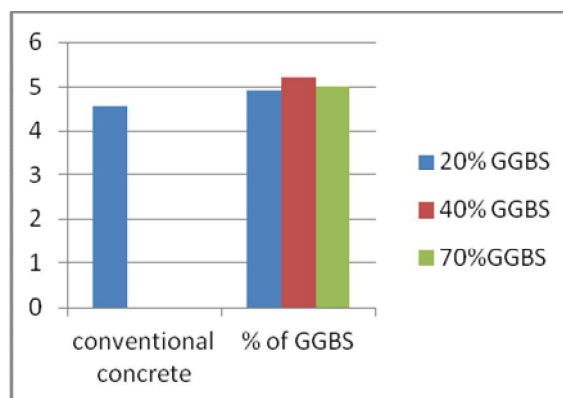


Figure – 5: Flexural strength test result

5. CONCLUSION

- The maximum compressive strength of 38.54 N/mm², 39.31 N/mm² and 38.86 N/mm² is achieved at 20%, 40% and 70% replacement of GGBS respectively as compare to 37.30 N/mm² of strength of conventional concrete for 60 days curing in potable water. Thus maximum strength is achieved in 40 % of GGBS replacement than other replacement levels.
- The maximum compressive strength of 34.13 N/mm² is achieved at 40% replacement of GGBS as compare to 32.25 N/mm² of strength of conventional concrete for 60 days curing in sea water.
- The maximum compressive strength of 32.04 N/mm² is achieved at 70% replacement of GGBS as compare to 30.60 N/mm² of strength of conventional concrete for 60 days curing in H₂SO₄.

- 40% replacement of GGBS has the equal weight of plain cement concrete (8.42 kg), when cured in sea water.
- Using GGBS instead of cement, not only provides the economy in the construction but it also facilitates environmental friendly disposal of the waste slag which is generated in huge quantities from the steel industries.
- Hopefully one day in the future GGBS will replace ordinary Portland cement as the most abundant man-made material in construction field.

6. REFERENCES

- (1) Syed Asif Ali, Shaik Abdullah, "Experimental study on partial replacement of cement by fly ash and GGBS." IJSRD vol.2, Issue 07, 2014
- (2) Yogendra O.Patil, Prof.P.N.Patil and Dr. Arun Kumar Dwivedi, "GGBS as partial replacement of OPC in cement concrete- An experimental study." IJSR vol.2, Issue11, 2013
- (3) A.H.L.Swaroop,K.Venkateswararao,Prof P Kondandaramarao, "Durability studies on concrete with fly ash & GGBS." IJERA vol.3, Issue4, jul-aug 2013, PP.285-289
- (4) Tanveer Asif Zerdi, Shaik Mohammed Athar, Shaik Abdul Mujeeb, Mohd Haroon, Tazeem-ul-haq-Zerdi, "Suitability & performance of concrete with the addition of GGBS as partial replacement of cement." IJR vol.3, Issue5, may 2016
- (5) D.Suresh and K.Nagaraju, "Ground granulated blast slag (GGBS) in concrete- a review" IOSR-JMCE vol.12, issue 4 ver. VI (Jul.-Aug. 2015), PP 76-82
- (6) Mr.Amit Gavali, Mrs.Sneha Sawant & Mr.Mithun Sawant, "Experimental study on ground granulated blast furnace slag in concrete" IJIR vol-2, Issue-7, 2016
- (7) Mohd Majiduddin, Md Muzzaffar Khan, Omer Zaheer Ahmed, Md.Hashmath, "Experimental investigation on the effect of physical,chemical and mechanical properties of fly ash and ground granulated blast furnace slag (GGBS) on concrete." IJESRT Majiduddin, 4(3): March, 2015
- (8) Yasutaka SAGAWA, Daisuke Yamamoto and Yoshikazu HENZAN, "Properties of concrete with GGBS and its applications for bridge superstructures" third international conference on sustainable construction materials and technologies.
- (9) Sonali K.Gadpalliwar, R.S.Deotale, Abhijeet R.Narde, "To study the partial replacement of cement by GGBS & RHA and natural sand by quarry sand in concrete" (IOSR-JMCE) vol 11, Issue 2 Ver II (Mar-Apr. 2014), PP 69-77
- (10) P.Vignesh, K.Vivek, "An experimental investigation on strength parameters of fly ash based geopolymer concrete with GGBS" IRJET Vol.02 Issue 02, may-2015
- (11) Santosh Kumar Karri, G.V.Rama Rao, P.Markandeya Raju, "Strength and durability studies on GGBS concrete" (SSRG-IJCE) - Vol 2, Issue 10, Oct 2015
- (12) IS 456: 2000, - Indian Standard Code of practice for plain and reinforced concrete, bureau of Indian Standard, New Delhi
- (13) IS 10262: 1982, - Recommended Guidelines for concrete mix design, Bureau of Indian Standard, New Delhi
- (14) IS 383: 1970, - specification for coarse aggregate and fine aggregate from natural sources for concrete, bureau of Indian Standard, New Delhi
- (15) IS 5816: 1999, - splitting tensile strength of concrete method of test, Bureau of Indian Standard, New Delhi
- (16) IS 516: 1959, - flexural strength of concrete, bureau of Indian standard, New Delhi
- (17) IS 9399: 1959, - specification for apparatus for flexural testing of concrete, bureau of Indian Standard, New Delhi

SINGLE PHASE BIDIRECTIONAL AC TO DC CONVERTER USING THREE PORT CONVERTER WITH MINIMISED POWER PROCESSING STAGE AND OVERALL IMPROVED EFFICIENCY**Chakkaravarthi C.¹ and J. Menaka²**PG Scholar¹ and Assistant Professor²

Department of Electrical and Electronics Engineering, E. G. S. Pillay Engineering College (Autonomous), Nagapattinam, Tamilnadu

ABSTRACT

Single-stage bidirectional AC to DC converters dependent on three-port converter (TPC) is proposed for vitality storage applications. Three power interfacing ports, i.e. a DC-bus port, a DC input port and an AC port, are given by the proposed converter. A battery, whose voltage is less than the pinnacle amplitude of the AC voltage, is associated with the DC input port of the TPC, with which vitality trade between the grid and battery is directly achieved. In this way, control prepared by the down-stream DC-DC converter is lessened, which can diminish the power misfortunes instigated by the down-stream DC-DC converter. In expansion, losses of switches of the TPC can be diminished as well because of multilevel characteristic. Subsequently, the generally speaking proficiency of the whole bidirectional AC-DC converter is enhanced fundamentally. Topologies, operation, regulation and control of the proposed TPC-based bidirectional AC to DC converter are dissected in detail. A 2-kW model is manufactured and tried to check the adequacy and focal points of the proposed arrangement.

Keywords: Three Port Converter, Bidirectional Converter.

I INTRODUCTION

ENERGY STORAG structure is a fundamental piece of various power systems, for instance, microgrids, electric-vehicles, uninterruptable power supplies, et cetera. The bidirectional AC-DC converter is a key equipment to interface the AC grid and a limit part .Profitable and versatile imperativeness exchange between AC system and storage segments is a significant test. A two-compose AC-DC converter is commonly used to interface a low voltage battery and the AC-grid. A bi-directional DC-DC converter is gotten to give an unflinching bus voltage V_{Bus} , whose voltage is higher than the peak abundance of the AC grid v_G . In inverting mode, the battery voltage V_B is wandered up to V_{Bus} by the DC-DC converter, while V_{Bus} is wandered down to V_B in the rectifying mode. An imperative issue of the two- stage sort out course of action lies in the multi-state power conversion. Since all the power must be arranged twice, the general efficiency of the entire AC-DC converter would be hurt. Various systems have been proposed to improve the efficiency of bidirectional AC-DC converters. Focuses are commonly just on the DC-DC orchestrates or the AC-DC sort out, autonomously. Though improved topologies and control can be associated with the AC-DC and DC-DC stages to achieve fragile trading or stunned movement to decrease trading adversities, the general change capability is so far certain to be hurt by the two change stages. Single-compose bidirectional AC-DC control change seems, by all accounts, to be charming since there is only a solitary power change sort out. It might be recognized using a bidirectional Z-wellspring of qZ-source AC-DC converter. Regardless, it is hard to achieve high capability with a single stage impedance-source converter in light of the limited development up limit, balance record and high-current/voltage weights on switches. Thusly, in practice, the full-associate AC-DC converter is altogether more standard. It is seen that there is a period changing voltage on the Cooling side. The voltage V_{Bus} is ordinarily picked by the most recognizably horrendous assignment case, i.e. the zenith abundance of AC cross section voltage, to ensure a controlled sinusoidal current on the AC system side of the AC-DC converter. The possibility of midway control planning is proposed and associated with DC-DC converters and AC-DC rectifiers to reduce the power.

II EXSITING METHOD

Efficient and adaptable vitality trade between AC lattice and capacity components is a noteworthy test. A two-organize AC-DC converter is generally used to interface a low voltage battery and the AC-network bidirectional DC-DC converter is received to give a consistent transport voltage V_{Bus} , whose voltage is higher than the pinnacle adequacy of the AC grid.

The existing system consists of the ac source with normal bi-directional AC-DC converter and bi-directional DC-DC converter connect to battery. The possibility of midway control planning is proposed and associated with DC-DC converters and AC-DC rectifiers to reduce the power change stages, anyway this thought has not been given a record of single stage bidirectional AC-DC change applications. Frankly, for the single-arrange bidirectional Cooling DC change showed up in Fig. 1, the low voltage battery V_B can moreover directly

exchange with AC grid, if the instantaneous estimation of v_G is lower than V_B . As demonstrated by the principle operation of multilevel converter, V_B can moreover exchange control with v_G through the AC-DC converter even exactly when V_B is lower than v_G .

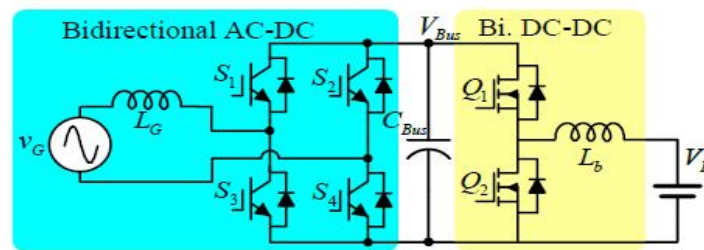


Fig-1: Two-stage AC-DC converter

III PROPOSED SYSTEM

1. Architecture of proposed converter

The design of the projected TPC-based single-stage bidirectional AC-DC converter is appeared in Fig. 2. It is seen that the fundamental thought of the proposed AC-DC converter is to present another DC power port in the AC-DC organize, so that the battery V_B can trade vitality with the AC grid as it were through the TPC inside single transformation stage.

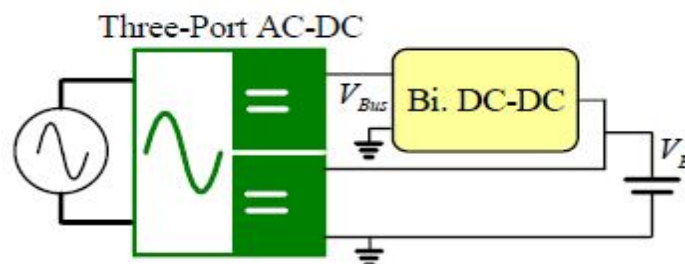


Fig-2: Architecture of proposed converter

Consequently, the power prepared by the bidirectional DC-DC converter can be lessened. The bidirectional DC-DC converter, or, in other words used to interface the DC transport and battery and gives a steady DC bus voltage V_{Bus} for the AC-DC state, can be the same as that in a traditional two-stage AC-DC converter appeared in Fig. 1. The bidirectional TPC is the keyform for the projected AC-DC converter. The topology of the proposed TPC is represented in Fig. 3, where it is seen that the bidirectional TPC is determined by including two bidirectional switches between the mid-focuses, of a regular full-connect inverter and the battery V_B . It ought to be noticed that, since voltage of V_B can be either higher or lower than the immediate estimation of v_G , bidirectional switch changes are important to ensure a controllable bidirectional power trading among V_B and v_G . The usage of the bidirectional switch is appeared at the base of Fig. 3 too.

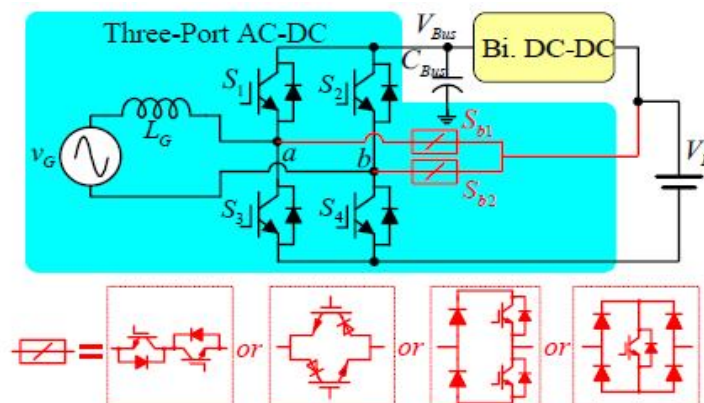
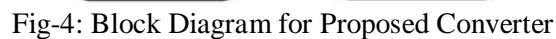


Fig-3: Topology of proposed converter and their switching design

Clearly, a bidirectional switch can be executed with two series connect MOSFETs/IGBTs, two parallel-associated switch blocked IGBT, or a blend of diodes and active switches. Bidirectional switches have been generally utilized in rectifiers and inverters, in spite of the fact that the execution and control of a bidirectional switch is somewhat muddled than a ordinary dynamic switch, the unwavering quality of the converter won't be influenced excessively by the bidirectional switches.



The proposed TPC-based bidirectional air conditioning DC converter appeared in Fig. 4, where the bidirectional switches are figured it out with two series connected switches, is taken to investigate the activity standards of the proposed arrangement. Since the topology and activity of the TPC in positive and negative cycle of AC voltage are symmetrical, just the positive half cycle is followed to be investigated in detail. It ought to be noticed that, in perspective of the whole AC-DC power system, just a single DC source, i.e. VB is utilized, the middle of intermediate DC bus V_{Bus} is given by the bidirectional DC-DC converter.

V_B trading power State: As appeared in Fig. 4, when Sb1 and S4 are both ON, V_B is associated with the inductor L_G. L_G can be charged (inverting mode with DC-AC change) or rectifying (rectifying mode with AC-DC change) by V_B as per the power stream bearing of the AC-DC converter. In this express, the mid-point voltage v_{ab}=V_B



86

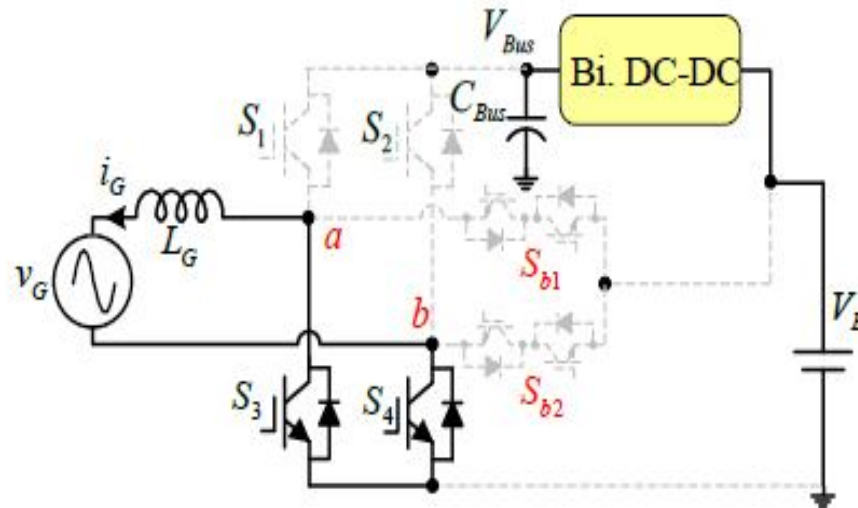


Fig-6: Frewelling state

2) Dual-port mode with $V_B < |v_G|$

At the point when V_B is lower than $|v_G|$, the voltage V_B can't satisfy the action essential of the AC-DC converter. Along these lines, the DC-bus must be used to ensure runoff the normal performance of AC-DC power stage. The converter works in twoport mode, in which V_B and V_{Bus} exchange control with v_G on the other hand. The converter has two switching states in this mode: V_B exchanging power state and V_{Bus} exchanging power state. The equivalent and performance of the V_B exchanging power state is the comparable as that in the single-port mode. The proportionate circuit of the V_{Bus} exchanging power state is showed up in Fig.6. As showed up in Fig. 6, when S_1 and S_4 are both ON, V_{Bus} is related with the inductor L_G . L_G can be charged (inverting mode) or discharged (rectifying mode) by V_{Bus} according to the power flow heading of the AC-DC converter. In this state, the mid-point voltage $v_{ab} = V_{Bus}$. As shown by the operation principle, plainly three voltage levels,

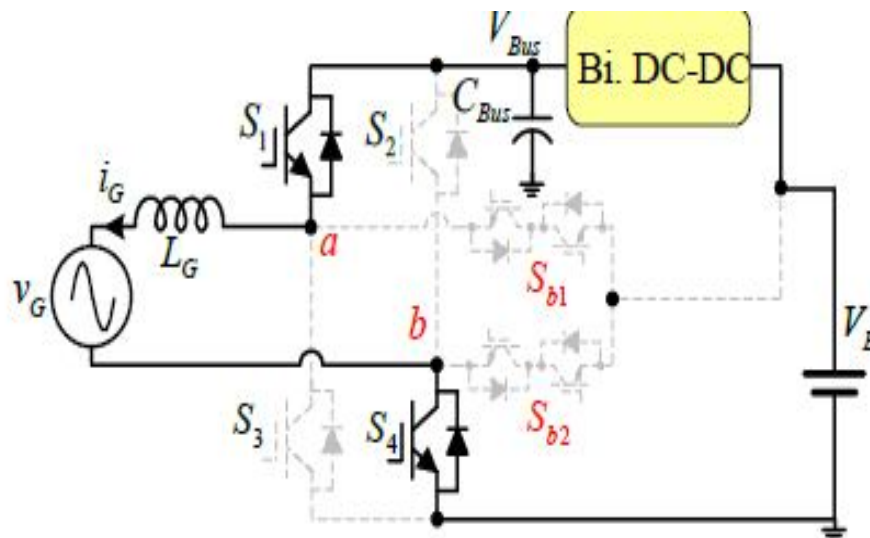


Fig-7: Circuit diagram for Vbus exchanging power stage in dual port mode

4. CONTROL SYSTEM FOR PROPOSED SYSTEM

Double bearer based SPWM balance technique can be connected to the proposed converter. Key waveforms of the proposed TPC where vc_{s1} , vc_{s2} , vc_{sb1} , vc_{sb2} are the bearer voltages of switches S_1 , S_2 , S_{b1} , S_{b2} , individually, and v_{ab} is the voltage between the mid-purposes of the switching bridges. Survey from the balance technique, the activity of the proposed converter is like a traditional multilevel converter. Be that as it may, not the same as indistinguishable voltage levels in a customary staggered converter, the low voltage level in the proposed converter is specifically dictated by V_B and will differ following the condition of-charge of the capacity battery. Considering the connection between the adequacy of V_B and the quick estimation of the matrix voltage v_G , the TPC has two activity modes, i.e. single-portmode and double port mode. Then, the TPC converter will work in the inverting mode when v_G and i_G are in same extremity, generally in correcting mode with v_G and i_G in inverse extremity. It ought to be noticed that the driving signs of every single activeswitch stay unaltered paying little mind to the course of the power flow.

IV MATLAB RESULT

1. Simulink Diagram

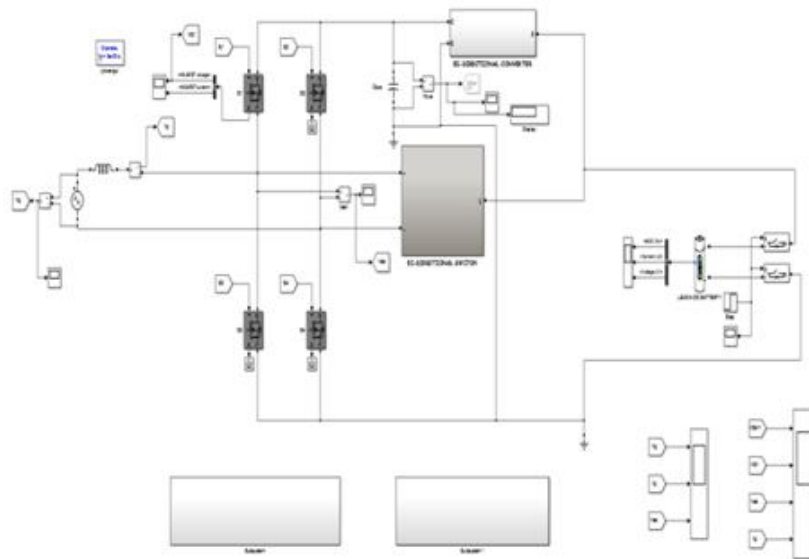


Fig-8: Simulation Diagram of Proposed system

2. Input

i) Input Voltage and current waveform

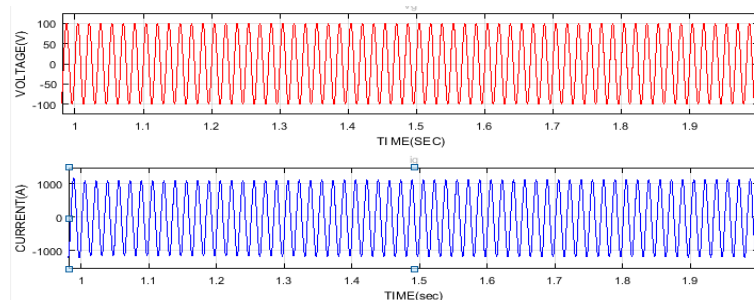


Fig-9: Input Voltage and current

ii) Output Voltage And Current Waveform

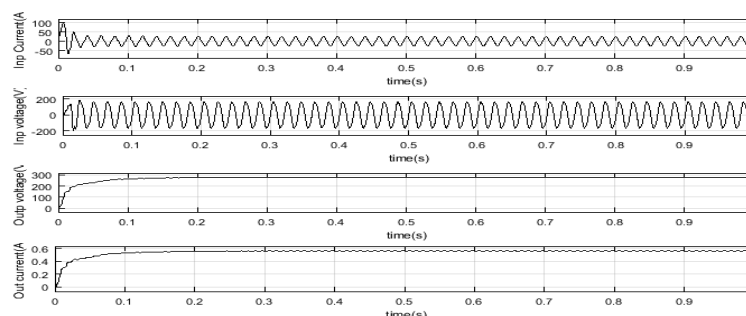


Fig-10: Output Voltage and current

V CONCLUSION

An epic three-port converter-based single-phase the bidirectional AC-DC converter has been proposed and analyzed for vitality storage systems. Another power flow route between the low voltage battery and the AC grid is gathered by the proposed three-port converter, with which imperativeness exchange between the battery and the grid can be refined directly through the three-port converter inside single power transformation stage. Since deficient power ought to be arranged by the down-stream bidirectional DC-DC converter in the proposed AC-DC converter, the power rating and losses of the DC-DC stage not can be diminished out and out. Theoretical examination shows that lower switching losses can be proficient with the three-port converter as a result of the various voltage-level character tics. Unmistakable examination on the basic idea, topology, assignment, equalization and control of the proposed three-port converter-based bidirectional AC-DC converter has been coordinated. Sufficiency and feasibility of the proposed bidirectional AC-DC converter is checked using a 2-kW demonstrate.

VI REFERENCE

1. E. Chatzinikolaou, D. J. Rogers, "A comparison of grid-connected battery energy storage system designs," *IEEE Trans. Power Electron.*, vol. 32, no. 9, pp. 6913-6923, Sep. 2017.
 2. N. Tashakor, E. Farjah, T. Ghanbari, "A bidirectional battery charger with modular integrated charge equalization circuit," *IEEE Trans. Power Electron.*, vol. 32, no. 3, pp. 2133-2145, Mar. 2017.
 3. Z. Liu, B. Li, F. C. Lee, Q. Li, "High-efficiency high-density critical mode rectifier/inverter for WBG-device-based on-board charger," *IEEE Trans. Ind. Electron.*, vol. 64, no. 11, pp. 9114-9123, Nov. 2017.
 4. H. Wu, K. Sun, L. Chen, L. Zhu, Y. Xing, "High step-up/step-down soft-switching bidirectional DC-DC converter with coupled-inductor and voltage matching control for energy storage systems," *IEEE Trans. Ind. Electron.*, vol. 63, no. 5, pp. 2892-2903, May 2017.
 5. L. Chen, C. Hu, Q. Zhang, K. Zhang, I. Batarseh, "Modeling and triple-loop control of ZVS grid-connected DC/AC converters for three-phase balanced microinverter application," *IEEE Trans. Power Electron.*, vol. 30, no. 4, Apr. 2015.
 6. B. D. Reddy, Anish N. K., M. P. Selvan, S. Moorthi, "Embedded control of n-level DC-DC-AC inverter," *IEEE Trans. Power Electron.*, vol. 30, no. 7, pp. 3703-3711, July 2015.
 7. S. Hu, Z. Liang, X. He, "Ultracapacitor-battery hybrid energy storage system based on the asymmetric bidirectional Z-source topology for EV," *IEEE Trans. Power Electron.*, vol. 31, no. 11, pp. 7489-7498, Nov. 2016.
- .

MANUSCRIPT SUBMISSION

GUIDELINES FOR CONTRIBUTORS

1. Manuscripts should be submitted preferably through email and the research article / paper should preferably not exceed 8 – 10 pages in all.
2. Book review must contain the name of the author and the book reviewed, the place of publication and publisher, date of publication, number of pages and price.
3. Manuscripts should be typed in 12 font-size, Times New Roman, single spaced with 1” margin on a standard A4 size paper. Manuscripts should be organized in the following order: title, name(s) of author(s) and his/her (their) complete affiliation(s) including zip code(s), Abstract (not exceeding 350 words), Introduction, Main body of paper, Conclusion and References.
4. The title of the paper should be in capital letters, bold, size 16” and centered at the top of the first page. The author(s) and affiliations(s) should be centered, bold, size 14” and single-spaced, beginning from the second line below the title.

First Author Name1, Second Author Name2, Third Author Name3

1Author Designation, Department, Organization, City, email id

2Author Designation, Department, Organization, City, email id

3Author Designation, Department, Organization, City, email id

5. The abstract should summarize the context, content and conclusions of the paper in less than 350 words in 12 points italic Times New Roman. The abstract should have about five key words in alphabetical order separated by comma of 12 points italic Times New Roman.
6. Figures and tables should be centered, separately numbered, self explained. Please note that table titles must be above the table and sources of data should be mentioned below the table. The authors should ensure that tables and figures are referred to from the main text.

EXAMPLES OF REFERENCES

All references must be arranged first alphabetically and then it may be further sorted chronologically also.

• Single author journal article:

Fox, S. (1984). Empowerment as a catalyst for change: an example for the food industry. *Supply Chain Management*, 2(3), 29–33.

Bateson, C. D.,(2006), ‘Doing Business after the Fall: The Virtue of Moral Hypocrisy’, *Journal of Business Ethics*, 66: 321 – 335

• Multiple author journal article:

Khan, M. R., Islam, A. F. M. M., & Das, D. (1886). A Factor Analytic Study on the Validity of a Union Commitment Scale. *Journal of Applied Psychology*, 12(1), 129-136.

Liu, W.B, Wongcha A, & Peng, K.C. (2012), “Adopting Super-Efficiency And Tobit Model On Analyzing the Efficiency of Teacher’s Colleges In Thailand”, *International Journal on New Trends In Education and Their Implications*, Vol.3.3, 108 – 114.

- **Text Book:**

Simchi-Levi, D., Kaminsky, P., & Simchi-Levi, E. (2007). *Designing and Managing the Supply Chain: Concepts, Strategies and Case Studies* (3rd ed.). New York: McGraw-Hill.

S. Neelamegham, "Marketing in India, Cases and Reading, Vikas Publishing House Pvt. Ltd, III Edition, 2000.

- **Edited book having one editor:**

Raine, A. (Ed.). (2006). *Crime and schizophrenia: Causes and cures*. New York: Nova Science.

- **Edited book having more than one editor:**

Greenspan, E. L., & Rosenberg, M. (Eds.). (2009). *Martin's annual criminal code: Student edition 2010*. Aurora, ON: Canada Law Book.

- **Chapter in edited book having one editor:**

Bessley, M., & Wilson, P. (1984). Public policy and small firms in Britain. In Levicki, C. (Ed.), *Small Business Theory and Policy* (pp. 111–126). London: Croom Helm.

- **Chapter in edited book having more than one editor:**

Young, M. E., & Wasserman, E. A. (2005). Theories of learning. In K. Lamberts, & R. L. Goldstone (Eds.), *Handbook of cognition* (pp. 161-182). Thousand Oaks, CA: Sage.

- **Electronic sources should include the URL of the website at which they may be found, as shown:**

Sillick, T. J., & Schutte, N. S. (2006). Emotional intelligence and self-esteem mediate between perceived early parental love and adult happiness. *E-Journal of Applied Psychology*, 2(2), 38-48. Retrieved from <http://ojs.lib.swin.edu.au/index.php/ejap>

- **Unpublished dissertation/ paper:**

Uddin, K. (2000). A Study of Corporate Governance in a Developing Country: A Case of Bangladesh (Unpublished Dissertation). Lingnan University, Hong Kong.

- **Article in newspaper:**

Yunus, M. (2005, March 23). Micro Credit and Poverty Alleviation in Bangladesh. *The Bangladesh Observer*, p. 9.

- **Article in magazine:**

Holloway, M. (2005, August 6). When extinct isn't. *Scientific American*, 293, 22-23.

- **Website of any institution:**

Central Bank of India (2005). *Income Recognition Norms Definition of NPA*. Retrieved August 10, 2005, from <http://www.centralbankofindia.co.in/home/index1.htm>, viewed on

7. The submission implies that the work has not been published earlier elsewhere and is not under consideration to be published anywhere else if selected for publication in the journal of Indian Academicians and Researchers Association.

8. Decision of the Editorial Board regarding selection/rejection of the articles will be final.

PUBLICATION FEE

The International Journal of Advance & Innovative Research is an online open access journals, which provides free instant, worldwide and barrier-free access to the full-text of all published manuscripts to all interested readers in the best interests of the research community. Open access allows the research community to view, any manuscript without a subscription, enabling far greater distribution of an author's work than the traditional subscription based publishing model. The review and publication fee of a manuscript is paid from an author's research budget, or by their supporting institutions.

As costs are involved in every stage of the publication process, like manuscript handling from submission to publication, peer-review, copy-editing, typesetting, tagging and indexing of articles, Electronic composition and production, hosting the final article on dedicated servers, electronic archiving, server and website update and maintenance and administrative overheads, each author is asked to pay certain fee as follows.

- The publication fee for the Online journal is Rs 1400. If the author wants a printed copy of the journal, then additional Rs.400/- have to be pay (which includes printing charges of the journal, hard copy of publication certificate for all authors, packaging and courier charges).
- The publication fee for the Online journal is Rs \$50. If the author wants a printed copy of the journal, then additional \$50 have to be pay (which includes printing charges of the journal, hard copy of publication certificate for all authors, packaging and courier charges).

The principal author will get one complimentary copy of journal (online / print) based on fee paid along with publication certificate (e copy / hard copy) after publication of the paper.

The publication fee, you can be deposited directly or can be transferred online in favour of “**Empyreal**”, **Current Account no 125505000329**, SWIFT No : ICICINBBCTS, IFS code : ICIC0001255, MICR No : 110229116, Branch code : 001255, Address: ICICI Bank, Plot No C-7, Sector-13, Opp. Jaipuria School, Vasundhara, Ghaziabad – 201012, Uttar Pradesh, India. **You can also transfer the publication fee through Paytm at Mobile no : 9999817591**

If anybody do not have funds to pay publication fee, he/she will have an opportunity to request the Editor for fee waiver through the Head of his/her Institution/Department/University with the reasons, because IARA does not want fee to prevent the publication of worthy work, however fee waivers is granted on a case-to-case basis to authors who lack funds. To apply for a waiver author/s must request during the submission process. Any request received thereafter will not be considered.

Indian Academicians and Researchers Association

1, Shanti Path ,Opp. Darwin Campus II, Zoo Road Tiniali, Guwahati, Assam
email : info@iaraedu.com / submission@iaraedu.com



INDIAN ACADEMICIANS & RESEARCHERS ASSOCIATION

Major Objectives

- To encourage scholarly work in research
- To provide a forum for discussion of problems related to educational research
- To conduct workshops, seminars, conferences etc. on educational research
- To provide financial assistance to the research scholars
- To encourage Researcher to become involved in systematic research activities
- To foster the exchange of ideas and knowledge across the globe

Services Offered

- Free Membership with certificate
- Publication of Conference Proceeding
- Organize Joint Conference / FDP
- Outsource Survey for Research Project
- Outsource Journal Publication for Institute
- Information on job vacancies

Indian Academicians and Researchers Association

Shanti Path ,Opp. Darwin Campus II, Zoo Road Tiniali, Guwahati, Assam

Mobile : +919999817591, email : info@iaraedu.com www.iaraedu.com



EMPYREAL PUBLISHING HOUSE

- Assistant in Synopsis & Thesis writing
- Assistant in Research paper writing
- Publish Thesis into Book with ISBN
- Publish Edited Book with ISBN
- Outsource Journal Publication with ISSN for Institute and private universities.
- Publish Conference Proceeding with ISBN
- Booking of ISBN
- Outsource Survey for Research Project

Publish Your Thesis into Book with ISBN “Become An Author”

EMPYREAL PUBLISHING HOUSE

Zoo Road Tiniali, Guwahati, Assam

Mobile : +919999817591, email : info@editedbook.in, www.editedbook.in